A CRITICAL STUDY OF THE HOPKINSON PRESSURE BAR

By R. M. DAVIES, *The Engineering Laboratory, University of Cambridge*

(*Communicated by Sir Geoffrey Taylor, F.R.S.—Received* 24 *January* 1947
—Read 13 *November* 1947

CONTENTS

The first part of this paper (§§ 1 to 9) contains a description of an electrical method for measuring the relation between pressure and time in experiments on high pressures of short duration. As in the method devised by Hopkinson, the pressure is applied normally to one end of a cylindrical steel bar, producing a stress pulse which gives rise to radial and longitudinal displacements in the bar.

The radial displacement, or the longitudinal displacement at the end of the bar remote from the applied pressure, is used to produce a change in the capacity of a suitable condenser unit which is charged to a high potential and connected through a feed circuit and an amplifier to a double-beam cathode-ray oscillograph. The change in capacity of the condenser unit gives rise to a vertical deflexion of one of the beams of the oscillograph, the other beam being used for time-marking. At the appropriate instant, the two beams are traversed rapidly in a horizontal direction across the screen by a sweep circuit triggered by a switch on the pressure bar. By photographing the traces on the screen, an oscillogram, giving the variation with time of the displacement in the bar, is obtained, and from this record the variation of the applied pressure with time can be deduced.

The second part of the paper (§§ 10 to 12) begins with a theoretical discussion of the propagation of extensional stress waves and pulses in a bar, using the exact equations due to Pochhammer and to Chree (§ 11), and also a less accurate wave equation due apparently to Love (§ 12). These investigations show that, owing to dispersion, a stress pulse is modified in its passage down the bar, the shorter waves lagging behind the longer ones. The theory provides a satisfactory explanation of certain features of the experimental results which are incompatible with elementary theory. It is found, for example, by the theory of group velocities, that a pulse whose initial duration is very short, becomes extended as it travels along the bar, its duration at distance x cm. from the origin being about $3{\cdot}3x$ μsec. In the early stages of the disturbance, extending for the first $1{\cdot}4x$ μsec., only one dominant group exists; the later portion, extending over $1{\cdot}9x$ μsec., is composed of two dominant groups which give the characteristic pattern of two superposed oscillations. These conclusions are confirmed by experiment.

The theory is used to discuss the errors in the experiments caused by the pressure bar itself, and it is shown that bars about 2 ft. long and 1 in. and 0·5 in. diameter can be used to measure pressures which last for about 20 and 10 μsec. respectively with an accuracy of about 2 to 3 %. This was confirmed by experiments with bullet impacts and detonation waves in gaseous mixtures, in which the measured values of the pressure could be checked by calculation.

List of symbols

A	area of cross-section of a pressure bar (general); amplitude of vibration (§ 11).
A'	area of application of a force on the pressure end of the bar.
a	radius of a pressure bar.
a'	internal radius of the insulated cylinder of a cylindrical condenser unit.
$C, C_1, \ldots$	capacity (general).
C	amplitude of vibration (§ 11).
c, c_g	phase and group velocities respectively of longitudinal waves of wave-length Λ in a bar.
c', c'_g	phase and group velocities respectively of flexural waves of wave-length Λ in a bar.
c_0 $(=\sqrt{[E/\rho]})$	velocity of longitudinal waves of infinite wave-length in a bar.
D	separation of the plates of a parallel-plate condenser unit.
d	distance between the axes of the cylinders in an eccentric cylindrical condenser; thickness of the plates of a parallel plate condenser.
E	Young's modulus.
E_p	e.m.f. used to polarize the condenser units.
$E_1, E_2, \ldots$	various e.m.f.'s and p.d.'s.
e_s	extension of a pressure bar under a static load.
$f_1 \ldots f_5$	functions of σ, a/Λ and r/a, defined by equations (11·8a) to (11·11a).

$H\ (=\sigma K/c_0)$	parameter of dimension of time (see equation (12·4)).
h	parameter defined in table 11·4.
i	current (general); $\sqrt{-1}$ (§§ 11 and 12).
K	radius of gyration of the cross-section of a bar about the axis.
K'	radius of gyration of the cross-section of a bar about an axis defined in appendix 3.
k	capacity per unit length of a coaxial cylindrical condenser.
k_e	capacity per unit length of a cylindrical condenser whose axes are parallel, but not coincident.
k'	constant used in connexion with figures 26 and 27.
L	self-inductance (general); overlap of cylindrical condenser unit (appendix 1).
L'	a length defined in appendix 1.
l	the length of a pressure bar.
l_b	the length of a bullet.
M	mass of a pressure bar (general); mutual inductance (§ 8).
$m\ (=\rho l)$	mass per unit area of a pressure bar.
$N,\ N'$	constants in equation (12·8).
n	a positive integer (§§ 11 and 12).
P	pressure (force per unit area) applied to the pressure end of a bar.
p	pressure (force per unit area) in a stress wave in a bar; a positive number in the Laplace transform.
p_0	pressure derived from the (displacement, time) curve of a distortionless bar.
q	electric charge (general); a positive number in a Laplace transform.
R	resistance.
R'	a non-dimensional constant defined in appendix 3.
r	distance measured at right angles to the axis of a cylinder.
$\widehat{rr}$	radial stress in a longitudinal stress wave (general case).
$S\ (=1-2\sigma/1-\sigma)$	parameter defined in table 11·4.
s	parameter in the trapezium-shaped wave of § 11.
T	period of a longitudinal wave of wave-length Λ, velocity c, in a bar.
T'	duration of a stress pulse.
$T_a\ (=a/c_0)$	time taken by a wave of velocity c_0 to traverse the radius, a, of a bar.
$T_0\ (=2l/c_0)$	period of longitudinal vibration of a free-free bar in the fundamental mode.
T_b	period of pressure bar swinging as a ballistic pendulum.
T_p	period of a dominant group.
T_w	period of a timing wave in an oscillogram.
t	time, reckoned from the instant of arrival of a stress pulse at the measuring end of a bar.
t'	time, reckoned from the instant of departure of a stress pulse from the pressure end of a bar.
U	initial velocity of swing of a pressure bar after a blow.

U_b	velocity of impact of a bullet.
u, $\dot{u}$	displacement and particle velocity in a stress wave when the stress is one-dimensional.
u_x, u_r	longitudinal and radial displacement in a stress wave in the general case.
u_y	lateral displacement in a flexural wave.
$\bar{u}$	Laplace transform of u.
V	p.d. across the input terminals of the amplifier due to the change in capacity of a condenser unit.
v, v_1, ...	p.d.
iw	the imaginary variable.
X	horizontal distance measured on a photographic plate.
X_b	the ballistic throw of a pressure bar.
Ox	axis of a pressure bar.
$\widehat{xx}$, $\widehat{xr}$	longitudinal stress and radial shear stress in a longitudinal wave (general case).
Y	vertical distance measured on a photographic plate.
Z	defined in table 11·4.
α	a parameter of dimension (length)$^{-1}$ defined in equation (5·14).
β	a parameter of dimension (e.m.f.)$^{-1}$; (see equation (5·10)).
β_n	amplitude of nth Fourier component in a periodic disturbance of arbitrary form.
γ	change in capacity of a bar condenser unit (general); $2\pi/\Lambda$ (see table 11·4 and appendix 3); real positive variable connected with the Laplace transform.
γ_r, γ_l	change in capacity of a cylindrical unit, due to the radial and longitudinal displacements of the bar (appendix 1).
δ	vertical deflexion of the recording spot of the oscillograph, measured on the photographic plate.
$\epsilon = 2R'(1+\sigma)$	a non-dimensional parameter defined in appendix 3.
ζ	radial displacement at the cylindrical surface of a bar.
κ	parameter defined in table 11·4.
Λ	wave-length of a longitudinal wave in a bar.
λ_1, λ_2	roots of the characteristic equation (general).
$\lambda = \gamma + iw$	complex variable (§ 12).
μ	modulus of rigidity (general).
μ_p, μ_{ce}, μ_{cr}	functions defined in equations (11·13) to (11·15).
ν	a constant factor used in connexion with similarity relationships.
ξ, $\dot{\xi}$	displacement and velocity of the measuring end of a pressure bar.
ξ_0, $\dot{\xi}_0$	displacement and velocity of the measuring end of a pressure bar free from distortion.
ρ	density of a pressure bar.
ρ_b	density of a bullet.
σ	Poisson's ratio (general); magnetic leakage factor (§ 8).
τ_1, τ_2	time constants.

ϕ correction term for the non-uniform distribution of the electric field in a parallel plate condenser.

ϕ_n phase of the nth Fourier component in a periodic disturbance of arbitrary form.

ψ $(= \pi H c_0/l)$ non-dimensional parameter (see equation (12·11)).

ω 2π (frequency).

ω_n 2π (frequency of the nth Fourier component in a periodic disturbance of arbitrary form).

1. Introduction

The accurate measurement of large pressures subject to very rapid changes presents a number of difficulties. Ordinary mechanical gauges which can withstand high pressures (say of order 5 to 25 tons/sq.in.) are severely limited by their free periods, and when dealing with changes of pressure taking place in times of the order of, say, 10 μsec. (1 μsec. $= 10^{-6}$ sec.) their readings are false. Piezo-electric gauges will faithfully record pressures which change in times of order 10 μsec., but their use is limited to the measurement of comparatively low pressures on account of the fragility of the piezo-electric crystal elements which they contain.

The most satisfactory method so far developed for dealing with the problem seems to be the pressure-bar method, devised originally by Hopkinson (1914) and developed by Robertson (1921) and by Landon & Quinney (1923). In this method, the pressure to be measured is applied normally to one end (the 'pressure' end) of a cylindrical steel bar; the magnitude of the pressure is deduced from measurement of the momentum trapped in detachable end-pieces wrung to the other end (the 'measuring' end) of the bar.

This apparatus is able to withstand high pressures (up to 60 tons/sq.in. or more with suitable steel), whilst pressure pulses are propagated along the bar without change of form so far as they can be regarded as travelling with velocity $c_0 = \sqrt{(E/\rho)}$, where E is the Young's modulus and ρ the density of the material of the bar. On this hypothesis, if the bar is so long that the whole pressure to be recorded is over before the pulse has had time to traverse the bar twice, the bar itself does not distort the pulse; analysis of the motion of the measuring end of the bar will thus give a true representation of events occurring at the pressure end at time l/c_0 sec. earlier, if l is the length of the bar.

Apart from any theoretical limitations associated with the distortion of a pressure pulse as it is propagated along a bar, the original Hopkinson method suffers from two disadvantages. On the one hand, the inevitable adhesion between the detachable end-pieces and the bar makes it difficult to obtain accurate results when the pressure is less than about 3 tons/sq.in. On the other hand, whereas the method can be used satisfactorily to measure maximum pressures and, with more difficulty, to measure the time during which the pressure exceeds any given value, it cannot give the relation between pressure and time.

This paper describes a development of the Hopkinson bar which retains the advantages of the original method and, at the same time, enables much smaller pressures to be measured and the relation between pressure and time to be determined. This new method consists in measuring electrically the variation with time t of either the longitudinal displacement ξ of the measuring end of the bar, or, alternatively, the radial displacement ζ of the cylindrical surface of the bar.

Considering the longitudinal displacement, ξ, let p and $\dot{u}$ be respectively the pressure and the particle velocity in the longitudinal elastic wave produced in the bar by the applied pressure. Then

$$p = \rho c_0 \dot{u}. \tag{1·1}$$

At the measuring end of the bar, because of the reflexion of the elastic wave, the velocity $\dot{\xi}$ of the end is double the particle velocity $\dot{u}$, and therefore

$$\dot{\xi} = 2\dot{u} = 2p/\rho c_0. \tag{1·2}$$

By differentiating the measured (ξ, t) curve, $\dot{\xi}$ is found and p is then determined by means of equation (1·2).

Considering next the radial displacement ζ, if a is the radius of the bar and σ the Poisson's ratio of the material of the bar, then

$$\zeta = \sigma a p/E. \tag{1·3}$$

It follows that if the (ζ, t) curve is determined experimentally, the (p, t) curve can be derived from it by multiplying the ordinates by the factor $\sigma a/E$.

At this point it is worth noticing the smallness of the magnitude of the quantities to be measured when the pressure pulse is produced in a bar 1 in. diameter by the impact of a 0·22 lead bullet of length 0·9 cm. = 0·228 in. The approximate values of ξ, ζ and the time of impact, together with other quantities associated with the pulses, are given in table 1·1.

TABLE 1·1. DIAMETER OF BAR = 1 IN.

	(1)	(2)
velocity of bullet (ft./sec.)	700	1200
duration of impact (μsec.)	42	25
length of the pulse in the steel bar: in.	8·6	5·0
cm.	22	13
maximum value of the total thrust produced by the impact on the end of the bar (tons)	1·3	3·8
maximum pressure over the area of contact of bullet and bar (tons/sq.in.)	34	100
maximum pressure in the bar: tons/sq.in.	1·6	4·8
dynes/sq.cm.	$2{\cdot}5 \times 10^8$	$7{\cdot}5 \times 10^8$
maximum velocity of the end of the bar (cm./sec.)	126	372
total longitudinal displacement of the end of the bar (cm.)	0·0042	0·0093
maximum radial displacement at the cylindrical surface (cm. $\times 10^{-5}$)	4·7	14

The original Hopkinson method and the new electrical methods are subject to three limitations, arising from the assumptions on which they are based and inherent in every method involving the propagation of a pulse along a bar of finite diameter.

(1) The equations (1·1) to (1·3), like the fundamental equations of the original method, assume that the waves propagated in the bar are *elastic* waves, i.e. the stress at every point in the bar must always lie within the region where the (stress, strain) curve is linear and reversible. With a given bar, this implies that there is an upper limit to the stress that can be measured with it, this limit being determined by the elastic and plastic properties of the material composing the bar.

(2) A second assumption common to the methods is that a pressure pulse is propagated without distortion. This assumption is only true when the wave-lengths of the elastic waves concerned in the propagation of the pulse are large compared with the lateral dimensions of the bar; when this condition is not fulfilled, the waves suffer dispersion and the form of the pulse is distorted as it travels along the bar.

The distortion of periodic disturbances and of pulses has been investigated theoretically and the results are given later (see §§ 11, 12); in the meantime it may be stated that experiment and theory tend to show that with bars about 2 ft. long and 1 and 0·5 in. diameter, pressures, which last only for 20 and 10 μsec. respectively, can be measured electrically with reasonable accuracy. Although this theoretical investigation is primarily concerned with the electrical methods of using the bar, some of the results are applicable to the mechanical methods. At some future date it may perhaps be worth while to make a more detailed investigation of the latter methods, based on the theory developed in §§ 10 to 12 below.

(3) A third assumption implicit in the methods is that the pressure in the pulse is uniformly distributed over the cross-section of the bar, even when the force acting on the pressure end is concentrated over a small area surrounding the centre. In the neighbourhood of the pressure end, this assumption is certainly not true, but experiments in which the end-pieces of the original method are replaced by small steel balls show that this uniform distribution of pressure does occur provided that the duration of the pulse due to the applied pressure is not so small that dispersion is important and provided that the length of the bar is more than four diameters. Under these conditions, if P is the applied pressure, assumed uniformly distributed over an area A' of the pressure end of the bar, then

$$p = PA'/A, \tag{1·4}$$

where A is the area of cross-section of the bar.

This paper falls naturally into three parts—the description of the apparatus and the experimental technique in §§ 2 to 9, the investigation of the theoretical limitations of the methods and the discussion of the accuracy of the results in §§ 10 to 12, and the detailed discussion of some points in the theory of the electrical parts of the apparatus in the appendices.

The experimental part of the paper is confined to the description of the determination of pressure from measurements of the longitudinal displacement ξ; the theoretical part, however, includes a discussion of the errors when the radial displacement is measured.

2. General description of the method

The longitudinal displacement ξ of the surface of the measuring end of the pressure bar is measured by using it as the earthed conductor of either a parallel plate or a cylindrical condenser (the 'bar' condenser). In the first case, the insulated conductor of the condenser consists of a brass plate parallel to the end-surface, and, in the second case, of a length of brass tube coaxial with the bar. In either case, the insulated conductor is part of a 'condenser unit' which enables this conductor to be supported elastically with respect to the pressure bar so that two conditions are fulfilled:

(1) During any slow movements of the bar, the two conductors move together so that there is no displacement of one relative to the other.

(2) During the rapid motion of the measuring end of the bar due to an impulse at the pressure end, the surface of the measuring end moves freely whilst the insulated conductor remains instantaneously at rest.

With this arrangement, a force applied to the pressure end of the bar will give rise to a change in the capacity of the bar condenser. By charging this condenser to a high voltage through a 'condenser feed-unit' which contains a condenser-resistance arrangement of high time constant, the charge on the bar condenser will be constant for small time intervals, and the change in its capacity will therefore be accompanied by a change in the potential difference (p.d.) between its conductors. This change in p.d. is amplified and recorded photographically with a cathode-ray oscillograph (c.r.o.) unit; the tube in this unit is of the 'double-beam' type, i.e. it has a system of deflecting plates which, by the application of suitable bias potentials, forms two spots on the oscillograph screen. These spots have identical horizontal motions, and at the same time they can be given independent vertical deflexions.

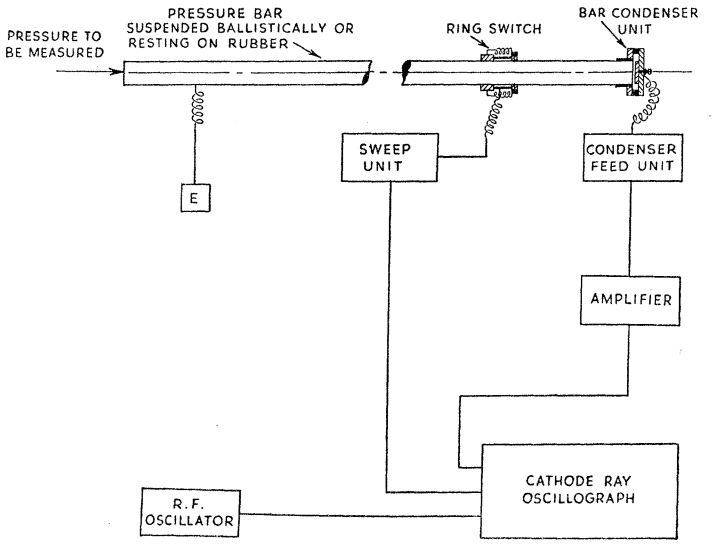

FIGURE 1. General arrangement of the apparatus.

The general arrangement of the apparatus is shown schematically in figure 1, which shows the condenser unit on the pressure bar connected to the c.r.o. through the amplifier and the condenser feed-unit. The amplified transient p.d. across the bar condenser due to a force at the pressure end of the bar is used to produce a vertical motion of one of the beams of the c.r.o. The vertical motion of the other beam is produced by the output from an oscillator of known frequency; this beam is used for giving the time scale of the record.

The horizontal motion of the oscillograph spots is produced by a sweep unit triggered by a switch on the pressure bar. Initially, the oscillograph spots are at rest on the left of the screen; they are then made to move horizontally to the right at high speed until they reach the extreme position of the sweep, whence they return at a slower speed towards their initial position. This type of sweep is obtained by using the transient p.d. produced across the secondary circuit of a transformer due to the establishment of a current in the primary circuit. Since bright stationary spots will destroy the c.r.o. screen and will fog the photographic plate used for recording, it is necessary to arrange that the brightness of the spots is small

when they are at rest and that they are modulated up to full intensity when they are in motion; to effect this, a voltage pulse, similar in form to the time-sweep pulse, is applied to the modulating grid of the oscillograph.

Normally the effects to be measured are of very short duration—as little as 25 μsec. in some instances. This means that the horizontal sweep must be synchronized with the transient p.d. across the bar condenser, so that the spots start their horizontal traverse just before the beginning of the motion of the measuring end of the bar. This requirement is met by arranging that the stress wave in the pressure bar, due to the applied pressure, breaks the ring switch shown on the bar in figure 1. This switch consists of an insulated brass ring mounted on a brass tube which can slide freely on the pressure bar; normally the ring is earthed, being held by thin rubber bands against three short brass studs which are screwed into the bar. When the stress wave due to the force applied at the pressure end reaches the studs, contact between them and the ring is momentarily broken, since the studs move forward whilst the ring, because of its inertia, remains instantaneously at rest. The ring switch forms part of the sweep circuit which contains a gas-filled relay valve which is normally non-conducting and which becomes conducting when the switch is broken; this initiates the horizontal traverse of the spots and simultaneously increases their intensity. The time between the beginning of the horizontal motion of the oscillograph spots and the arrival at the oscillograph of the amplified transient p.d. from the bar condenser is determined by the time lag in the electrical circuits, by the delay in the action of the ring switch, and by the time taken by the elastic wave in the pressure bar to travel from the switch to the bar condenser. By varying the distance between the ring switch and the end of the bar, it is possible to arrange that the vertical motion of the recording spots starts at a suitable time after the beginning of the horizontal motion.

The traces of the fluorescent spots on the screen of the c.r.o. are photographed using a stationary plate camera, and the experimental results are deduced from analysis of these records which are measured with a Hilger travelling microscope fitted with two independent motions at right angles to one another and reading directly to 0·01 mm.

3. The pressure bar

The stress waves set up in the pressure bar by the application of a force at the pressure end are assumed to be elastic waves, and it is therefore essential to make certain in any given experiment that the material of the bar is homogeneous and is nowhere stressed beyond the limit of proportionality. The majority of the bars used in this work have been made from bright, annealed tool steel, with a limit of proportionality of 30 to 40 tons/sq.in.; for most purposes this limit is high enough and, at the same time, bars obtainable commercially are reasonably homogeneous, uniform in diameter, and they can be sawn, drilled, tapped and ground with reasonable ease.

In many cases it is possible to protect the pressure end of the bar by using an anvil consisting of a short length of hardened alloy steel, equal in diameter to the bar; the front surface of the anvil is exposed to the pressure to be measured and the back surface is ground flat and lapped, and wrung with a slight smear of grease to the surface of the bar, which is similarly ground plane and lapped. A well-made joint of this type will transmit an elastic wave without distortion.

In experiments involving bullet impacts, the gun is placed some distance away from the pressure end of the bar and the bullet passes through a directing cone before striking the bar. This cone consists of a steel cylinder machined so that the internal surface consists of a truncated cone followed by a cylinder whose internal diameter is equal to the calibre of the rifle (0·22 in.). The axial length of the truncated cone is 3 in., the diameter of the larger end is about $\frac{3}{8}$ in. and the length of the cylindrical portion is about 1 in.

The directing cone ensures that the projectile strikes the end surface of the pressure bar accurately when the apparatus has been carefully set up. It also helps to reduce the disturbing effect of blast from the rifle on ballistic measurements, since it allows the rifle to be placed at a sufficient distance from the pressure bar to enable the blast to expand laterally so as to give no forward momentum to the bar.

The factors which determine the minimum length of bar to be used in any given circumstance have been stated in § 1. In the present work, bars ranging in length from 2 to 22 ft. have been used; with a force uniformly distributed over the pressure end, the bars are capable of dealing with pressures which last for $2{\cdot}4 \times 10^{-4}$ and $2{\cdot}6 \times 10^{-3}$ sec. respectively.

For most purposes, bars of diameter 0·5, 1 and 1·5 in. are suitable. The smaller the diameter of the bar, the less is the distortion of the elastic waves in the bar due to dispersion, but the diameter cannot be reduced indefinitely since the sensitivity of the apparatus decreases when the diameter of the bar decreases. The minimum pressures which can be measured with reasonable accuracy are about 0·05 ton/sq.in. with a bar 1·5 in. diameter, about 0·1 ton/sq.in. with a bar 1 in. diameter and about 0·3 ton/sq.in. with a bar 0·5 in. diameter.

When it is necessary to use the bar as a ballistic pendulum, it is hung by two bifilar suspensions; in this case all electrical connexions to the bar are made by thin flexible wires arranged so as not to disturb the motion; when measurements of momentum are not required, the bar can be supported on rubber in V-blocks.

In order to deduce the pressure from the observed (ξ, t) curve, it is necessary to know the values of ρ and c_0 (see equation (1·2)); because of the variability of tool steel, these quantities were determined for each pressure bar. The value of c_0 was found by a dynamical method, and for this purpose the bar of length l was supported on two knife-edges each at a distance $0{\cdot}25l$ from the ends, i.e. at the nodes appropriate to the stationary vibrations of a free-free bar in its first overtone of frequency c_0/l. One end of the bar was placed near an electromagnet with two windings, one carrying d.c. to magnetize the bar whilst the other was fed with variable-frequency a.c., generated by a beat-frequency oscillator whose signal was amplified by an audio-frequency amplifier with an output of 30 W. The bar was set in resonant vibration by varying the frequency of the oscillator, and, since the bar was magnetized, the frequency of its vibration was then equal to the known frequency of the oscillator. From this frequency and the length of the bar, the value of c_0 was calculated.

4. The bar condenser units

The method of attachment of the insulated conductor of the bar condenser to the bar itself must fulfil the requirements stated in § 2.

Figure 2 shows in elevation the construction of the parallel-plate unit used with a bar 1 in. diameter. In this diagram, A represents the steel pressure bar, the end-surface being

ground plane. The brass disk B is the insulated plate of the condenser, and it is mounted centrally in the ebonite disk C which is connected elastically by a rubber ring D to the ebonite ring E; the joints between the rubber ring and the ebonite disk C and ebonite ring E are made with sealing wax, and a number of holes are bored in the rubber to allow free passage of air. The ebonite ring E is firmly fixed to a brass tube F which can make contact with the pressure bar over the two cylindrical surfaces G, G; these portions are scraped so that their internal diameter exceeds the external diameter of the bar by about 0·001 in., thus making the sleeve an easy piston fit on the bar.

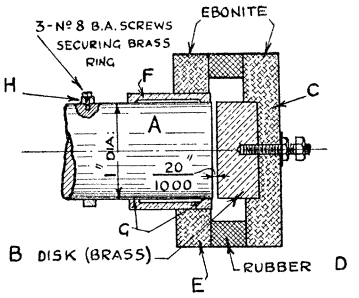

FIGURE 2. The parallel-plate condenser unit.

When the end A of the pressure bar moves forward under the action of a pressure pulse, the tube F and its attachments remain stationary because of their inertia, whilst the smallness of the clearance between the tube and the bar ensures that the insulated disk remains parallel to the end of the bar; at the same time, the clearance is sufficient to allow free motion of F and its attachments. As an extra precaution, the rubber ring D is inserted between the ebonite disks C and E; it makes the period of the system, D, B and C, sufficiently long to ensure that B remains sensibly at rest irrespective of what happens between A and F during the very short time of motion of the end of the bar.

The distance between the end-surface of the bar and the disk B is normally between 0·01 and 0·04 in., depending on the displacement to be measured. The disk can be set at a given distance from the end of the bar by means of a narrow brass ring H, which is screwed to the bar, and a removable brass half-ring (not shown in the diagram) which acts as a gauge. By placing the gauge between F and H, then pressing F so as to make contact on both sides of the gauge, and finally removing the gauge, the gap between the insulated plate and the end of the bar is set to a given value and the tube F is left free to move on the bar.

In practice, it is convenient to arrange that the gap between B and the end of the bar is between ten and thirty times the displacement of the end of the bar due to the pressure to be measured; at the same time, the gap should be at least 0·01 in. in order to avoid errors in setting it.

The cylindrical condenser units are constructed on the same principles as the parallel-plate units, and the construction of a unit for use with a bar 1·5 in. diameter is shown in elevation in figure 3. The insulated conductor consists of a brass cylinder A which is insulated by the mica plates B and supported elastically relative to the pressure bar by the system consisting of the brass sleeve G, the ebonite ring F, the outer earthed brass cylinder E and the short rubber cylinders C. The internal diameter of the sleeve G is about two-thousandths of an inch greater than the diameter of the pressure bar, so that the unit as a whole can slide

freely on the bar. The adjusting screws pressing the brass disks D are carefully set so that the insulated cylinder is coaxial with the sleeve G. In the unit shown in the diagram, the diameter of the insulated cylinder is $\frac{1}{8}$ in. greater than the diameter of the pressure bar; a condenser unit with these dimensions can be used with the apparatus described below to measure displacements of the order of 2 mm.

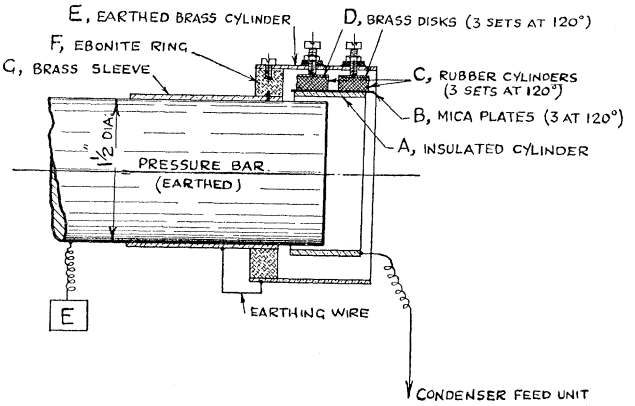

FIGURE 3. The cylindrical condenser unit.

When a force is applied to the pressure end of the bar, the longitudinal wave of compression, travelling towards the measuring end, causes lateral expansion of the bar, and since this wave is reflected as a longitudinal wave of extension, lateral contraction of the bar will accompany the extension. It follows that the change in the capacity of a cylindrical condenser unit of this type is caused by (i) the change in the length of the common portion of the bar and the insulated cylinder due to the longitudinal waves of compression and extension, and (ii) the change in the radius of the bar due to its lateral expansion and contraction. The response of a cylindrical condenser unit when the two effects are present is discussed in appendix 1, where it is shown that the results are difficult to interpret unless the second effect is small in comparison with the first; the gap between the bar and the insulated conductor must therefore be large. For this reason, the sensitivity of this type of unit is small in comparison with that of the parallel-plate type; on the other hand, the cylindrical unit can be used to measure displacements which are too large to be measured with the parallel-plate unit, and the unit shown in figure 3 has been used successfully to measure the pressure due to an underwater explosion where the maximum pressure was about 35 tons/sq.in. and the displacement of the end of the bar about 0·25 cm., i.e. about 0·1 in.

5. THE THEORY OF THE METHOD

The electrical circuit, the condenser feed-unit of figure 1, which is associated with the condenser unit, is shown in figure 4, in which the condenser C represents the bar condenser whose initial capacity is normally of order 10 $\mu\mu$F. The lower plate of C is the earthed surface of the pressure bar and the upper plate is the insulated conductor of the condenser unit. The insulated plate of C is connected through a high resistance R, 50 MΩ, to a dry battery of e.m.f. E_p, which can be set to values lying between 200 and 1000 V. The insulated plate of C is also connected through a condenser C_0, 0·1 μF, to the shunt capacity C_s and the shunt resistance R_s which are in parallel with the input terminals of the amplifier. It is essential that

all parts of this circuit, together with the leads to the amplifier, should be adequately screened to avoid pick-up from extraneous sources. The shunt capacity C_s is made up of the input capacity of the amplifier, the capacity of the screened lead to the amplifier and the capacity of any loading condensers which are used to bring up the time constant C_sR_s to the value required in a particular experiment; usually C_s exceeds $1000\,\mu\mu$F. The shunt resistance R_s consists of the leakage resistance of the screened lead to the amplifier—which is usually negligible—together with the resistance of loading resistors used to adjust the value of C_sR_s; to avoid instability in the particular amplifier used in these experiments, it is essential that R_s should not exceed $5\,\text{M}\Omega$, and in most experiments its value is about $2\,\text{M}\Omega$. The components R, C_0 and the loading condensers and resistors are contained in an earthed screening box.

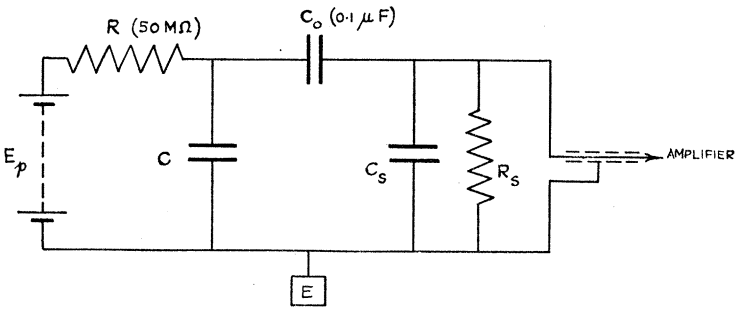

FIGURE 4. The condenser feed-unit circuit.

The action of the circuit is as follows. Before the pressure to be measured acts on the pressure bar, the condensers C and C_0 are charged by the battery E_p through the high resistance R; the condenser C_0 isolates the amplifier from the high-tension battery, and the charge on C_s is zero at this stage, because it is short-circuited by the resistance R_s. The effective time constant, as far as the charging of the condensers C, C_0 and C_s through R is concerned, is the product of R into the resultant capacity of C in parallel with C_0 and C_s in series; since C is much less than C_s, and C_0 is much greater than C_s, this resultant capacity is practically equal to C_s and the time constant is thus RC_s. C_s is usually greater than $1000\,\mu\mu$F, and hence the time constant is normally greater than 0·05 sec.

When the measuring end of the pressure bar begins to move forward, at time $t = 0$ say, the value of C changes, the change being completed at a time $t = T'$, say, which is usually less than $100\,\mu$sec. Since RC_s is of order $50{,}000\,\mu$sec., the charge which flows from the battery to the condensers C, C_0 and C_s in time $100\,\mu$sec. is negligibly small, and the charge on the system C, C_0 and C_s may therefore be considered to be constant.

The change in the capacity of C gives rise to a p.d. across C_s which is transmitted through the amplifier to the c.r.o. By making the time constant R_sC_s sufficiently large in comparison with the time T', the effect of the current through R_s during the time T' on the charge and on the p.d. of C_s can be made so small as to be negligible in comparison with other errors in the experiment. For example, if $T' = 10^{-4}$ sec. and $R_sC_s = 10^{-2}$ sec. (e.g. $R_s = 2\,\text{M}\Omega$, $C_s = 5000\,\mu\mu$F), then the decrease, due to the presence of R_s, in the charge or the p.d. of C in time T' will not exceed 1 %. To derive the theory of the method it will be assumed that the effect of the current through R_s is negligible, so that R_s will be considered to be infinite. (A more exact theory of the circuit, taking the leakage through R_s into account, is given in

appendix 2.) At the same time it will be assumed that $RC_s \gg T'$, so that the system can be regarded as being charged by the battery to a potential E_p at time $t = 0$, and isolated from it during the period $0 < t < T'$. With these assumptions, the circuit of figure 4 can be replaced by that shown in figure 5. Considering the latter, at time t $(0 < t < T')$, let v = p.d. across C_s, q = charge on the plates of C, q' = charge on the plates of C_0 and C_s. Let the values of C, v, q, q' be respectively C_1, v_1, q_1, q_1' at time $t = 0$, and C_2, v_2, q_2, q_2' at time $t = T'$.

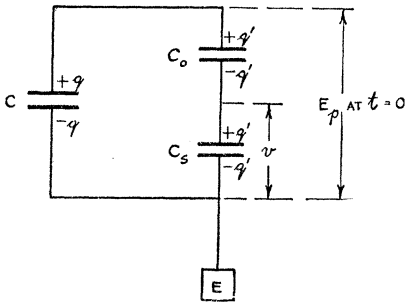

FIGURE 5. Equivalent circuit of condenser system.

At time $t = 0$, $$E_p = q_1/C_1 = q_1'(1/C_0 + 1/C_s) = q_1'/C_e, \tag{5·1}$$

where $C_e = C_0 C_s/(C_0 + C_s)$ = the capacity of C_0 and C_s in series.

Since it is assumed that R_s of figure 4 is infinite, the p.d. across C_s at time $t = 0$ will not be zero now, but will be given by the equation

$$v_1 = q_1'/C_s = C_e E_p/C_s. \tag{5·2}$$

Since the system is electrically isolated, the total charge is the same for all values of t between the limits 0 and T'. Hence

$$q + q' = q_1 + q_1' = q_2 + q_2'. \tag{5·3}$$

Now $$q_1 + q_1' = q_1'(1 + C_1/C_e) \quad \text{from equation (5·1)}$$
$$= C_s v_1 (1 + C_1/C_e) \quad \text{from equation (5·2)}.$$

Similarly $$q + q' = C_s v (1 + C/C_e), \quad q_2 + q_2' = C_s v_2 (1 + C_2/C_e).$$

Hence $$v_1(C_1 + C_e) = v(C + C_e) = v_2(C_2 + C_e). \tag{5·4}$$

If $C = C_1 + \gamma$, $v = v_1 + V$, so that γ is the change in the capacity of the bar condenser and V is the change in the p.d. across C_s, i.e. the p.d. applied to the input terminals of the amplifier, then from equations (5·2) and (5·4)

$$\left(1 + \frac{VC_s}{E_p C_e}\right)\left(1 + \frac{\gamma}{C_1 + C_e}\right) = 1,$$

which gives $$V = -\frac{\gamma E_p C_e}{C_s(C_e + C)}. \tag{5·5}$$

In many cases, C is sufficiently small in comparison with C_e to allow $(C_e + C)$ to be replaced by C_e; in these circumstances,

$$V = -\gamma E_p/C_s. \tag{5·5a}$$

Equations (5·5) and (5·5*a*) give the relation between the p.d. V applied to the input terminals of the amplifier, the change in capacity γ of the bar condenser and the electrical constants of the circuit. It is now necessary to find the relationship between γ and the displacement ξ of the measuring end of the bar, and finally the equation connecting ξ with V and the circuit constants.

(*a*) *The parallel-plate condenser unit*

Let D be the initial separation of the earthed and insulated plates of the bar condenser. Then the initial capacity C_1 of the bar condenser is

$$C_1 = A(1+\phi)/4\pi D, \tag{5·6}$$

where A = cross-sectional area of the gap, and ϕ = correction term for the non-uniform distribution of the field between the plates due to the fact that the plates are not infinitely close together.

At time t, the separation of the plates is $(D-\xi)$, and the capacity C is therefore

$$C = \frac{A(1+\phi)}{4\pi(D-\xi)}, \tag{5·7}$$

assuming that the displacement ξ is sufficiently small in comparison with D to leave the correction term ϕ unchanged.

From equations (5·6) and (5·7),

$$\gamma = \xi C/D = \xi C_1/(D-\xi), \tag{5·8}$$

and substituting in equation (5·5), after some reduction, it is found that

$$\xi = -\frac{VDC_s(C_1+C_e)}{C_e(C_1E_p - C_sV)}, \tag{5·9}$$

or, if $\beta = C_s/C_1E_p$,

$$\xi = -\frac{\beta VD(1+C_1/C_e)}{1-\beta V}, \tag{5·10}$$

which gives ξ expressed in terms of V and the circuit constants.

If $C_1 \ll C_e$, as is often the case, then equation (5·10) becomes

$$\xi = -\beta VD/(1-\beta V). \tag{5·10a}$$

It will be noticed that the sensitivity of this type of unit, i.e. the ratio of V to ξ, is not constant unless βV is small in comparison with unity; this is often the case in practice, e.g. if $C_s/C_1 = 100$, $E_p = 600$ V, $V = 0{\cdot}03$ V, then $\beta V = 0{\cdot}005$.

(*b*) *The cylindrical condenser unit*

It will be assumed that the insulated cylinder of the condenser unit is adjusted initially so as to ensure that there is no change in the end-effect during the displacement of the end of the bar; this condition will be amply fulfilled if the measuring end of the bar projects into the insulated cylinder to a distance which is five to ten times the difference in radius between the bar and the cylinder. Under these conditions, the increase in the capacity of the bar condenser will be proportional to the displacement ξ, so that if k is the capacity per unit

length of the condenser, its capacity C at time t will be $(C_1+k\xi)$, where, as before, C_1 is the initial capacity of the condenser. From equation (5·5) it follows that

$$\xi = -\frac{VC_s(C_e+C_1)}{k(E_pC_e+VC_s)}. \tag{5·11}$$

E_p is never less than 100 V, whilst V never exceeds about 0·07 V, and C_e and C_s are nearly equal; VC_s can therefore be neglected in comparison with E_pC_e, and equation (5·11) then becomes

$$\xi = -\frac{VC_s}{E_pk}\left(1+\frac{C_1}{C_e}\right). \tag{5·11a}$$

If $C_1 \ll C_e$, this equation becomes $\xi = -VC_s/E_pk.$ (5·11*b*)

(*c*) *Calibration of the condenser units*

From equations (5·10) and (5·11) it is theoretically possible to deduce the displacement ξ at time t from the p.d. V across the input terminals of the amplifier, the charging voltage E_p, and the dimensions of the condensers. In practice, difficulties arise in the case of the parallel-plate unit, where it is necessary to set the insulated disk accurately parallel to the end-surface of the bar so that the distance D between the surfaces, which is of order 0·02 in., is known; it is also necessary that the centre of the insulated disk should lie on the axis of the bar produced. In addition, the correction factor $(1+\phi)$ of equation (5·6), representing the edge-effect, complicates matters. For these reasons it was decided, in the case of the parallel-plate units, to determine the value of D for each unit, with its gauge ring, by finding the p.d. corresponding to a measurable displacement of the measuring end of the bar. Such a displacement can be produced by an impulse of short duration acting at the pressure end of the bar, e.g. by the impact of a lead bullet or a steel ball at this end, whilst the total displacement of the measuring end of the bar can be deduced from the momentum communicated to the bar by the impulse.

Let p be the pressure in the stress pulse produced in the bar by the impact, $\dot{\xi}$ the velocity of the measuring end of the bar at any instant, and $\hat{\xi}$ the total displacement of this end due to the impact. Then

$$\hat{\xi} = \int \dot{\xi}\, dt,$$

where the integral is taken over the duration of the pulse. From equation (1·2), $\dot{\xi} = 2p/\rho c_0$, and therefore, whatever be the form of the pulse,

$$\hat{\xi} = \frac{2}{\rho c_0}\int p\, dt. \tag{5·12a}$$

If the duration of the impact is less than the time taken by the stress pulse to traverse the bar twice, and if A is the area of cross-section of the bar, then

$$A\int p\, dt = \text{momentum acquired by the bar} = MU,$$

where M is the mass of the bar, and U its initial velocity after impact. Thus

$$\hat{\xi} = 2MU/\rho c_0 A. \tag{5·12b}$$

U is measured by suspending the bar as a ballistic pendulum and determining the ballistic throw, X_b, say. If T_b is the period of the bar as a ballistic pendulum, then

$$U = 2\pi X_b/T_b, \tag{5·13}$$

if, as in these experiments, the damping of the vibrations of the pendulum is negligible and if X_b is small in comparison with the length of the pendulum.

$\hat{\xi}$ can thus be determined from measurements of X_b, T_b, M, A, ρ and c_0.

If $\hat{V}$ is the p.d. across the input of the amplifier due to the displacement $\hat{\xi}$ of the measuring end of the bar, we have next to express D in terms of $\hat{\xi}$, $\hat{V}$, E_p, etc. Let

$$\alpha = \beta\hat{V}/D = C_s\hat{V}/(C_1 D)\,E_p. \tag{5·14}$$

Neglecting the sign of the p.d. $\hat{V}$, equation (5·10) then becomes

$$\hat{\xi} = \alpha D^2(1+C_1/C_e)/(1-\alpha D), \tag{5·15}$$

which reduces to

$$\alpha(1+C_1/C_e)\,D^2+\alpha\hat{\xi}D-\hat{\xi} = 0.$$

The solution of this equation, which is physically significant, is

$$D = \frac{\hat{\xi}}{2(1+C_1/C_e)}\left\{\sqrt{\left[1+\frac{4}{\alpha\hat{\xi}}(1+C_1/C_e)\right]}-1\right\}. \tag{5·16}$$

From this equation the value of D can be found, since $\hat{\xi}$ can be measured as described above, C_e and C_s measured with a capacity bridge and the terms $(1+C_1/C_e)$, which do not differ much from unity, can be evaluated by calculating the initial capacity C_1 of the bar condenser from the simple formula for the capacity of a parallel-plate condenser, the distance D being found as accurately as possible by means of feeler gauges and slip gauges of known thicknesses. It remains to determine the parameter α of equation (5·14). C_s, E_p and $\hat{V}$ are measurable, the latter from the oscillograph record as described later in this report; the remaining quantity which enters into α, the product $C_1 D$, is calculated from Kirchhoff's expression for the capacity C_1 of a parallel-plate condenser consisting of one insulated and one earthed circular disk, each of radius a, thickness d, placed parallel to each other at distance D apart (see, for example, Kohlrausch 1930, p. 658). This expression can be written in the form

$$C_1 = a^2(1+\phi)/3{\cdot}6D \quad (\mu\mu\text{F}), \tag{5·17}$$

where

$$\phi = \frac{D}{\pi a}\left\{1+\ln\frac{16\pi a}{D}+\left(1+\frac{d}{D}\right)\ln\left(1+\frac{d}{D}\right)-\frac{d}{D}\ln\frac{d}{D}\right\} \quad (\ln = \log_e). \tag{5·18}$$

Thus

$$C_1 D = a^2(1+\phi)/3{\cdot}6 \quad (C_1 \text{ in } \mu\mu\text{F}, D \text{ in cm.}). \tag{5·17a}$$

If $a = 0{\cdot}5$ in. $= 1{\cdot}27$ cm., $D = 0{\cdot}0162$ in. $= 0{\cdot}0411$ cm. and $d = 0{\cdot}25$ in. $= 0{\cdot}635$ cm., then $\phi = 0{\cdot}125$; if $a = 0{\cdot}25$ in. $= 0{\cdot}635$ cm., $D = 0{\cdot}0124$ in. $= 0{\cdot}0316$ cm., $d = 0{\cdot}125$ in. $= 0{\cdot}317_5$ cm., then $\phi = 0{\cdot}178_5$.

Considering equation (5·17a), the value of a is easily determined to a high degree of accuracy. ϕ is only a correction term and the value of the factor $(1+\phi)$ is insensitive to small variations in the values of D and d; in fact, when evaluating ϕ from equation (5·18) and $C_1 D$ from equation (5·17a), it is found that sufficient accuracy for most purposes is obtained if D is determined approximately by feeler gauges, etc., and if d is taken as the thickness of the insulated plate of the condenser unit.

In this way all the quantities on the right-hand side of equation (5·16) can be measured and the value of D calculated from the equation.

This process of calibrating the condenser unit consists essentially in starting with a reasonably good approximation to the value of D, and combining it with measurements of $\hat{\xi}$, C_e, C_s, $\hat{V}$ and E_p, together with the calculation of the value of $C_1 D$, to derive a much more accurate value of D by using equation (5·16).

It is clear that, if necessary, this new value of D can be used in equation (5·18) to calculate a more accurate value of ϕ, of $C_1 D$ and therefore of α; using this new value of α in equation (5·16), we obtain a still more accurate value of D. In practice, this second step is hardly ever necessary.

The accurate value of D, in conjunction with the value of $C_1 D$, is then used in subsequent experiments to determine the values of ξ, corresponding to the measured values of V, C_0, C_s and E, using equations (5·10) or (5·10a).

To illustrate the procedure, the following are results obtained with a bar 1 in. diameter, 2 ft. 2 in. long:

Mass of bar $= M = 2790$ g.; area of cross-section $= A = 5{\cdot}06$ sq.cm.; $\rho = 7{\cdot}85$ g./c.c.; $c_0 = 5{\cdot}23 \times 10^5$ cm./sec.; $\rho c_0 = 4{\cdot}10 \times 10^6$ g./sq.cm.sec. From equation (5·12b),

$$\hat{\xi} = 2MU/\rho c_0 A = 2{\cdot}69 \times 10^{-4}\, U \text{ cm.}$$

Length of wires used to suspend bar as a ballistic pendulum = 15 in. = 38 cm. approximately; period $= T_b = 1{\cdot}16$ sec. From equation (5·13),

$$U = 2\pi X_b/T_b = 5{\cdot}41_5 X_b \text{ cm./sec.}$$

Hence
$$\hat{\xi} = 2{\cdot}69 \times 10^{-4} U = 1{\cdot}45_5 \times 10^{-3} X_b \text{ cm.}$$

By measurement with feeler gauges, etc., the value of D was found to be approximately

$$0{\cdot}02 \text{ in.} = 5{\cdot}08 \times 10^{-2} \text{ cm.}; \quad d = 0{\cdot}25 \text{ in.} = 0{\cdot}635 \text{ cm.}; \quad a = 0{\cdot}5 \text{ in.} = 1{\cdot}27 \text{ cm.}$$

From equation (5·18) it is found that

$$\phi = 11{\cdot}64D/\pi a = 0{\cdot}148.$$

Hence
$$C_1 D = a^2(1+\phi)/3{\cdot}6 = 0{\cdot}514\,\mu\mu\text{F cm.}; \quad C_s = 1310\,\mu\mu\text{F.}$$

Therefore, from equation (5·14),

$$\alpha = C_s \hat{V}/C_1 D E_p = 1310\hat{V}/0{\cdot}514E_p = 2{\cdot}55 \times 10^3 \hat{V}/E_p;$$

$$C_1 D = 0{\cdot}514\,\mu\mu\text{F cm.}; \quad D = 5{\cdot}08 \times 10^{-2} \text{ cm.};$$

thus
$$C_1 = 10{\cdot}1\,\mu\mu\text{F}; \quad C_s = 1310\,\mu\mu\text{F}; \quad C_0 = 100{,}000\,\mu\mu\text{F};$$

hence
$$C_e = C_0 C_s/(C_0 + C_s) = 1294\,\mu\mu\text{F} \quad \text{and} \quad C_1/C_e = 10{\cdot}1/1294 = 0{\cdot}007_8.$$

Hence, from equation (5·16),

$$D = \frac{\hat{\xi}}{2{\cdot}016}\left\{\sqrt{\left(1 + \frac{4 \times 1{\cdot}008 E_p}{2{\cdot}55 \times 10^3 \hat{V}\hat{\xi}}\right)} - 1\right\},$$

i.e.
$$D = \frac{\hat{\xi}}{2{\cdot}016}\left\{\sqrt{\left(1 + 0{\cdot}00158\frac{E_p}{\hat{V}\hat{\xi}}\right)} - 1\right\}. \qquad (5{\cdot}16a)$$

The results of the experiments and the calculations are summarized in table 5·1, and from this it will be seen that the average value of $D = 5{\cdot}42 \times 10^{-2}$ cm.

TABLE 5·1

projectile used for the impulse	X_b (cm.)	$\hat{\xi}$ (10^{-3} cm.)	$\hat{V}$ (volts)	E_p (volts)	D (10^{-2} cm.)
1·25 in. steel ball	$1{\cdot}56_5$	2·28	0·0525	193	5·60
	1·62	$2{\cdot}35_5$	0·0549	193	5·56
1 in. steel ball	$0{\cdot}88_6$	1·29	0·0536	352	5·69
	1·14	1·66	0·0524	242	5·36
	1·10	1·60	0·0632	305	5·39
0·75 in. steel ball	$0{\cdot}38_6$	$0{\cdot}56_2$	0·0591	719	5·11
	$0{\cdot}46_6$	$0{\cdot}68_0$	0·0645	719	5·39
lead bullet (700 ft./sec.)	2·68	3·90	0·0656	128	5·25

In this set of results, the maximum deviation of D from the mean value is about 5 %; in spite of the differences in the impulses, together with the sevenfold variation in $\hat{\xi}$, and the fivefold variation in E_p, there does not appear to be any systematic error in the results. The average value of D is thus probably accurate to within 2 or 3 %.

It will be noticed that this value of D differs by about 6 % from the value previously measured approximately with slip gauges and assumed for the calculation of ϕ and α. The effect of this discrepancy on the value of $C_1 D$ and α is, however, small, and calculation shows that when $D = 5{\cdot}42 \times 10^{-2}$ cm. = 21·5/1000 in., $\phi = 11{\cdot}56D/\pi a = 0{\cdot}147$. With this new value of ϕ, $C_1 D = 0{\cdot}513_5$, which differs from the previous value by one in a thousand; the effect of this difference on the values of D deduced from the observations is negligible.

To derive the relationship connecting ξ with the values of V obtained in subsequent experiments in which this bar with its condenser unit and gauge ring are used, the values just derived for D and $C_1 D$ are substituted in equation (5·10). In this equation

$$\beta = C_s/C_1 E_p = C_s D/C_1 D \,.\, E_p = 3{\cdot}6 C_s D/a^2(1+\phi)\, E_p. \qquad (5{\cdot}10b)$$

Here $$\beta = 5{\cdot}42 \times 10^{-2} C_s/0{\cdot}513_5 E_p = 0{\cdot}105_6 C_s/E_p$$

and $$\beta D = 0{\cdot}105_6 \times 5{\cdot}42 \times 10^{-2} C_s/E_p = 0{\cdot}00572 C_s/E_p.$$

From equation (5·10), neglecting the negative sign,

$$\xi = \frac{\beta V D(1+C_1/C_e)}{1-\beta V} = \frac{0{\cdot}00577 C_s V/E_p}{1-0{\cdot}105_6 C_s V/E_p}.$$

If C_s is the same as before, namely, 1310 $\mu\mu$F, this equation becomes

$$\xi = \frac{7{\cdot}56 V/E_p}{1-138 V/E_p}. \qquad (5{\cdot}16b)$$

It is worth noticing that when other quantities are constant, ξ is proportional to βD (equation (5·10)), and β is proportional to D (equation (5·10b)); under these conditions, ξ is therefore proportional to D^2, and fractional error, ϵ say, in the determination of D leads to a fractional error of 2ϵ in the values of ξ calculated from this value of D.

Turning now to the case of the *cylindrical* condenser units, calibration experiments on the lines just described for the parallel-plate condenser units are unnecessary, since equations

(5·11 *a*) and (5·11 *b*) show that ξ is derivable from the measurable quantities V, E_p, C_s, C_0, C_1 and k. C_1 occurs only in the factor $(1+C_1/C_e)$, which is normally so near to unity that C_1 needs only to be known with moderate accuracy. The value of k (in $\mu\mu$F/cm.) is given by the expression

$$k = \frac{0{\cdot}2416}{\log a'/a} \quad (\log = \log_{10}), \tag{5·19}$$

where a is the radius of the bar and a' the internal radius of the insulated cylinder. Thus k can be accurately determined from measurements of a and a' if the condenser unit is constructed and adjusted so that the axes of the insulated cylinder and the bar are coincident. By careful construction and manipulation in a lathe, it is possible to adjust the condenser unit so as to make the axis of the brass sleeve G of figure 3 coincide with the axis of the insulated cylinder A. When, however, the unit is slipped on the pressure bar, the clearance between G and the bar will result in the axis of the insulated cylinder being displaced slightly relative to the axis of the bar, although they will still remain parallel. This will alter the value of k from that given by equation (5·19) by an amount which can be estimated from the known expression for the capacity of cylinders whose axes are parallel but not coincident. If d is the distance between the axes of the two cylinders of radii a and a', and if d and $(a'-a)$ are small, then it can be shown from the formulae given, for example, by Russell (1914, p. 167), that the capacity per unit length, k_e, when the cylinders are eccentric is given by

$$k_e = k\Big/\sqrt{\left[1-\frac{d^2}{(a'-a)^2}\right]} \simeq k\left[1+\frac{1}{2}\frac{d^2}{(a'-a)^2}\right]. \tag{5·20}$$

If $2a' = 1\frac{1}{16}$ in., $2a = 1$ in. and $d = 0{\cdot}004$ in., which corresponds to an extremely slack fit of the sleeve on the bar, $d/(a'-a) = 0{\cdot}128$, and $k_e = 1{\cdot}008k$; normally d will be about 0·002 in., which gives $k_e = 1{\cdot}002k$. The effect of the eccentricity of the cylinders can therefore be neglected in most cases, and k determined from accurate measurements of a and a'.

6. The cathode-ray oscillograph

The transient p.d., V, developed across C_s and R_s of figure 4, after amplification, is applied between earth and one of the Y-plates of the c.r.o., so as to give a vertical deflexion to one of the beams of the tube. The short duration of V makes it essential to obtain the maximum possible writing speed on the photographic plate used for recording. The writing speed is determined by three factors: (1) the type of cathode-ray tube; (2) the camera lens, and (3) the photographic plate.

(1) For high-speed recording, it is desirable to use a high-vacuum tube in which the beam is focused by an electron lens system; by running the tube at a high anode voltage and temporarily intensifying the spot during its motion, a high writing speed on the oscillograph screen is readily obtained. In these experiments, a Cossor indirectly heated electrostatic high-vacuum tube, type 3259 J (double beam) has been used; this tube is fitted in the Cossor Oscillograph Tube Unit, Model 3402, which enables the tube to be run at a maximum anode voltage of 3000 V. Under these conditions, the writing speed is adequate for the present experiments; the low sensitivity of the tube, about 0·22 mm./V (d.c.) can be offset by using an amplifier with a sufficiently high gain.

The diameter of the fluorescent screen of tube type 3259J is 9 in. = 22 cm.; it is, however, advisable to avoid using the curved marginal portions of the screen since distortion would be introduced, and in the present experiments only the central flat region of the screen, measuring about 10 by 5 cm., has been used.

(2) The camera must be fitted with a high-quality lens of large aperture. In these experiments, the camera lens is a Kodak Ektar lens, $f/2$ aperture and 4·5 cm. focal length, mounted in a Compur shutter.

The distance from the lens to the photographic plate in the camera is such that the size of the image is about one-third of the size of the object; the intensity of the image formed by a lens is inversely proportional to the square of {1 + (length of image)/(length of object)}, other quantities remaining constant, and the reduction of one-third in size gives an image of reasonable size without excessive loss in intensity.

(3) The J type screen used in the cathode-ray tube gives a light blue fluorescent spot with an afterglow which persists only for a time of the order of a microsecond. With this type of screen, Ilford 'Selochrome', 'Zenith' and 'Golden Iso-Zenith' plates have been found to give very satisfactory records, particularly when developed in a high-contrast developer. With records of low intensity, it is advisable to increase contrast still further by developing at a temperature of 70 to 75° F; this results in a plate in which the background is fogged compared with one developed at the normal temperature of 65° F, but the increase in contrast gives greater accuracy when the plates are measured with a travelling microscope.

7. The amplifier

The voltage V developed at time t across the shunt condenser and resistance, C_s and R_s of figure 4, due to the displacement ξ of the measuring end of the pressure bar, requires amplification before it can be used to deflect the beam of the c.r.o. In most experiments, according to equation (5·5a), the factors which determine the maximum value $\hat{V}$ of the p.d. V are (1) the polarizing voltage, E_p; (2) the shunt capacity, C_s; (3) the maximum change in capacity, $\hat{\gamma}$, corresponding to the total displacement $\hat{\xi}$ of the measuring end of the pressure bar.

By suitably designing the condenser unit and choosing the values of E_p and C_s, it is possible to arrange that the value of $\hat{V}$ is about 0·04 to 0·09 V (d.c.), and to ensure at the same time that the value of R_s in conjunction with the chosen value of C_s is sufficient to make the value of the time constant $R_s C_s$ large enough to make the correction for leakage through R_s negligible. In most cases, a photographic plate on which the maximum vertical deflexion, $\hat{\delta}$, due to $\hat{V}$, is about 3 or 4 mm. will give reasonably accurate values of ξ when measured carefully with a good travelling microscope. A deflexion of 3 mm. on the photographic plate corresponds to about 9 mm. on the oscillograph screen, and since the sensitivity of the oscillograph tube is about 0·22 mm./V (d.c.) it follows that the p.d. required to produce the desired deflexion of 9 mm. is 9/0·22 = 41 V. Taking 0·07 V as the average value of the maximum input voltage, $\hat{V}$, the gain of the amplifier must be about 41/0·07 = 585.

The amplifier must also fulfil three further conditions:

(1) The relation between the deflexion δ finally recorded on the photographic plate and the input voltage V must be linear up to a value of, say, 0·07 V (d.c.).

(2) Since the displacements ξ which have to be measured often change suddenly in times of order 5 μsec., the amplifier must faithfully amplify transient p.d.'s which vary similarly with time; it is also desirable that the amplifier should be capable of amplifying without distortion transient voltages which last for times of order 5 msec. Broadly speaking, this implies that the high-frequency response of the amplifier should be very good and its low-frequency response moderately good.

(3) Since the gain of an amplifier varies somewhat during the course of a series of experiments, it is necessary to arrange means whereby the amplifier can be calibrated frequently.

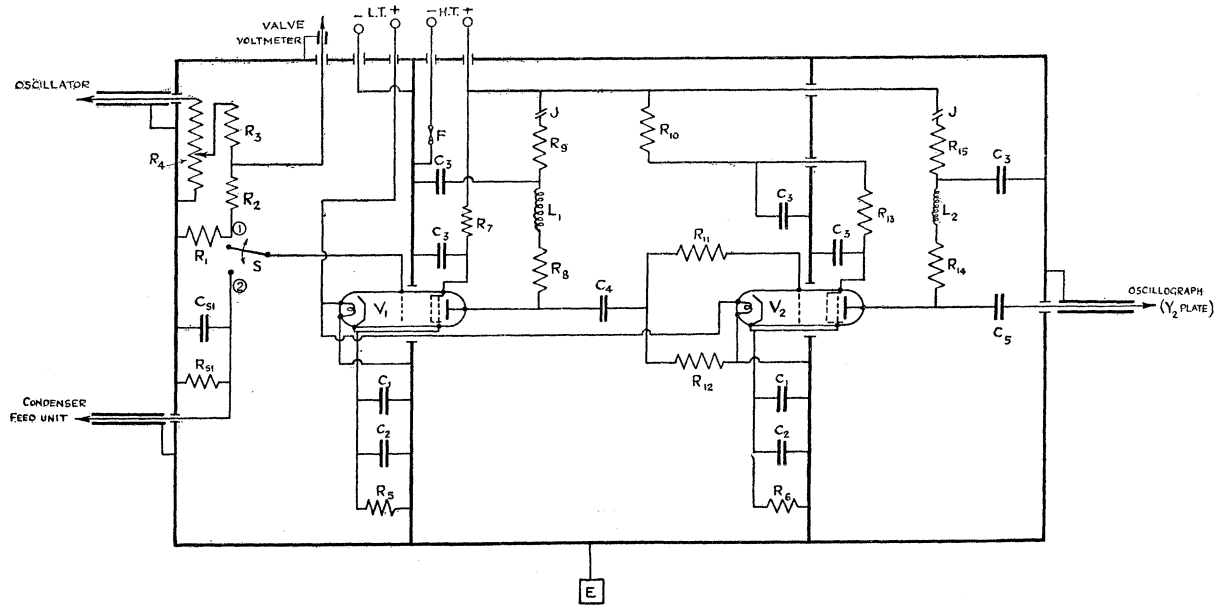

FIGURE 6. Circuit diagram of the amplifier. Thick lines denote earthed screens. S, single-pole, double-throw switch; J, jacks (closed circuit type); F, fuse. V_1, Mazda S.P.41; V_2, Mazda S.P.42. C_{s1}, 0·0005μF; C_1, 0·05μF (mica); C_2, 200μF (electrolytic); C_3, 2μF; C_4, 0·01μF; C_5, 0·1μF. R_{s1}, 5 MΩ; R_1, 100Ω; R_2, 3000Ω; R_3, 20,000Ω; R_4, 0·25 MΩ; R_5, 54Ω; R_6, 100Ω; R_7, 27,000Ω; R_8, 4400Ω; R_9, 3300Ω; R_{10}, 29,000Ω; R_{11}, 5000Ω; R_{12}, 0·1 MΩ; R_{13}, 11,000Ω; R_{14}, 2500Ω; R_{15}, 3400Ω. L_1, 24μH; L_2, 25μH. H.T. 310 V; L.T. 4 V.

The circuit diagram of the amplifier used in this work is shown in figure 6. It has two stages in order to give sufficient gain, and the coupling circuits are designed so that the distortion of the signals is negligibly small. The output p.d. is proportional to the input p.d. when the latter does not exceed 0·095 V (d.c.); the deflexion on the photographic plate corresponding to this value of input p.d. is about 4 mm.

When C_4 in figure 6 is 0·01 μF, the (gain, frequency) curve of the amplifier is linear from 800 to 10^5 cyc./sec., the gain in this region being 550; the gain drops to half this value at 8×10^5 and 80 cyc./sec. at the upper and lower ends. When C_4 in figure 6 is 0·1 μF, the gain at the lower end drops to half value at 8 cyc./sec., whilst the high-frequency portion of the curve remains unchanged.

In order to calibrate the amplifier, a signal of sine-wave form is fed from an oscillator into the input circuit containing the potentiometer R_4, the switch S being in position 1. The resistance R_3 serves to maintain a reasonably high load across the oscillator, thus avoiding

distortion of the wave form, whatever be the position of the variable contact on R_4. The p.d. across R_1 and R_2, which can be varied by means of R_4, is measured by a valve voltmeter, and the voltage across R_1 is applied between the grid of the first valve and earth; thus the fraction $R_1/(R_1+R_2)$ of the voltage, V_v V (r.m.s.) say, indicated by the valve voltmeter is applied to the input terminals of the amplifier.

This signal, when amplified, gives a vertical line on the c.r.o. screen, and if the line is photographed an overall calibration of the amplifier and the camera will be obtained. Actually, if the length of this vertical line is measured, the measurement will be in error because of the unknown but finite size of the oscillograph spot, and in order to avoid this, the trace is photographed when it is swept across the screen by the sweep unit. If δ_v is the vertical distance from the centre of a crest to the centre of a trough of the sine-wave trace obtained in this way, then δ_v corresponds to a p.d. $R_1V_v/(R_1+R_2)$ V (r.m.s.), i.e. to $2\sqrt{2}R_1V_v/(R_1+R_2)$ V (d.c.). In order to avoid errors due to stray capacities associated with the R_1, R_2 circuit, and the decrease of the gain of the amplifier at high and low frequencies, the frequency of the signal used for calibration is about 2000 cyc./sec.

When a transient voltage pulse from the bar condenser is to be recorded, the switch S is placed in position 2. If δ is the vertical deflexion on the photographic plate at any instant, then the corresponding p.d., V, across the input terminals of the amplifier, i.e. across C_s and R_s in figure 4, is

$$V=\frac{2\sqrt{2}R_1V_v}{R_1+R_2}\frac{\delta}{\delta_v}\text{ (V (d.c.))}, \tag{7·1}$$

provided that the camera setting and the gain of the amplifier have not changed between the bar experiment and the calibration experiment. When the deflexions δ and δ_v are expressed in mm. on the photographic plate, the value of the factor $2\sqrt{2}R_1V_v/(R_1+R_2)\,\delta_v$ in this apparatus is about 0·025 V(d.c.)/mm.

8. The sweep circuit

Consider the circuit shown in figure 7, in which a battery of e.m.f. E_1 is shown connected in series with a key K, which is initially open, and the primary coil of an iron-cored transformer. The total inductance of the primary circuit is denoted by L_1 and its resistance by R_1, the inductance of the secondary circuit by L_2, its resistance by R_2, and the mutual inductance between the primary and secondary coils by M.

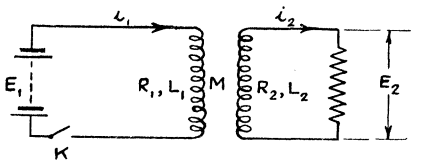

FIGURE 7. Transformer circuit.

Let the key K be closed at time $t=0$. At time t, let i_1 be the current in the primary circuit, i_2 the current in the secondary circuit, and E_2 the p.d. across R_2.

Let $\tau_1=L_1/R_1$ be the time constant of the primary circuit, $\tau_2=L_2/R_2$ the time constant of the secondary circuit and $\sigma=1-(M^2/L_1L_2)$ the magnetic leakage factor of the transformer.

The equations of the circuit are

$$L_1\frac{di_1}{dt}+M\frac{di_2}{dt}+R_1 i_1 = E_1, \quad L_2\frac{di_2}{dt}+M\frac{di_1}{dt}+R_2 i_2 = 0, \quad E_2 = R_2 i_2. \tag{8·1}$$

The solution for E_2, subject to the initial conditions $i_1 = i_2 = 0$ at $t = 0$ is

$$E_2 = \frac{-E_1 R_2(1-\sigma)}{M\sqrt{\left\{\left(\frac{1}{\tau_1}+\frac{1}{\tau_2}\right)^2-\frac{4\sigma}{\tau_1\tau_2}\right\}}}\{e^{-\lambda_1 t}-e^{-\lambda_2 t}\}, \tag{8·2}$$

where

$$\left.\begin{matrix}-\lambda_1\\-\lambda_2\end{matrix}\right\} = \frac{1}{2\sigma}\left\{-\left(\frac{1}{\tau_1}+\frac{1}{\tau_2}\right)\pm\sqrt{\left[\left(\frac{1}{\tau_1}+\frac{1}{\tau_2}\right)^2-\frac{4\sigma}{\tau_1\tau_2}\right]}\right\}. \tag{8·3}$$

From equation (8·2) it follows that E_2 is zero at $t = 0$ and $t = \infty$, and that it reaches a maximum value E_{2m} at $t = t_m$, where

$$t_m = \frac{\ln \lambda_2/\lambda_1}{\lambda_2-\lambda_1}. \tag{8·4}$$

The exact shape of the (E_2, t) curve depends on the values of τ_1, τ_2 and σ; with the values which these parameters usually assume with a step-up transformer, it is found that, as shown in figure 8, E_2 initially increases very rapidly as time increases; E_2 then attains its maximum value E_{2m} and finally decreases slowly as time increases.

Suppose that the terminals of R_2 in figure 7 are connected to the X-plates of the cathode-ray tube, giving a horizontal deflexion of the spots. When K is open, the spots are at rest; when K is closed, the spots will be swept to one side of the initial position (the forward stroke). They will momentarily come to rest when E_2 is a maximum, and finally they will return to their initial position (the return stroke). From figure 8 it is clear that the forward stroke is more rapid than the return stroke.

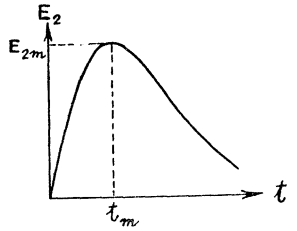

FIGURE 8. (E_2, t) curve for transformer circuit.

This is the principle of the sweep unit used in these experiments. The complete circuit diagram is shown in figure 9, in which T represents the iron-core transformer and L_1, L_2 the windings corresponding to the primary and secondary coils of figure 7; the components of the circuit, together with the various leads, are screened. It will be seen that the key K of figure 7 is replaced by the circuit containing the gas-filled relay valve V with its associated resistances and batteries, etc.

The grid circuit of this valve can be closed by means of the switch S_2 and the ring switch on the bar (see figure 1), connected in series with each other and with the grid battery B_2 across the resistance R_3; the function of R_3 is to earth the grid of V when S_2 or the ring switch are open, whilst R_4 prevents excessive grid current when V is in the conducting state. The anode circuit of the valve can be opened or closed by means of the switch S_1.

The e.m.f.'s of the anode battery B_1 and the grid battery B_2 are adjusted so that (1) the valve is non-conducting when the grid circuit is closed before the anode circuit, and (2) with S_1 closed, the valve becomes conducting when the bias on the grid is removed by breaking the grid circuit either by opening S_2 or the ring switch. Thus, after the valve has been 'set' by closing the grid circuit before the anode circuit, the current in the anode circuit of the valve and in the winding L_1 of the transformer begins to flow almost immediately, when the ring switch or S_2 is broken. Once the anode current is started, the grid loses control and the sweep will therefore be completed irrespective of what happens in the grid circuit; this feature is very useful because it makes the sweep independent of events such as 'chattering', which may occur at the ring switch after the initial break. The circuit must be reset each time the valve has become conducting.

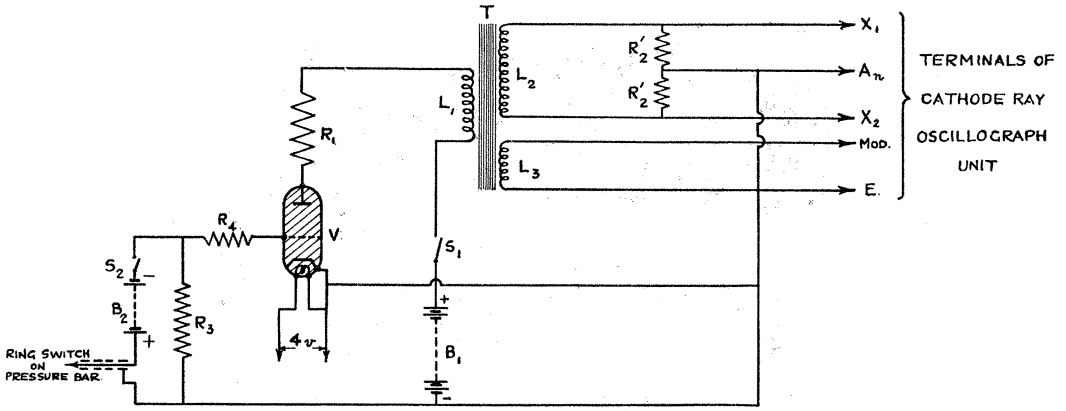

FIGURE 9. Circuit of sweep unit. V, Cossor G.D.T. 4B gas-filled relay valve. T, Pye mains transformer for television sets. L_1, 375–0–375 V secondary winding; inductance = 100 H; resistance = 200 Ω. L_2, 5000 V secondary winding; inductance = 500 H; resistance = 15,000 Ω. L_3, 200 V primary winding; inductance = 17 H; resistance = 12 Ω. E.m.f. of B_1 = 150–250 V; e.m.f. of B_2 = 12 V.

(I) For rapid sweep (working on forward stroke): $R_1 = 20{,}000\,\Omega$; $R_4 = 100\,\Omega$; $R_3 = 5000\,\Omega$; $R'_2 = 2\,\mathrm{M}\Omega$.

To eliminate return stroke.

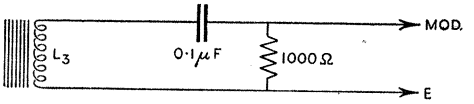

(II) For slow sweep (working on return stroke): $R_1 = 20{,}000\,\Omega$; $R_4 = 2000\,\Omega$; $R_3 = 10{,}000\,\Omega$; $R'_2 = 0{\cdot}5\,\mathrm{M}\Omega$.

To eliminate forward stroke.

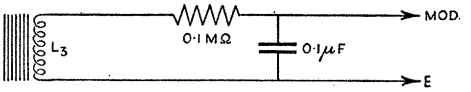

In order to preserve the focus of the spots of the c.r.o. when they traverse the screen, it is essential that the p.d.'s applied to the two X-plates should be symmetrical with respect to earth potential. To satisfy this condition the resistance connected across L_2 consists of two equal resistances R'_2 joined in series, with their common point earthed.

As stated in § 2, the horizontal traverse of the beam is normally timed relative to the vertical deflexion due to the output from the bar condenser by adjustment of the distance from the ring switch to the measuring end of the bar. An additional adjustment can be provided by connecting a condenser across the resistance R_3; if the values of this condenser and R_3, together with the e.m.f.'s of the batteries B_1 and B_2, are suitably chosen, then any desired delay can be introduced between the opening of S_2 or the ring switch and the firing of the relay valve.

The third winding, L_3, of the transformer T is used to apply an impulse to the modulating grid of the c.r.o.; this impulse is of the form shown in figure 8, and if its sign is correct it will intensify the beams during their traverse, thus allowing the intensity of the stationary spots or lines to be kept low and avoiding the destruction of the oscillograph screen and the fogging of the photographic plate.

When dealing with transient p.d.'s from the bar condenser which last only for times of order 20 to 40 μsec., the rapid forward stroke is used, and typical values of the resistances, etc., are given in figure 9. This figure also shows how a resistance-capacity filter, which is really one element of a high-pass filter, can be connected between L_3 and the modulating circuit of the c.r.o. in order to eliminate the major part of the slow return trace to avoid confusion of the record.

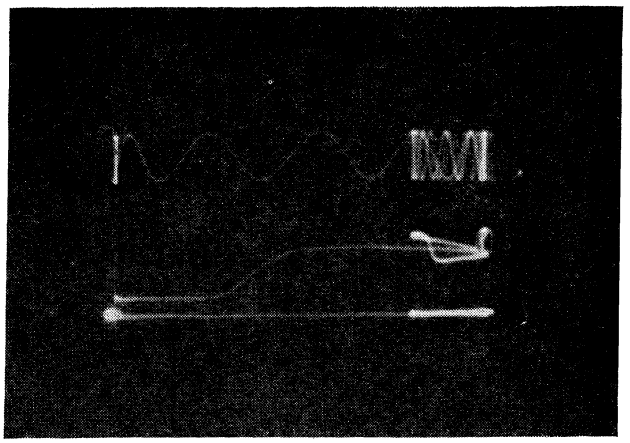

FIGURE 10. Oscillogram of a pulse due to the impact of a bullet. Pressure bar: length = 2 ft. 2 in., diameter = 1 in. Condenser unit: parallel-plate type. Velocity of bullet = 998 ft./sec. Upper trace: timing wave of period $40{\cdot}3_2$ μsec. Middle trace: amplified p.d. from condenser unit. Lower trace: datum line.

When the p.d. from the bar condenser lasts for a time of order 1 to 2 msec., the slow return stroke is used, and appropriate values of the resistances, etc., are given in figure 9. The elimination of the forward stroke is not very important in this case, since the writing speed on the forward stroke is very much greater than on the return stroke and the photographic intensity is therefore much less; furthermore, the undeflected forward stroke is useful in that it provides a datum line from which the vertical deflexion of the recording spot can be measured. If, however, it is necessary to eliminate the forward stroke, a resistance-capacity filter, which is virtually an element of a low-pass filter, can be inserted between L_3 and the modulating terminal of the c.r.o., as shown in figure 9.

In general, the speed of traverse is not constant; this is no disadvantage with a double-beam tube in which a timing trace is recorded simultaneously with the transient p.d. In practice the rapid forward stroke and the slow return stroke can be arranged so that they do not differ greatly from constant-speed strokes except at the ends, and by making a small correction for the deviation it is easy to find the time corresponding to any given abscissa on the record. With the values of the resistances, etc., given in figure 9, 1 msec. corresponds to about 15 cm. on the photographic plate in the case of the rapid sweep, and to about 1·5 cm. in the case of the slow sweep.

The photographs of figures 10 and 11 show the types of records obtained when working on the fast forward stroke and the slow return stroke respectively. In both photographs, the spots and the lines on the c.r.o. screen are initially at the left of the photographs, and, in fact, the initial positions of the spot and the line are visible in figure 10. In each case, the forward stroke is from left to right and the return stroke from right to left.

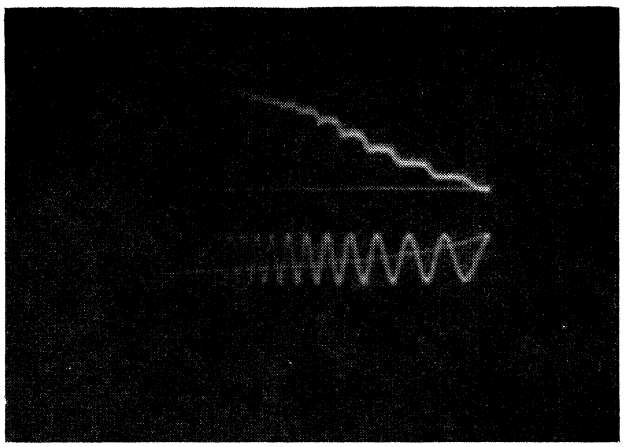

FIGURE 11. Oscillogram showing the discontinuous motion of the measuring end of a bar, caused by the impact of a steel ball on the pressure end. Pressure bar: length = 3 ft. $9\frac{1}{2}$ in., diameter = $1\frac{1}{2}$ in. Condenser unit: parallel-plate type. Upper trace: amplified p.d. from condenser unit. Lower trace: timing wave of period 435 μsec.

The photograph of figure 10 is an enlargement from a plate obtained in an experiment which was carried out to test the accuracy of the calibration experiments summarized in table 5·1 above; the results of this experiment are analyzed in § 9 below. The upper curve in the photograph is the timing wave whose frequency was $24{\cdot}8_0$ kcyc./sec. and whose period was therefore $40{\cdot}3_2\,\mu$sec. The middle curve is due to the amplified transient p.d. from the bar condenser which was a parallel-plate unit with the distance D equal to $0{\cdot}054_2$ cm. The pressure bar was 2 ft. 2 in. long and 1 in. in diameter; the stress pulse was produced by the normal impact of a 0·22 lead bullet, velocity 998 ft./sec., on the pressure end of the bar. The circuit shown in figure 9 was used to eliminate the return stroke, and, over the important part of the record, the forward traces are clear of the return traces.

The lower trace in figure 10 is a datum line from which the vertical deflexions, δ, on the condenser output trace were measured. This line was photographed separately after the two upper traces had been obtained. The oscillator setting was left undisturbed, and the region of the screen on which the timing trace would appear was blacked out; the lower spot was displaced on the screen by the X-shift control on the c.r.o. unit, so that it would not confuse the existing record when traversing the screen from its new initial position. The position of the photographic plate was kept unchanged, and the beams were swept across the screen by the switch S_2 of figure 9 when the camera shutter was open. With these adjustments, the path of the lower spot will be parallel to its undeviated path in a pressure measurement, except in so far as its motion is affected by coupling between the two beams of the oscillograph. The straightness of the lower trace in the photograph shows that the interaction between the two beams is negligibly small.

The maximum writing speed of the spot on the photographic plate in this record is about 12·5 km./sec. or 7·75 miles/sec.

In figure 11, the trace due to the transient p.d. from the bar condenser is above the timing trace, which in this instance has a period of 435 μsec. The length of the pressure bar used in this experiment was 3 ft. $9\frac{1}{2}$ in. and its diameter was $1\frac{1}{2}$ in.; a parallel-plate condenser unit was used, the distance D being about 1 mm. The impulse on the pressure end of the bar was produced by the impact of a steel ball, 2 in. diameter, suspended in pendulum fashion, and displaced and released so as to hit the centre of the pressure end of the bar normally. The forward stroke was not eliminated, and in the period covered by the return stroke the photograph shows the arrival at the measuring end of the first pulse, followed by a large number of pulses due to repeated reflexions at the pressure end of the bar. The vertical deflexion corresponding to the later pulses is less than that corresponding to the earlier ones on account of saturation of the amplifier, although this is partly offset by the increase in the sensitivity of the bar condenser as the distance D decreases when the measuring end jerks forward on the arrival of each pulse.

The velocity, c_0, of longitudinal elastic waves in the pressure bar can be estimated from this photograph; the time corresponding to the horizontal distance between two successive knees on the condenser record is approximately equal to the period of the timing wave; c_0 is therefore approximately

$$(2\times 3{\cdot}79)/(4{\cdot}35\times 10^{-4}) = 17{,}400\,\text{ft./sec.} = 5{\cdot}31\times 10^5\,\text{cm./sec.}$$

9. The calculation of experimental results

The results of the measurement of the plate corresponding to figure 10 and the calculation of ξ (see §§ 5, 7) and t are shown in the curve marked 'ξ (experiment)' in figure 12, the dots indicating the values which have been calculated from the readings of the measuring microscope. $\dot{\xi}$ is found by differentiating the (ξ, t) curve and p determined from equation (1·2) with $\rho c_0 = 4{\cdot}10\times 10^6$ g./sq.cm.sec.; the relationship between p and t obtained in this way is shown by the curve marked 'p (experiment)' in the figure.

To compare this (p, t) curve with theory, let l be the length of the pressure bar and A its area of cross-section; if the bullet is assumed to behave as a fluid, then the pressure p at a point just within the measuring end of the bar at time t, reckoned from the instant of arrival of the stress pulse at the measuring end, is

$$p = \rho_b U_b^2 A'/A, \tag{9·1}$$

where ρ_b = the density of the bullet = 11·34 g./c.c.; U_b = the velocity of the bullet; A' = the area of cross-section of the bullet in contact with the pressure end of the bar at time $(t-l/c_0)$.

The duration T' of the impact of the bullet is

$$T' = l_b/U_b, \tag{9·2}$$

where l_b is the length of the bullet.

The values of p and T' can thus be calculated from measurements of U_b, l_b and the radius of the bullet at different points along its length. In the experiment relating to figure 12, $U_b = 998$ ft./sec. $= 3{\cdot}04_2\times 10^4$ cm./sec., $l_b = 0{\cdot}87_7$ cm., and therefore $T' = 28{\cdot}8\,\mu$sec.; the

relationship between p and t, calculated from the size and shape of the bullet, assuming it to behave as a fluid, is shown in the broken-line curve labelled 'p (theoretical, fluid theory)' in figure 12. This curve is subject to large errors in its initial and final portions, i.e. in the regions corresponding to the nose and the tail of the bullet, because of the difficulty of accurate measurement of the dimensions of the bullet near the nose, and because of the presence of a ridge and a concavity near the tail.

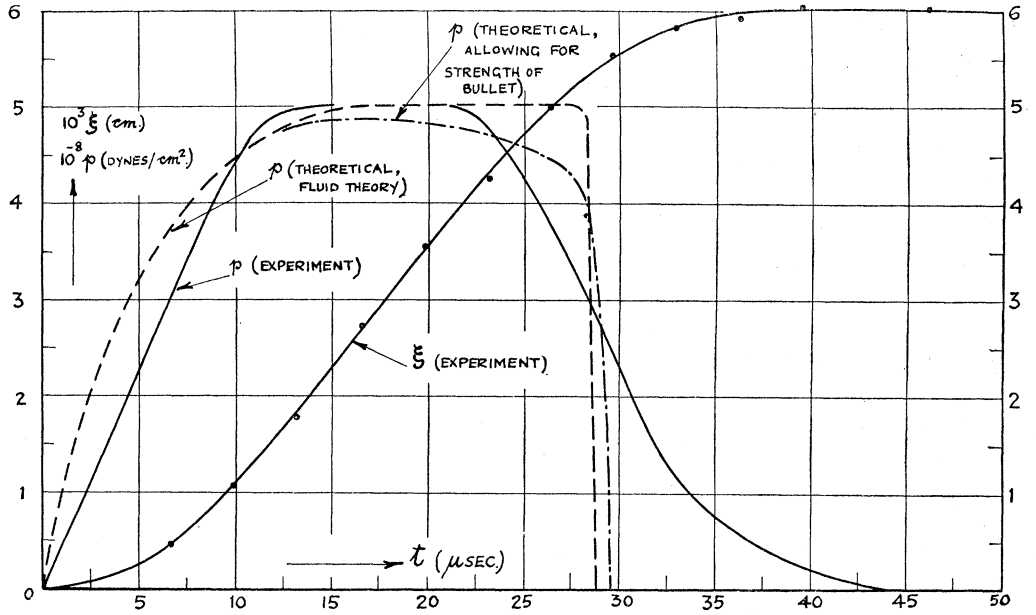

FIGURE 12. Analysis of the record shown in figure 10. t = time, reckoned from the instant of arrival of the pulse at the measuring end of the bar; p = pressure in the bar; ξ = displacement of measuring end of the bar.

Apart from this, the calculated (p, t) curve is in error because of the finite value of the yield stress of the material of the bullet; the value of this stress (reckoned as 'true stress') was found by experiment to be 2·1 tons/sq.in.

The effect of finite yield stress on the pressure due to the impact of a bullet has been considered by Hopkinson (1914), assuming that the stress system in the bullet is one-dimensional; calculations on the lines indicated in this paper show that during the first 10 μsec., the effect of the finite strength is too small to be shown in figure 12, and that the pressure is reduced in the later stages, the duration of the impact being increased by about 3 %. The calculated pressure, when allowance has been made for finite strength, is shown in figure 12 by the chain-dotted curve labelled 'p (theoretical, allowing for the strength of the bullet)', extending from $t = 11\,\mu$sec. to $t = 29{\cdot}6\,\mu$sec.

The diagram shows that the qualitative agreement between the theoretical and experimental (p, t) curves is rather better when the effect of the strength of the bullet is taken into account. There is still considerable discrepancy in the later stages of the impact, where the assumption that the stress system in the bullet is one-dimensional undoubtedly breaks down. This is clearly shown to be the case by examining the residue of the bullets after impact. In one experiment, with a bullet moving at 741 ft./sec., the weight of the residue was found to be about one-third of the weight of the bullet, whereas the theory used here shows that

the ratio should be 0·0014; the diameter of the residue was about 0·375 in. compared with 0·22 in. for the bullet. These facts indicate that Hopkinson's theory of the effect of the strength of a bullet on the force which it exerts needs modification in the light of recent work on the propagation of plastic waves.

The curves shown in figure 12 satisfy the momentum relationships, since the value of $\int p\,dt$ taken over the duration of the pulse is $12{\cdot}0\times10^3$ g./cm.sec. when evaluated from the experimental (p, t) curve and $11{\cdot}9\times10^3$ g./cm.sec. when evaluated from the theoretical (p, t) curve, after allowance has been made for the finite strength of the bullet. From equation (5·12a), the integral should be equal to $\frac{1}{2}\rho c_0\xi'$ which has here the value $12{\cdot}3\times10^3$ g./cm.sec.

Further discussion of the agreement between the theoretical and experimental (p, t) curves in figure 12 will be deferred until the more accurate theory of the pressure bar has been discussed in the next sections.

10. Introduction to a more accurate theory of the pressure bar

In order to discuss the accuracy of the method used in these experiments, it is necessary to examine in greater detail the propagation of pulses in the cylindrical pressure bar, since the elementary result that such pulses are propagated without change of form with constant speed $c_0 = \sqrt{(E/\rho)}$ is only a first approximation which cannot be expected to hold when the variations in pressure occur in times which are of the order of the time taken by a stress wave to traverse distances equal to the diameter of the bar, i.e. when the wave-lengths of the vibrations concerned in the propagation of the pulse are comparable with the lateral dimensions of the bar.

The exact equations of longitudinal vibrations of a circular cylinder, due originally to Pochhammer (1876) and to Chree (1889), are given by Love (1934, § 201).

These equations are very complex, but it is possible to deduce from them the phase and group velocities of sinusoidal waves in a bar of finite radius and to calculate the distribution of the stresses and displacements over the cross-section of the bar. Although it is possible, by using Kelvin's method of stationary phase, to obtain information about the periods of the dominant groups involved in the propagation of an infinitely intense disturbance concentrated initially in a very short length of the bar, it is difficult to use the equations to study, in a general way, the change in form of a pressure *pulse* as it travels along the bar. The values of the phase velocities derived from the exact equations can, however, be used in conjunction with Fourier's theorem to find the motion at various points in the bar due to any arbitrary *periodic* disturbance originating at a given point in the bar. These matters are discussed in § 11.

By using the form of the wave equation (due apparently to Love (1934, § 278)), which includes a term representing the effect of the lateral inertia, or the radial forces acting in the bar, it becomes possible to calculate the displacement at the measuring end of the bar due to the action on the pressure end of a force which rises instantaneously from zero to a finite constant value. The results of calculations based on this equation cannot be regarded as exact, but since they are more accurate than the simple theory they are useful in indicating

the order of magnitude, at any rate, of the effects of dispersion on the propagation of a pulse as distinct from a periodic disturbance. This problem is discussed in § 12, which also includes a comparison between theory and experiment.

11. The propagation of waves in a bar of infinite length according to the exact equations of Pochhammer and Chree

Considering a cylindrical bar of radius a, let the axis of the bar be taken as the axis of x and let r denote distances measured at right angles to Ox. Let c be the velocity of propagation of extensional sinusoidal waves of wave-length Λ and period T in the bar.

The main differences between the elementary theory and the exact general theory of Pochhammer and Chree are as follows: (1) According to the simple theory, the velocity of a sinusoidal wave is independent of Λ and is equal to c_0 $(= \sqrt{(E/\rho)})$; according to the general theory, c is determined by a, Λ, c_0 and σ, where σ is Poisson's ratio, and, in fact, (c/c_0) is a function of σ and (a/Λ), which is unity only in the limit when a/Λ is zero. Dispersion will therefore occur in the general case, and if an arbitrary disturbance, originating at $x = 0$, say, is resolved into its Fourier components, the relative phases of these components vary with the distance from the origin and the disturbance suffers distortion as it travels along the bar. (2) According to the simple theory, the longitudinal stress and displacement are uniform over the cross-section of the bar, the radial stress is everywhere zero and the radial displacement at distance r from the axis is $\sigma pr/E$. In the general case, the longitudinal stress and displacement vary over the cross-section of the bar, the radial stress is finite and the radial displacement does not follow the simple linear law.

The discussion which follows deals with the effects of these differences on the response of the various types of condenser units which can be used with the pressure bar.

The boundary conditions at free ends of a bar cannot be satisfied exactly in the general case (see Love 1934, § 201); to avoid this difficulty and, in addition, complications due to reflected waves, the length of the bar will be assumed to be infinite.

(*a*) *The phase and group velocities of sinusoidal waves in a bar*

The relation between c/c_0, σ and a/Λ can be expressed in terms of the roots of an equation (the frequency equation) involving Bessel functions, which can be derived from equation (54) on p. 289 of Love's book. This equation has multiple roots, and solutions were found for the first three roots differing from zero, assuming σ to be 0·29. A year or so after the completion of these calculations, a paper by Bancroft (1941) appeared on the same subject, and it is now unnecessary to give the details of the calculation. Bancroft's calculations refer to the lowest root of the frequency equation which differs from zero, and they are carried out for values of σ ranging from zero to one-half. The results obtained by interpolation to $\sigma = 0{\cdot}29$ between the values given by Bancroft for $\sigma = 0{\cdot}25$ and $\sigma = 0{\cdot}30$ agree with the present results, which are summarized in table 11·1 and shown graphically in figure 13.

The columns and the curves marked (1), (2) and (3) refer respectively to the first, second and third roots of the frequency equation differing from zero. The results are given in non-dimensional form, namely, c/c_0 as a function of a/Λ.

Since $\Lambda = cT$, $a/\Lambda = a/cT$, i.e. a/Λ is equal to the time taken by an extensional wave to traverse the radius of the bar divided by the period of the wave. Furthermore, $ac/\Lambda c_0$ is equal to a/Tc_0, so that, if the material of the bar is unchanged and its radius is multiplied by a factor ν, say, and the period of the wave is simultaneously multiplied by the same factor, a/Λ and c/c_0 remain unchanged, since $(ac/\Lambda c_0)$ is a function of σ and a/Λ only.

TABLE 11·1. VELOCITY OF SINUSOIDAL WAVES IN STEEL CYLINDERS ($\sigma = 0{\cdot}29$)

	a/Λ		
c/c_0	(1)	(2)	(3)
1·536	—	0·232	0·390
1·448	—	0·251	0·425
1·254	—	0·313	0·560
1·200	—	0·342	0·615
1·168	—	0·371	0·675
1·150	—	0·388	0·709
1·130	—	0·415	0·751
1·116	—	0·442	0·796
1·086	—	0·506	0·892
1·023	—	0·605	1·008
1·000	0·000	0·636	—
$0{\cdot}985_3$	0·1259	—	—
0·978	0·1505	—	—
0·958	0·1968	0·715	—
0·886	0·2875	0·846	1·345
0·809	0·3625	1·020	1·649
0·724	0·4550	1·395	2·242
0·687	0·5049	1·71	2·81
0·650	0·5868	—	—
0·627	—	5·61	9·84
0·600	0·8191	—	—
0·590	0·9355	—	—
0·580	$1{\cdot}1794_0$	—	—
0·579	$1{\cdot}2239_8$	—	—
0·578	$1{\cdot}2815_1$	—	—
0·577	$1{\cdot}3549_7$	—	—
0·576	$1{\cdot}4575_6$	—	—
0·575	$1{\cdot}6188_5$	—	—
0·574	$2{\cdot}0936_4$	—	—
0·5764	∞	—	—

Figure 13 also shows the values of the ratios c_1/c_0, c_2/c_0 and c_s/c_0, where c_1 is the velocity of the wave of dilatation in an infinite medium, c_2 the velocity of the wave of distortion in an infinite medium and c_s the velocity of the Rayleigh surface waves in a semi-infinite medium. In terms of σ

$$\frac{c_1^2}{c_0^2} = \frac{1-\sigma}{(1+\sigma)(1-2\sigma)}, \quad \frac{c_2^2}{c_0^2} = \frac{1}{2(1+\sigma)}. \tag{11·1}$$

As Bancroft has shown, the velocity corresponding to the first root of the frequency equation approaches the value c_s asymptotically as a/Λ becomes infinite.

The dotted curve (1 *a*) in figure 13 gives the relationship between c/c_0 and a/Λ when c is given by the formula derived from the wave equation used in the next section.

The curves (1), (2) and (3) in the diagram relate to different modes of vibration of the cylindrical bar. From the expressions given later for the longitudinal displacement at distance r from the axis of the bar, it can be shown that curve (1) (the first mode) corresponds

to vibration either without a nodal cylinder, or with one nodal cylinder, depending on the value of a/Λ; curve (2) (the second mode) corresponds to vibration with one or more nodal cylinders, and so on. The particular mode of vibration excited in any given instance depends on the initial conditions. Under the conditions which prevail in these experiments, it is unlikely that the vibrations of curves (2) and (3) are ever excited,* since they correspond to waves of extremely short periods and to forces applied over very small portions of the cross-section of the bar.

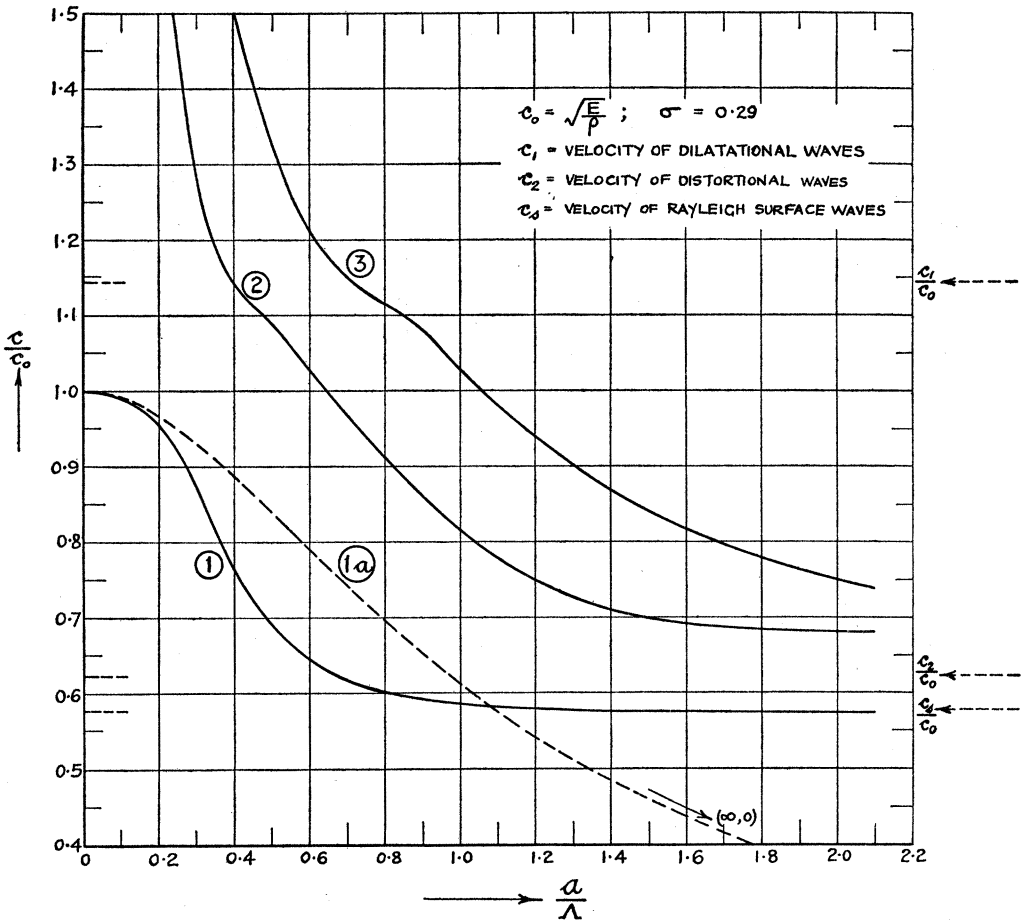

FIGURE 13. Phase velocity c of extensional waves of wave-length Λ in cylindrical bars of radius a.

The velocities c, c_0, c_1, c_2 and c_s are phase velocities, i.e. they give the velocity of transmission of surfaces of constant phase defined by the equation $2\pi(x-ct)/\Lambda = \text{constant}$. In dispersive media, the group velocity, i.e. the velocity of propagation of a wave packet consisting of waves whose wave-lengths do not differ greatly from a certain fixed value, is more important than the phase velocity, since, for example, the rate of transmission of energy is equal to the group velocity rather than the phase velocity. If c_g is the group velocity, then

$$c_g = c - \Lambda \frac{dc}{d\Lambda} \quad \text{or} \quad \frac{c_g}{c_0} = \frac{c}{c_0} + \frac{a}{\Lambda}\frac{d(c/c_0)}{d(a/\Lambda)}. \tag{11·2}$$

* This conclusion is supported by experiment (see the discussion on p. 427 in connexion with figure 23).

The values of c_g/c_0 for branches (1), (1*a*) and (2) of figure 13 have been calculated by differentiating the appropriate curves and using equation (11·2); the variation of c_g/c_0 with a/Λ is shown in figure 14. It is worth noticing that although the phase velocity in the second branch of figure 13 exceeds the velocity c_1 of the fastest possible wave in an infinite medium, the group velocity never exceeds c_0.

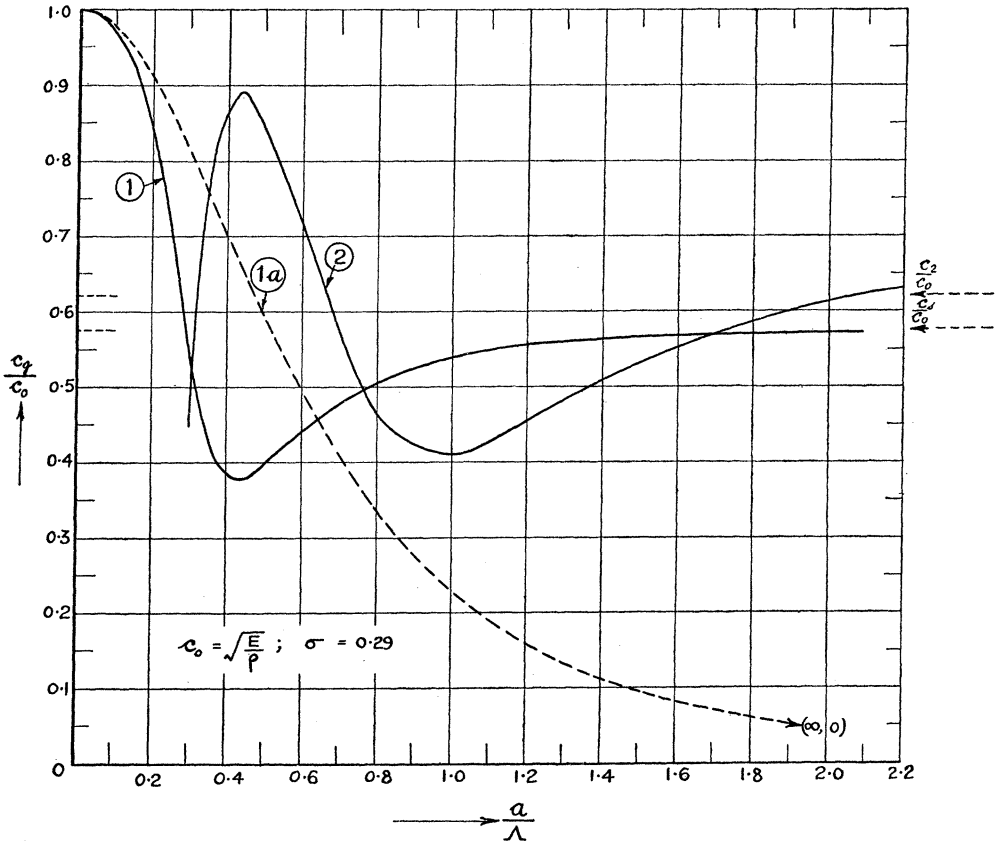

FIGURE 14. Group velocity, c_g, of extensional waves of wave-length Λ in cylindrical bars of radius a.

(*b*) *The propagation of a pulse according to the method of stationary phase*

Considering a bar of infinite length, let the axis of the bar be taken as the axis of x; let the bar be stressed initially so that the pressure is zero everywhere except at a certain cross-section, where it is infinite; take the origin of x at this cross-section. If this distribution of stress is released at time $t' = 0$, the stress at time t' at a cross-section of abscissa x can be derived by Kelvin's method of stationary phase, if certain conditions are fulfilled.

In this method, the initial distribution of stress is expressed as a Fourier integral, and it may be regarded as the superposition of the stresses due to an infinite number of trains of sinusoidal stress waves of equal amplitude, all of which agree in phase at the origin; at every other point in the bar, the various waves are out of phase, and, in the optical sense, they 'interfere' destructively, giving zero stress. At time t', the effect at a point abscissa x is obtained by summing the effects due to all the waves, supposing that each wave has travelled the distance ct'; in this way, phase differences are introduced between the various waves, and they interfere, so that the main effect is produced by a small group of waves whose

phase velocities, periods and wave-lengths are nearly equal, and which are in the same phase at x at time t'.

Let T_p be the mean period of the waves which coincide in phase at a point of abscissa x at the time t'; T_p may be termed the predominant period. The waves which reinforce each other at x at time t' must satisfy the condition that the phase, $2\pi(x-ct')/\Lambda$, is stationary, and this condition is easily shown to be equivalent to $x-c_g t' = 0$; from this equation and the curves given in figures 13 and 14, the value of T_p can be calculated. In representing the relationship between T_p, x and t' in non-dimensional form, it is convenient to plot T_p/T_a as ordinate and $t'/\frac{1}{2}T_0$ as abscissa, where $T_a = a/c_0$ and $\frac{1}{2}T_0 = x/c_0$, representing respectively the time taken by a stress wave of infinite wave-length to traverse the radius of the bar and the distance x.

Since
$$\frac{T_p}{T_a} = \frac{\Lambda}{a}\frac{c_0}{c} \quad \text{and} \quad \frac{t'}{\frac{1}{2}T_0} = \frac{x}{c_g}\frac{1}{\frac{1}{2}T_0} = \frac{c_0}{c_g},$$

the values of the non-dimensional variables can be found, and the $(T_p/T_a,\ t'/\frac{1}{2}T_0)$ curves derived from the curves marked (1), (1 a) and (2) in figures 13 and 14 are shown in figure 15; the curves for the various modes are labelled similarly in the three diagrams. Figure 15 also shows the values of a/Λ corresponding to various values of T_p/T_a for curve (1).

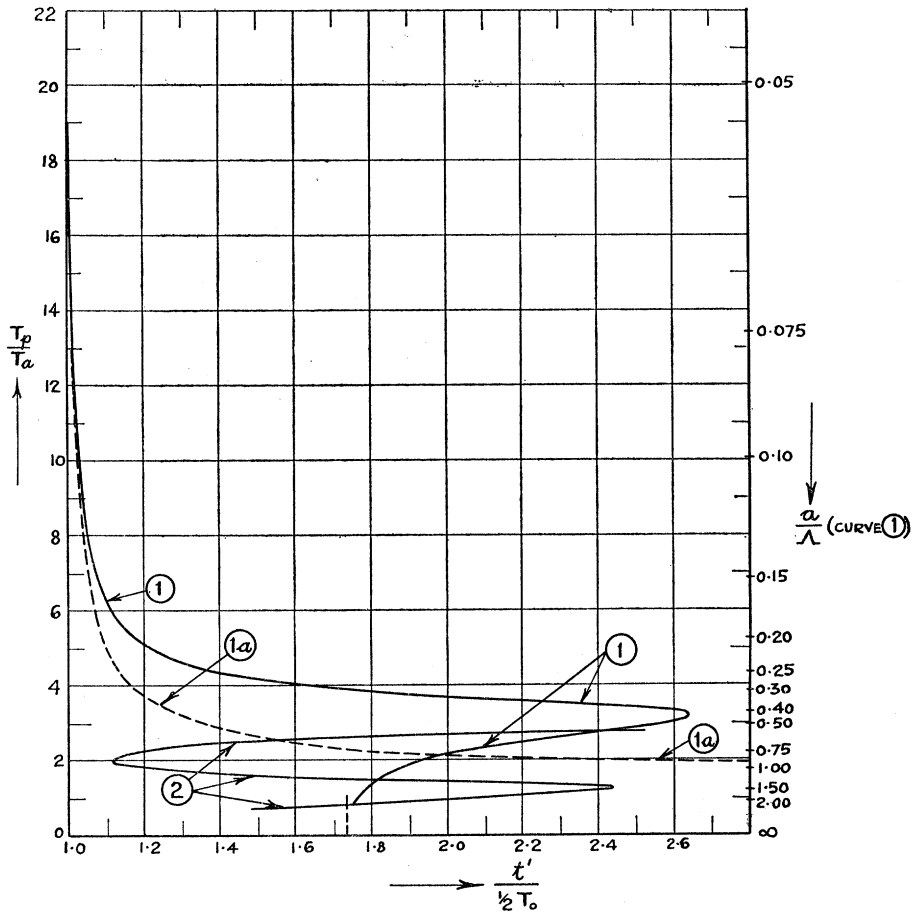

FIGURE 15. The period T_p of the dominant group in a bar of length l, radius a, at a point abscissa x, at time t' after the departure of an infinitely thin pulse from the origin. $T_a = a/c_0$; $\frac{1}{2}T_0 = x/c_0$.

The $(T_p/T_a, t'/\frac{1}{2}T_0)$ curves are useful for describing, in general terms, the motion at a point abscissa x in the bar when an infinite pressure of infinitely short duration, built up of stress waves of all possible wave-lengths, is released at the origin at time $t' = 0$. If dispersion were absent, all the waves would arrive simultaneously at the point at time $t' = \frac{1}{2}T_0$, giving an exact reproduction of the original pulse, whilst the $(T_p/T_a, t'/\frac{1}{2}T_0)$ curve would consist of a vertical straight line of abscissa unity, extending from $T_p/T_a = 0$ to $T_p/T_a = \infty$.

Considering only the vibrations represented by the first mode, the curve (1) in figure 15 extends from $t' = \frac{1}{2}T_0$ to $t' = 2{\cdot}64\,(\frac{1}{2}T_0)$, showing that a pulse propagated in this mode, originally of infinitely short duration, is distorted as it passes down the bar into a disturbance of duration $1{\cdot}64(\frac{1}{2}T_0)$. Since $\frac{1}{2}T_0 = x/c_0$, it is clear that the duration of the disturbance increases progressively with distance from the origin. The finite duration of the disturbance is clearly due to the fact that the $(c_g/c_0, a/\Lambda)$ curve of figure 14 shows a minimum which corresponds to a value of c_g/c_0 differing from zero.

As regards the sequence of events at a given point in a bar, it follows from curve (1) of figure 15 that when $t' = \frac{1}{2}T_0$, the dominant group at the point is composed of very long waves, all of which have travelled with the same velocity c_0. As t' increases, the values of T_p and a/Λ decrease, showing that the infinitely long waves are followed by shorter waves. We would therefore expect the (pressure, time) curve at a given point to consist of a pulse which may be regarded as a highly distorted form of the main pulse, followed by a tail consisting of oscillations of high frequency; since the waves mainly concerned in the propagation of sharp discontinuities have short wave-lengths, the infinitely sharp discontinuities present in the original pulse will be rounded off.

Considering the structure of the tail of the disturbance in greater detail, it will be noticed that T_p is a single-valued function of $t'/\frac{1}{2}T_0$ when t' lies between $\frac{1}{2}T_0$ and $1{\cdot}73_5(\frac{1}{2}T_0)$; in this region, there is therefore only one dominant group for a given value of t', and it follows from the curve that the period of the dominant group decreases progressively as t' increases. When t' exceeds $1{\cdot}73_5(\frac{1}{2}T_0)$, there are two possible values of T_p for each value of t', i.e. two dominant groups, differing in period and wave-length, arrive simultaneously at the point considered. In the limiting case of $t' = 1{\cdot}73_5(\frac{1}{2}T_0)$, the lower branch of the curve becomes practically a vertical straight line, implying that, at this instant, *all* the waves with periods less than about $0{\cdot}5T_a$ arrive simultaneously at the point considered; these waves, which include the Rayleigh surface waves, are accompanied by a dominant group of period $3{\cdot}9T_a$.

It follows that the portion of the tail immediately following the deformed main pulse consists of a sequence of high-frequency oscillations, approximately sinusoidal in form, whose frequency decreases rapidly at first, and then more slowly. The character of these oscillations suddenly changes when t' is about $1{\cdot}73_5(\frac{1}{2}T_0)$; from this point on, the oscillations become more complex in shape, since they are composed of two or more superposed oscillations, both of which vary in period as t' increases. The difference between the periods of the two constituent oscillations decreases as the end of the disturbance is approached, and furthermore the variation of these periods with t' is much slower; the oscillations should therefore become more regular towards the end.

So far discussion has centred only on the periods of the dominant groups. Provided that certain conditions are fulfilled, the Kelvin theory also enables one to estimate the magnitude of the pressure, and the relevant approximate formulae are given in the texts. In the present

notation, the condition for the validity of the approximate expressions (Lamb 1924, § 241) is the smallness of the ratio

$$\left\{\frac{1}{2\pi}\frac{a}{x}\frac{1}{t'/\frac{1}{2}T_0}\right\}^{\frac{1}{2}}\frac{d^2(c_g/c_0)}{d(a/\Lambda)^2}\Big/\left(\frac{d(c_g/c_0)}{d(a/\Lambda)}\right)^{\frac{3}{2}}.$$

Unfortunately, the values of the derivatives in this expression and the values of a/x and $t'/\frac{1}{2}T_0$ corresponding to the present experiments are such that the value of the ratio is usually so large that the approximate expressions for the magnitude of the pressure cease to hold.

It should be emphasized that the discussion given above refers to a disturbance which is initially of infinitely short duration. This case obviously cannot be realized in practice, but, by superposing the results of a number of disturbances of this simple type, it is possible to proceed to the case of a disturbance of finite initial duration.

(c) *The distortion of a periodic disturbance due to dispersion*

If a periodic disturbance of arbitrary form is supposed to act at the origin of x, it is possible from the curves of figure 13 to determine the distortion of this disturbance when it has travelled a distance x along the bar. For this purpose, the initial disturbance is decomposed into its Fourier components of frequencies $\omega_0/2\pi \ldots n\omega_0/2\pi$, where n is an integer and $\omega_0/2\pi$ is the frequency of the component of lowest frequency in the disturbance. The nth component will be of the form $\beta_n\left\{\begin{matrix}\sin\\ \cos\end{matrix}\right\}(n\omega_0 t'-\phi_n)$, where β_n is the amplitude, ϕ_n the phase angle, and t' the time reckoned from an instant at which the magnitude of the component at $x=0$ is $\beta_n\left\{\begin{matrix}\sin\\ \cos\end{matrix}\right\}(-\phi_n)$.

If c_n is the phase velocity of the nth component, and if damping is absent, the contribution of the nth component to the disturbance at distance x from the origin is

$$\beta_n\left\{\begin{matrix}\sin\\ \cos\end{matrix}\right\}\left[n\omega_0\left(t'-\frac{x}{c_n}\right)-\phi_n\right], \tag{11·3}$$

since x/c_n is the time taken by this component to travel the distance x.

In order to evaluate the terms (11·3), it becomes necessary to determine the values of c_n corresponding to the values of $n\omega_0$; now

$$\frac{a}{\Lambda}=\frac{an\omega_0}{2\pi c_n},$$

and therefore

$$\frac{an\omega_0}{c_0}=2\pi\frac{c_n}{c_0}\frac{a}{\Lambda}. \tag{11·4}$$

The quantities on the right of this equation can be evaluated from figure 13, and the curve showing the relationship between c_n/c_0 and $an\omega_0/c_0$ can therefore be plotted; from this curve the value of c_n corresponding to a given value of n can be determined when a and c_0 are given.

For a given value of t', the resultant displacement at the point abscissa x can now be found by evaluating and summing terms of type (11·3); from the nature of the case this sum must be found numerically, a sufficient number of terms being taken to ensure that no appreciable error is caused by the omission of the remaining terms of the infinite series.

For comparison with the type of pressure pulse which is transmitted along the bar in a pressure measurement, it will be assumed that the relation between $[u_{x0}]_0$, the displacement at $x = 0$ parallel to Ox (i.e. the longitudinal displacement) on the axis of the bar, and time t' is of the form shown in figure 16. The $([u_{x0}]_0, t')$ curve is trapezium-shaped; its amplitude is $[\hat{u}_{x0}]_0$, its period, represented by OE, is $2\pi/\omega_0$, and the duration of the inclined portions, AB and CD, is $2\pi s/\omega_0$. Figure 16 shows the (pressure, time) curve corresponding to figure 16*a*, assuming the relation $p = \rho c_0 v$ of the simple theory.

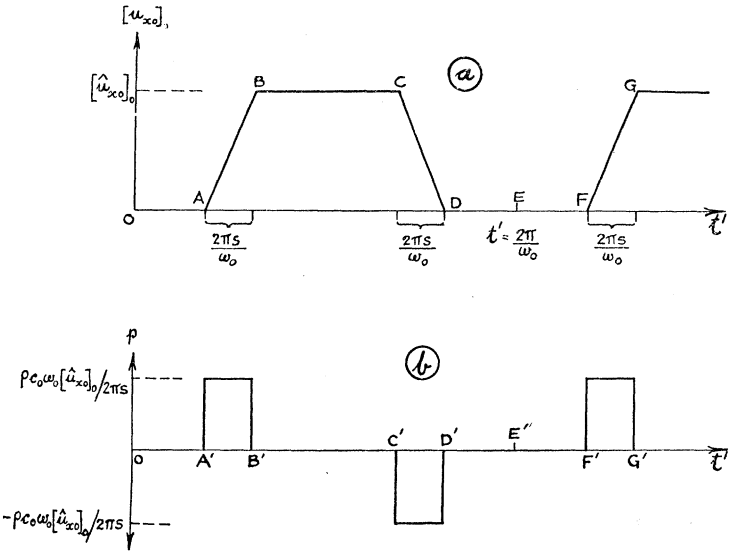

FIGURE 16. (*a*) Trapezium-shaped (displacement, time) curve.
$[u_{x0}]_0$ = displacement parallel to Ox on the axis of the bar at $x = 0$ at time t';
$[\hat{u}_{x0}]_0$ = maximum value of $[u_{x0}]_0$; $OE = 2\pi/\omega_0$ = period; $2\pi s/\omega_0$ = duration of rising and falling portions of the curve.
(*b*) (pressure, time) curve corresponding to (*a*); points A', B', ... correspond to A, B, ... in (*a*).

The Fourier expansion of the curve of figure 16*a* is

$$[u_{x0}]_0 = \tfrac{1}{2}[\hat{u}_{x0}]_0 - \frac{2[\hat{u}_{x0}]_0}{\pi^2 s} \sum_{n=1,\,3,\,5,\,\ldots} \frac{(-1)^{\frac{1}{2}(n-1)}}{n^2} \sin \pi n s \cos n\omega_0 t', \tag{11·5}$$

so that the phase angles ϕ_n in expression (11·3) are zero, whilst the amplitudes are given by the equation

$$\beta_n = \frac{2[\hat{u}_{x0}]_0}{\pi^2 s} \frac{(-1)^{\frac{1}{2}(n-1)}}{n^2} \sin \pi n s \quad (n = 1, 3, 5, \ldots). \tag{11·6}$$

It follows from equations (11·3), (11·5) and (11·6) that the displacement $[u_{x0}]_x$ parallel to Ox on the axis of the bar at a distance x from the origin is given by

$$[u_{x0}]_x = \tfrac{1}{2}[\hat{u}_{x0}]_0 - \frac{2[\hat{u}_{x0}]_0}{\pi^2 s} \sum_{n=1,\,3,\,5,\,\ldots} \frac{(-1)^{\frac{1}{2}(n-1)}}{n^2} \sin \pi n s \cos n\omega_0 \left(t' - \frac{x}{c_n}\right). \tag{11·7}$$

The value of $[u_{x0}]_x$ will clearly depend on the values of $[\hat{u}_{x0}]_0$, s, ω_0, x, a, t' and the elastic constants of the bar. Remembering that a/A and c/c_0 remain unchanged if the material of the bar remains the same and if the radius and the period of the wave are multiplied by the same factor ν, it follows from equation (11·7) that for a bar of given material, if all linear dimensions and all times are multiplied by the same factor ν, $[u_{x0}]_x/[\hat{u}_{x0}]_0$ will remain

unchanged. Thus, for example, $[u_{x0}]_x/[\hat{u}_{x0}]_0$ will be the same for two bars A and B if the radius of A is double the radius of B and if the distance x for bar A is double that for bar B, provided that the period of the displacement $[u_{x0}]_0$ and the value of s for bar A is double that for bar B.

Assuming $\sigma = 0{\cdot}29$ and $c_0 = 5 \times 10^5$ cm./sec., calculations have been carried out for $s = \frac{1}{20}, \frac{1}{10}$ and $\frac{1}{3}$ when

$$x = 200\,\text{cm.} = 6{\cdot}56\,\text{ft.}, \quad a = 0{\cdot}5\,\text{in.} = 1{\cdot}27\,\text{cm.}, \quad 2\pi/\omega_0 = 100\,\mu\text{sec.}$$

and for $s = \frac{1}{10}$ when

$$x = 600\,\text{cm.} = 19{\cdot}7\,\text{ft.}, \quad a = 1{\cdot}27\,\text{cm.}, \quad 2\pi/\omega_0 = 100\,\mu\text{sec.}$$

When $2\pi/\omega_0 = 100\,\mu$sec. and $s = \frac{1}{20}, \frac{1}{10}, \frac{1}{3}$, the duration of the inclined portions AB, CD of figure 15a is 5, 10 and $33\frac{1}{3}\,\mu$sec. respectively; when $x = 200$ and 600 cm., the times taken by waves propagated with velocity c_0 to travel the distance x are 400 and 1200 μsec. respectively. In each calculation, the summation in equation (11·7) was taken up to $n = 29$, and table 11·2, giving the values of $[u_{x0}]_0/[\hat{u}_{x0}]_0$ calculated with this limit from equation (11·5) for the points O and A in figure 16a, shows that the error due to the omission of the higher terms is not excessive even at the point A for $s = \frac{1}{20}$, where, as one would expect, the error is greatest.

TABLE 11·2. VALUES OF $[u_{x0}]_0/[\hat{u}_{x0}]_0$

	$s = \frac{1}{20}$	$s = \frac{1}{10}$	$s = \frac{1}{3}$
point O	0·0007	0·0011	0·0005
point A	0·0343	0·017	0·0047

The results of the calculations are shown in figures 17 and 18 in which t' is plotted as abscissa and $k'[u_{x0}]_x/[\hat{u}_{x0}]_0$, where k' is a constant, as ordinate; each diagram covers a complete period and the points actually calculated are marked in the diagrams. The diagrams also show the (displacement, time) curve for a distortionless bar, i.e. one in which dispersion is absent.

Figure 17 shows how the (displacement, time) curve at a given distance from the origin changes when the period is kept constant and the parameter s is varied; in this diagram, the values of k' have been chosen so that the slope of the (displacement, time) curve for a distortionless bar is the same for the three values of s.

Figure 18 shows how the (displacement, time) curve changes when the distance from the origin is varied, the period and s being kept constant; the value of k' in this diagram is unity. The crosses surrounded by circles in figure 18 show the values of $[u_{x0}]_x/[\hat{u}_{x0}]_0$ calculated from equation (11·7), using terms up to $n = 29$ and assuming the absence of dispersion. The small deviation of these points from the curve for a distortionless bar shows that the large oscillations in the curves of figures 17 and 18 are really due to dispersion and not to errors of computation caused by the neglect of terms beyond $n = 29$ in the infinite series.

The chief features of the distortion shown by the curves in figures 17 and 18 are as follows:

(*a*) The sharp corners at A, B, C and D in figure 16 are rounded off.

(*b*) The straight portions OA, AB, BC, CD and DE of figure 16 become oscillatory curves.

(*c*) Corresponding to the inclined portions AB, CD of figure 16, the distorted curves show regions in which the relation between displacement and time is approximately linear. As the curve $s = \frac{1}{3}$ in figure 17 shows very clearly, in these regions the distorted curve oscillates

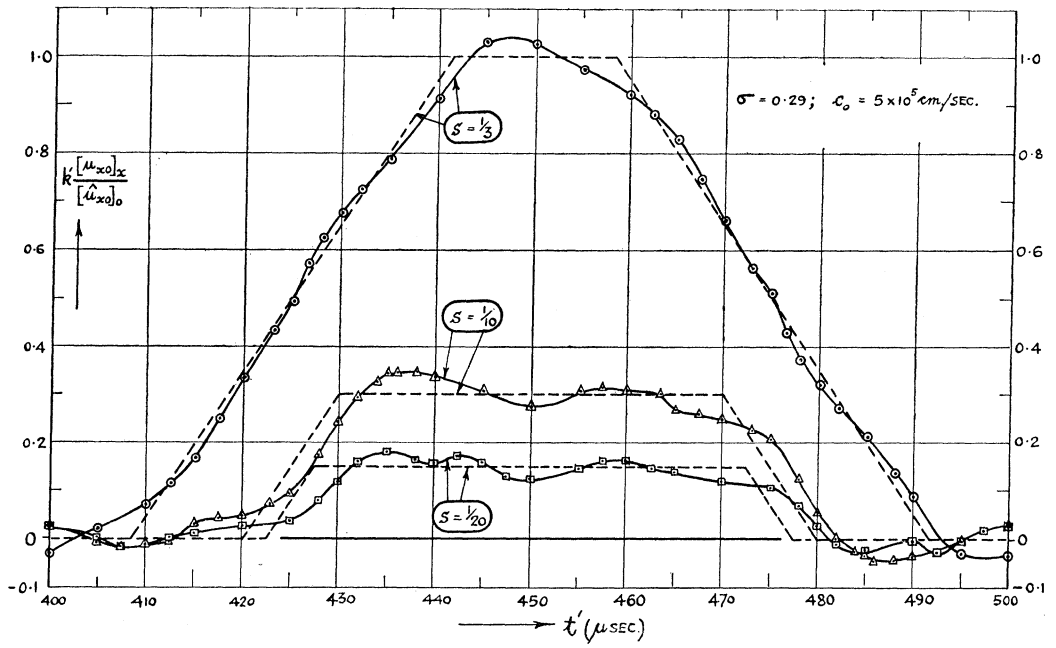

FIGURE 17. The longitudinal displacement $[u_{x0}]_x$ on axis of bar, at a distance $x = 200$ cm. from the origin, due to the trapezium-shaped wave of figure 16 acting at $x = 0$. Broken lines: distortionless bar. Full lines: allowing for dispersion. Period: 100 μsec. Radius of bar = 1·27 cm.

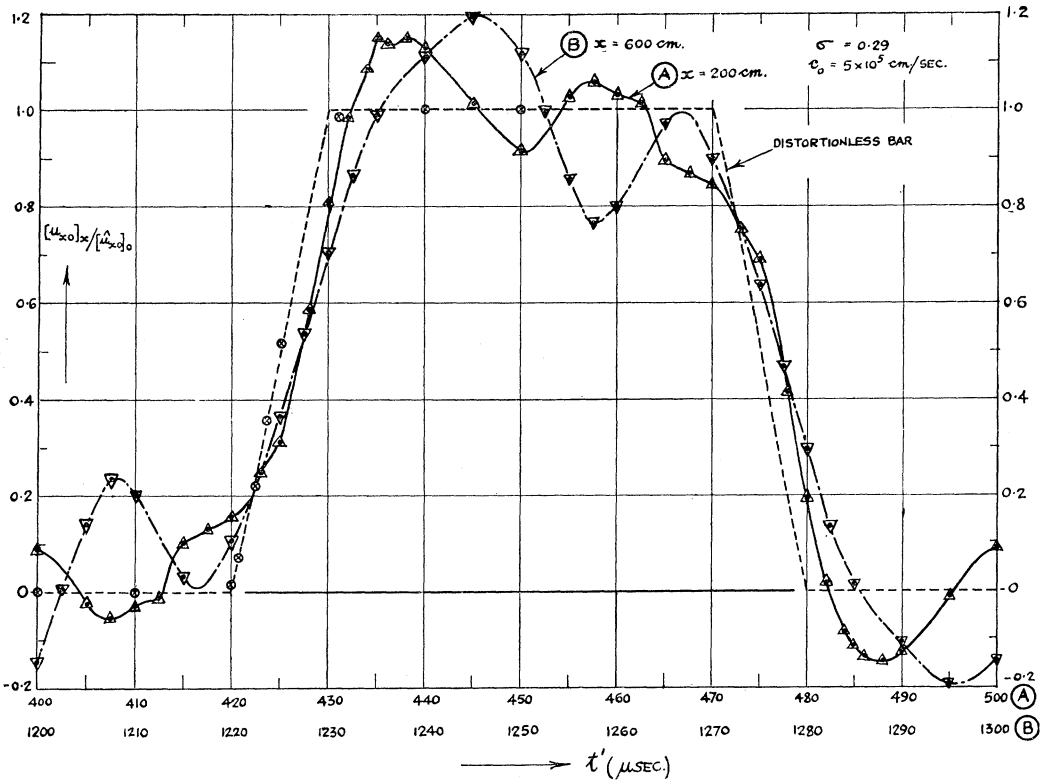

FIGURE 18. The longitudinal displacement $[u_{x0}]_x$ on the axis of the bar, at distances of 200 cm. (curve A) and 600 cm. (curve B) from the origin, due to the trapezium-shaped wave of figure 16 acting at $x = 0$. $s = \frac{1}{10}$. Period = 100 μsec. Radius of bar = 1·27 cm. Broken line: distortionless bar. Full lines: allowing for dispersion. ⊗ values calculated for distortionless bar from equation (11·7) with $n = 29$.

about a straight line whose slope is approximately the same as that of the undistorted curve. The ratio of the slope of the straight line of closest fit drawn through the points of the distorted curve, where it is approximately linear, to the slope of the inclined portion of the undistorted curve gives an idea of the error in the value of the pressure when it is deduced from the (displacement, time) curve by differentiation and calculation using equation (1·2). The values of this ratio are given in table 11·3. As far as they go, these figures show that results derived in this way can be considerably in error, and that the error appears to increase as x increases when s and other quantities remain constant.

TABLE 11·3

	$x = 200$ cm.			$x = 600$ cm.
s	$\frac{1}{20}$	$\frac{1}{10}$	$\frac{1}{3}$	$\frac{1}{10}$
ratio of slopes	$0{\cdot}67_7$	$1{\cdot}00_4$	$1{\cdot}06_4$	0·665

It is worth while noticing that the approximately linear portions of the distorted (displacement, time) curves are shifted horizontally relative to the inclined portions of the undistorted curves. This implies that the mean velocity of propagation of the disturbance is decreased by dispersion, as one would expect from the curves of figures 13 and 14; the decrease amounts to about 1 % for the curves $s = \frac{1}{20}$ and 0·5 % for the curve $s = \frac{1}{10}$ in figure 17.

Comparing the curve $s = \frac{1}{3}$ of figure 17 with curve A of figure 18, it is clear that the distortion increases when s decreases, other quantities remaining constant; comparing curves A and B in figure 18, it is seen that the distortion increases as x increases, when the remaining variables are unchanged. Thus, to minimize the distortion due to dispersion, it is advisable to use a pressure bar whose radius and length are as small as possible.

These general conclusions agree with those derived from the investigation of the propagation of a pulse (see § 12), and they are confirmed by experiments to be described later.

(*d*) *The variation of stress and displacement over the cross-section of the bar*

The non-uniformity of the longitudinal stress and displacement over the cross-section of the bar, the deviation of the radial displacement from the simple linear law, and the fact that the radial stress does not vanish have already been mentioned as results of the general theory of the vibrations of a cylinder. These results have an important bearing on the measurement of pressure by the condenser units used in this work, since the aim in all the experiments is to determine the average normal pressure over the cross-section of the bar.

When a parallel-plate condenser unit is used, it is the longitudinal displacement averaged over the measuring end of the bar that is measured, and the non-uniformity of longitudinal stress and displacement means in general that the ratio of the mean normal pressure to the mean longitudinal velocity will be a function of a/A and σ instead of being equal to ρc_0. In experiments with a cylindrical condenser unit placed so as to project over the measuring end of the bar, as described in § 4, the quantity measured is the longitudinal displacement at the surface of the bar; in this case, the ratio of mean normal pressure to the longitudinal velocity at the surface will only be equal to ρc_0 in the limiting case where a/A is zero. Finally,

a cylindrical unit placed on the bar itself, as indicated in § 1, measures the radial displacement at the cylindrical surface of the bar and in general the ratio of this displacement to the mean normal pressure will not be equal to $\sigma a/E$.

To determine the errors introduced into the measurements by these effects, it is first necessary to determine the radial displacement at the cylindrical surface of the bar and the distribution of longitudinal stress and displacement over the cross-section of the bar for various values of σ and a/Λ, and then to find the mean values of the stress and displacement over the cross-section of the bar. The necessary equations for these quantities are easily obtained from the relationships given by Love (1934), and the expression for the longitudinal displacement is in fact given by Bancroft (1941).

The differences between our notation and that used by Love and by Bancroft are shown in table 11·4. The remainder of the notation agrees with that used by Love and by Bancroft. No confusion need arise from the fact that γ, A and C are here used to denote respectively $2\pi/\Lambda$ and constants connected with the amplitude of vibration, whereas they have been used in preceding sections to denote change in capacity, area of cross-section and capacity.

TABLE 11·4

description	present work	Love	Bancroft
axis of the bar	Ox	Oz	Oz
frequency	$\omega/2\pi$	$p/2\pi$	$p/2\pi$
wave-length	$\Lambda = 2\pi/\gamma$	$2\pi/\gamma$	L
velocity of a wave	$c = \omega/\gamma$	p/γ	v
$\sqrt{(E/\rho)}$	c_0	—	v_0
diameter of bar	$2a$	$2a$	d
$(1-2\sigma)/(1-\sigma)$	S	—	β
$(1+\sigma)\,c^2/c_0^2$	Z	—	$\varkappa$
$\gamma(SZ-1)^{\frac{1}{2}}$	h	h'	h
$\gamma(2Z-1)^{\frac{1}{2}}$	κ	κ'	k

At time t', at the point (x, r), let u_x, u_r, $\widehat{xx}$, $\widehat{xr}$, $\widehat{rr}$* be the longitudinal displacement, the radial displacement, the longitudinal stress, the shearing stress, and the radial stress respectively. From equations (46), (53) and (54) and the equations immediately preceding equation (57) in § 201 of Love's book, it can be shown that

$$\widehat{xx} = -2\mu\gamma^2 A \frac{J_1(ha)}{ha} f_1 e^{i(\gamma x+\omega t')}, \tag{11·8}$$

$$u_x = i\gamma A \frac{J_1(ha)}{ha} f_2 e^{i(\gamma x+\omega t')}, \tag{11·9}$$

$$u_r = -\gamma A \frac{J_1(ha)}{ha} f_3 e^{i(\gamma x+\omega t')}, \tag{11·10}$$

$$\widehat{xr} = -2i\mu\gamma A h J_1(ha) f_4 e^{i(\gamma x+\omega t')}, \tag{11·11}$$

$$\widehat{rr} = 2\mu\gamma^2 A \frac{J_1(ha)}{ha} f_5 e^{i(\gamma x+\omega t')}, \tag{11·11b}$$

* The values of $\widehat{xr}$ and $\widehat{rr}$ are not required for determining the errors under discussion, but they have been calculated for one or two values of a/Λ as a matter of interest. It should be noted that the angular displacement u_θ and the stresses $\widehat{r\theta}$, $\widehat{x\theta}$ and $\widehat{\theta\theta}$ vanish everywhere.

where μ = the rigidity modulus of the material of the bar $= \frac{1}{2}E/(1+\sigma)$, A = a constant determined by the amplitude of vibration, and f_1, f_2, f_3, f_4 and f_5 are functions of σ, a/Λ and r/a determined by the equations

$$f_1 = (1+Z-SZ)\frac{haJ_0(hr)}{J_1(ha)} + \frac{(1-SZ)}{(Z-1)}\frac{\kappa a J_0(\kappa r)}{J_1(\kappa a)}, \tag{11·8a}$$

$$f_2 = \frac{haJ_0(hr)}{J_1(ha)} + \frac{(1-SZ)}{(Z-1)}\frac{\kappa a J_0(\kappa r)}{J_1(\kappa a)}, \tag{11·9a}$$

$$f_3 = (SZ-1)^{\frac{1}{2}}\frac{haJ_1(hr)}{J_1(ha)} - \frac{(1-SZ)}{(Z-1)}\frac{1}{(2Z-1)^{\frac{1}{2}}}\frac{\kappa a J_1(\kappa r)}{J_1(\kappa a)}, \tag{11·10a}$$

$$f_4 = \frac{J_1(hr)}{J_1(ha)} - \frac{J_1(\kappa r)}{J_1(\kappa a)}, \tag{11·11a}$$

$$f_5 = (1-Z)\,ha\frac{J_0(hr)}{J_1(ha)} + (SZ-1)\frac{a}{r}\frac{J_1(hr)}{J_1(ha)} + \frac{SZ-1}{1-Z}\kappa a\frac{J_0(\kappa r)}{J_1(\kappa a)} - \frac{SZ-1}{1-Z}\frac{a}{r}\frac{J_1(\kappa r)}{J_1(\kappa a)}. \tag{11·11c}$$

Equations (11·9) and (11·9a) for the longitudinal displacement agree (apart from a constant factor) with the equation given by Bancroft who points out in connexion with this particular case that the value of u_x is independent of the sign chosen in extracting the square root when evaluating h and κ and that the function f_2 cannot be complex. These considerations hold for all the above equations, and the fact that f_1, f_2, f_3, f_4 and f_5 cannot be complex means that each of the quantities $\widehat{xx}$, u_x, u_r, $\widehat{xr}$ and $\widehat{rr}$ must be in the same phase or in antiphase at any instant at all points on a cross-section of the bar.

In order to find the mean values $\overline{\widehat{xx}}$ and $\bar{u}_x$ of $\widehat{xx}$ and u_x over a cross-section of the bar for given values of σ and a/Λ it is necessary to calculate the values of f_1 and f_2 for different values of r/a and then find their mean values $\bar{f}_1, \bar{f}_2$. It is easy to see that

$$\bar{f}_1 = \frac{2}{a^2}\int_0^a r f_1\,dr = 2\int_0^1 \frac{r}{a} f_1\,d\left(\frac{r}{a}\right), \tag{11·12}$$

and similarly for $\bar{f}_2$. This equation, together with equations (11·8a) and (11·9a), gives

$$\bar{f}_1 = 2\left\{1+Z-SZ+\frac{1-SZ}{Z-1}\right\}, \quad \bar{f}_2 = 2\left\{1+\frac{1-SZ}{Z-1}\right\}. \tag{11·12a}$$

In considering the response of the various condenser units, it is convenient to form the quotients $\bar{\dot{u}}_x/\overline{\widehat{xx}}$, $\dot{u}_{xa}/\overline{\widehat{xx}}$ and $u_{ra}/a\overline{\widehat{xx}}$, where $\dot{u}_x = i\omega u_x$ = the particle velocity parallel to Ox, $\bar{\dot{u}}_x$ = the mean value of $\dot{u}_x$ over a cross-section, $\dot{u}_{xa}$ = the value of $\dot{u}_x$ at the cylindrical surface of the bar, u_{ra} = the radial displacement at the cylindrical surface.

From equations (11·8) to (11·11a), it can be shown that

$$\frac{E}{c_0}\frac{\bar{\dot{u}}_x}{\overline{\widehat{xx}}} = (1+\sigma)\frac{c}{c_0}\frac{\bar{f}_2}{\bar{f}_1} = \mu_p \quad \text{(say)}, \tag{11·13}$$

$$\frac{E}{c_0}\frac{\dot{u}_{xa}}{\overline{\widehat{xx}}} = (1+\sigma)\frac{c}{c_0}\frac{f_{2a}}{\bar{f}_1} = \mu_{ce} \quad \text{(say)}, \tag{11·14}$$

$$-\frac{E}{\sigma}\frac{u_{ra}}{a\overline{\widehat{xx}}} = -\frac{\Lambda}{2\pi a}\frac{1+\sigma}{\sigma}\frac{f_{3a}}{\bar{f}_1} = \mu_{cr} \quad \text{(say)}, \tag{11·15}$$

where f_{2a} and f_{3a} are the values of f_2 and f_3 when $r = a$.

It follows from the discussion given above that the value of $\bar{u}_x/\overline{\widehat{xx}}$ for a given value of a/Λ divided by its value when $c = c_0$, or $a/\Lambda = 0$ is a measure of the error which would occur if a parallel-plate condenser unit were used to determine the pressure when the bar is traversed by a sinusoidal stress wave corresponding to the assumed value of a/Λ. Similarly, the ratios of the values of $\bar{u}_{xa}/\overline{\widehat{xx}}$ and $u_{ra}/a\overline{\widehat{xx}}$ for given values of a/Λ to their values for $a/\Lambda = 0$ determine the errors in measurements of pressure made with cylindrical condenser units situated so as to measure the longitudinal and radial displacements respectively.

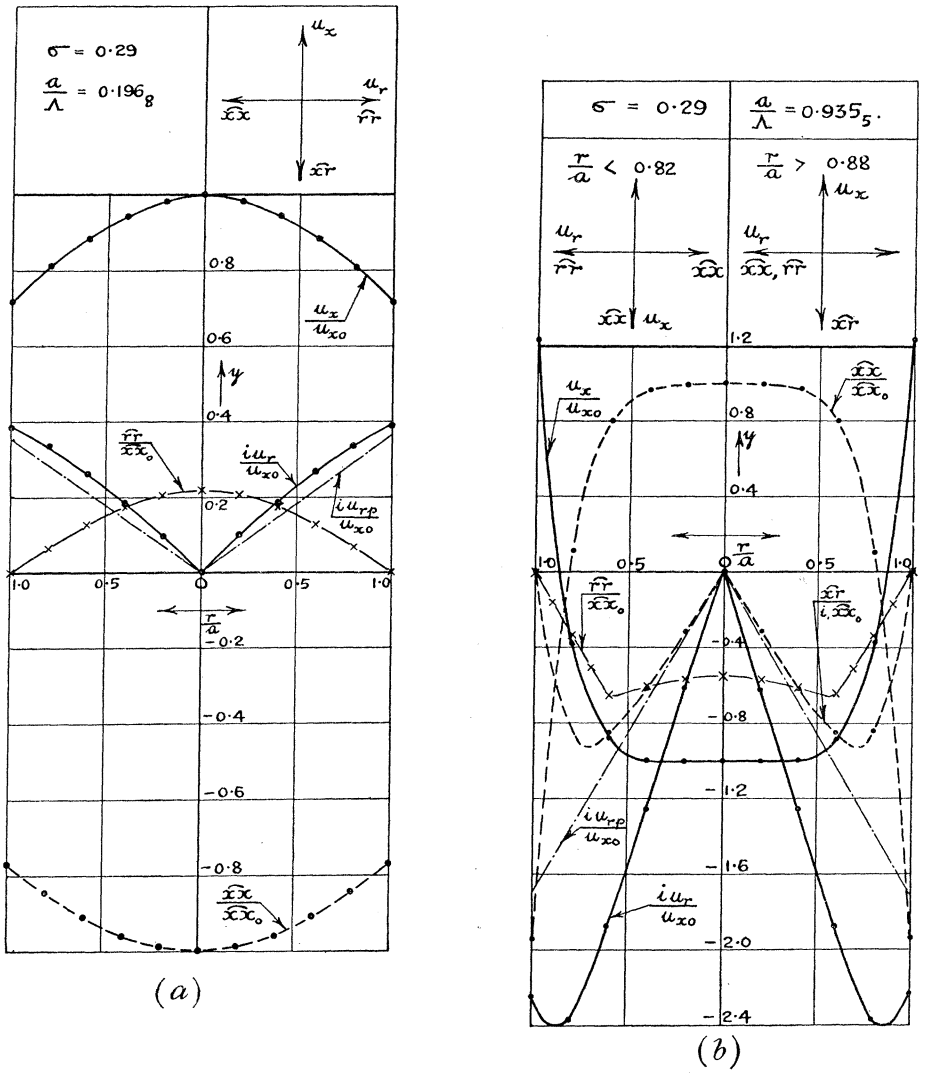

FIGURE 19. The variation of the displacements and the stresses over the cross-section of a bar of radius a. $\widehat{xx}$ = longitudinal stress; $\widehat{xr}$ = shearing stress; $\widehat{rr}$ = radial stress; u_x = longitudinal displacements; u_r = radial displacement; u_{rp} = radial displacement in distortionless bar.

When $a/\Lambda = 0$, it can be shown that the expressions in equations (11·13), (11·14) and (11·15) become equal to unity; from the curves connecting the quantities μ_p, μ_{ce}, μ_{cr} with a/Λ it will be possible to estimate the errors of the various types of condenser units when the pressure bar is traversed by sinusoidal waves.

The results of the numerical calculations are shown in figures 19, 20 and 21; as before, σ has been assumed to be 0·29.

Figures 19*a* and 19*b* show the variation of the stresses and displacements over the cross-section for two typical values of a/Λ, namely, $0{\cdot}196_8$ and $0{\cdot}935_5$. In each case, the ratio r/a is taken as abscissa, and the ratios $\pm\widehat{xx}/\widehat{xx}_0$, $\pm u_x/u_{x0}$, $\pm iu_r/u_{x0}$, $\pm\widehat{xr}/i\widehat{xx}_0$ and $\pm\widehat{rr}/\widehat{xx}_0$ are plotted as ordinates, the suffixes '0' indicating values at $r = 0$. The scale of the ordinates in the two diagrams differs by a factor 2.

Assuming the constant A to be positive, these ratios are taken with the plus sign when the displacements and stresses near the axis are of the form $+(Re)\,e^{i(\gamma x+\omega t')}$ or $+i(Re)\,e^{i(\gamma x+\omega t')}$, where (Re) denotes a positive real quantity, and with the minus sign when they are of the form $-(Re)\,e^{i(\gamma x+\omega t')}$ or $-i(Re)\,e^{i(\gamma x+\omega t')}$. Vector diagrams of the type used in a.c. theory are given in the figures to show the relative phases of the stresses and the displacements. When a/Λ is very small, the $(u_x/u_{x0}, r/a)$ and $(\widehat{xx}/\widehat{xx}_0, r/a)$ curves are horizontal straight lines of ordinates ± 1 respectively, $\widehat{xr}$ and $\widehat{rr}$ are everywhere zero, and if u_{rp} denotes the radial displacement, it is easily shown that

$$\frac{u_{rp}}{u_{x0}} = -2\pi i\sigma\frac{a}{\Lambda}\frac{r}{a}; \qquad (11{\cdot}16)$$

the curves $(iu_{rp}/u_{x0}, r/a)$ are shown in figures 18*a* and 18*b* by chain-dotted straight lines.

When $a/\Lambda = 0{\cdot}196_8$, the values of $\widehat{xx}$ and u_x decrease as r/a increases, whilst the values of iu_r/u_{x0} are greater than their values according to the simple theory; the maximum value of $\widehat{rr}$ is about one-fifth that of $\widehat{xx}$ and the shearing stress is small, the maximum value of the ratio $\widehat{xr}/i\widehat{xx}_0$ being about $-0{\cdot}007$.

Comparison of figures 19*a* and 19*b* brings out the change in the distribution of the stresses and displacements when a/Λ becomes large. At the cylindrical surface, the signs of $\widehat{xx}$ and u_x are the same in the two diagrams; when $a/\Lambda = 0{\cdot}935_5$, the signs change as r/a decreases from unity to zero, and in the case of u_x there is a nodal cylinder, over which the displacement vanishes, of radius $0{\cdot}85a$. Compared with the case of $a/\Lambda = 0{\cdot}196_8$, the radial displacement is much greater and its sign is reversed, whilst the radial and shearing stresses have become comparable with the longitudinal stress.

Figure 20 shows the variation with a/Λ of the ratio of the longitudinal displacements u_{xa} and u_{x0} at the cylindrical surface and the axis respectively. This ratio gradually decreases from unity as a/Λ increases from zero and it becomes zero at about $a/\Lambda = 0{\cdot}37_5$, corresponding to zero longitudinal displacement at the cylindrical surface. As a/Λ increases, u_{xa}/u_{x0} becomes negative and a nodal cylinder appears within the bar. When a/Λ is about 0·85, $u_{xa}/u_{x0} = -1$; beyond this point the displacement at $r = a$ is greater than the displacement at $r = 0$, and $|\,u_{xa}/u_{x0}\,|$ increases as a/Λ increases, as one would expect, since the waves degenerate into Rayleigh surface waves when a/Λ becomes large.

The $(u_x/u_{x0}, r/a)$ curves of figure 19 and the $(u_{xa}/u_{x0}, a/\Lambda)$ curve of figure 20 differ from those given by Bancroft for $\sigma = 0{\cdot}25$. Calculation shows that the difference is not due to the different values of σ assumed in the two cases, and since the equations (11·9) and (11·9*a*) agree with equation (6) in Bancroft's paper, the discrepancy is probably to be attributed to a numerical error in Bancroft's calculations.

The effect of the non-uniform distribution of stress and displacement on the response of the condenser units, when the bar is traversed by sinusoidal waves, can be seen from figure 21, which shows the functions $\mu_p, \mu_{ce}, \mu_{cr}$ defined in equations (11·13) to (11·15) plotted against a/Λ as abscissa. The values of a/Λ for which these functions were found are indicated in the diagram.

When a/Λ is small, the functions μ_p, μ_{ce}, μ_{cr} are each equal to unity, and all waves of unit amplitude traversing the bar produce equal response in the particular condenser unit which is used for a pressure measurement. Beyond the initial region, μ_p and μ_{cr} increase and μ_{ce} decreases as a/Λ increases. As the frequency of the waves increases, the response of the condenser units to waves of unit amplitude therefore increases when the unit is a parallel-plate unit or a cylindrical unit measuring radial displacements, and decreases when the unit is a cylindrical unit measuring longitudinal displacements; this is equivalent to a magnification of high frequencies relative to low frequencies in the former cases, and conversely in the latter case. When $a/\Lambda = 0{\cdot}37_5$, $\mu_{ce} = 0$, which is what one would expect from figure 20; when a/Λ exceeds $0{\cdot}37_5$, μ_{ce} becomes negative, i.e. the p.d. developed by the condenser unit changes sign. When a/Λ is greater than $0{\cdot}485$, μ_{ce} is negative and is numerically greater than unity; in this region, the reversal of sign is accompanied by magnification relative to low frequencies.

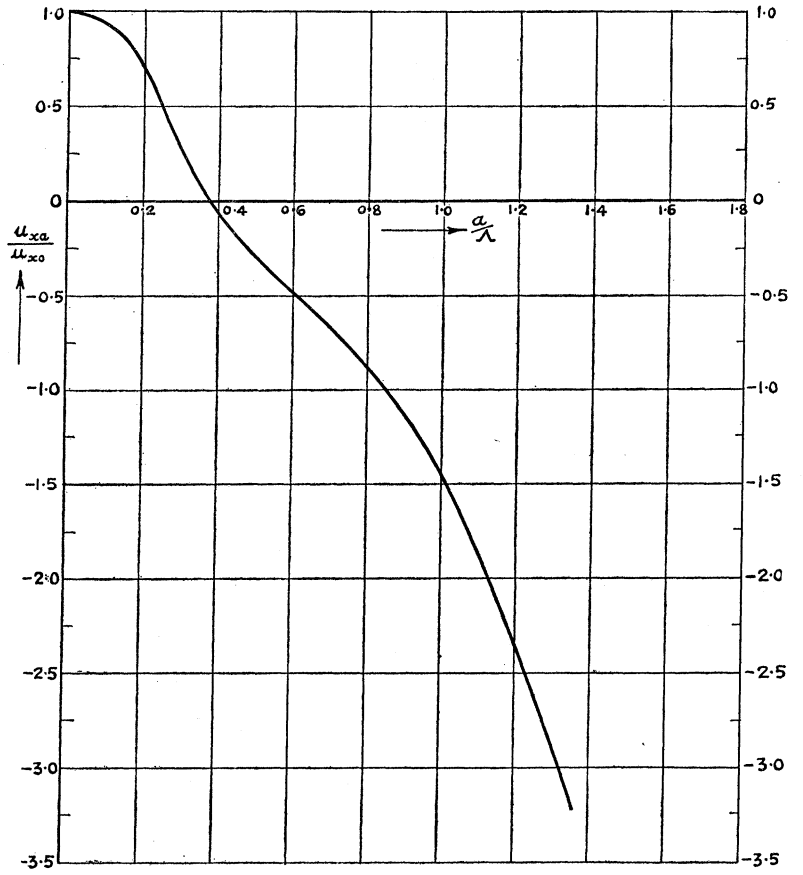

FIGURE 20. The longitudinal displacements u_{x0}, u_{xa} at the axis and at the cylindrical surface of a bar of radius a.

In the limit when a/Λ becomes infinite, $c/c_0 = 0{\cdot}5764_2$, $Z = 0{\cdot}4286_2$, $SZ = 0{\cdot}2535_5$. It is easily shown that in this limit, $\mu_p = 1{\cdot}734_8$, $\mu_{cr} = 9{\cdot}482_5$, $\mu_{ce} = -6{\cdot}587_6\, a/\Lambda$. These limiting values are indicated in figure 20 by the lines marked '$a/\Lambda \to \infty$'.

It is obvious that the parallel-plate unit is far superior to the two types of cylindrical condenser units in the range covered in figure 21. The reason for this is clear from figures

19*a* and 19*b*, where the $(u_x/u_{x0}, r/a)$ curves are seen to be similar in form to the $(\widehat{xx}/\widehat{xx}_0, r/a)$ curves; on the other hand, the values of u_{xa} and u_{ra} are noticeably different from their values when dispersion is absent.

An estimate of the error when the condenser units are used with a bar traversed by a non-sinusoidal wave involves a long calculation. In general, the magnitude of the error for any particular wave form will be determined by μ_p, μ_{ce}, μ_{cr} and the amplitudes and frequencies of the Fourier components of the wave, and since the functions μ_p, μ_{ce}, μ_{cr} refer to the quotient of particle velocity or gradient of displacement divided by stress, the relevant Fourier components are those of particle velocity rather than displacement.

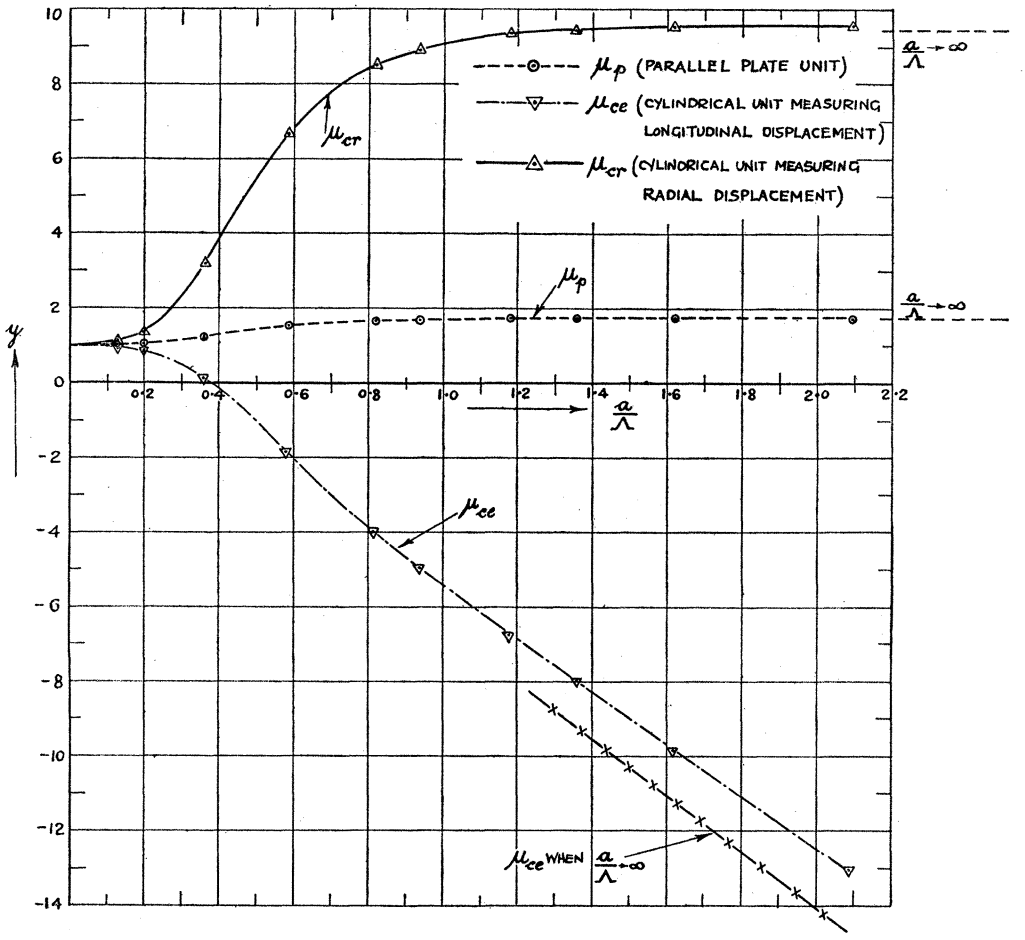

FIGURE 21. The behaviour of various types of condenser units with sinusoidal waves of wave-length Λ.

Qualitatively, with the parallel-plate unit and the cylindrical unit measuring radial displacements, one may anticipate that the effect of non-uniform distribution of stresses and displacements will be to magnify the high-frequency Fourier components relative to the low-frequency components; this will tend to increase an effect mentioned earlier, namely, the rounding-off of discontinuities and the superposition of oscillations on the linear portions of the waves. Considering a cylindrical unit measuring longitudinal displacements, the peculiar form of the $(\mu_{ce}, a/\Lambda)$ curve will lead to a very odd form of distortion, since the Fourier components for which a/Λ lies between 0 and $0{\cdot}37_5$ are partially or wholly cut off

and components for which a/Λ exceeds $0{\cdot}37_5$ are reversed in sign; in addition, the components for which a/Λ lies between $0{\cdot}37_5$ and $0{\cdot}485$ are again wholly or partially cut off, whilst those components for which a/Λ exceeds $0{\cdot}485$ are magnified.

As an example, consider the case of a wave in which the longitudinal displacement on the axis is trapezium-shaped, as shown in figure 16, with $s = \frac{1}{10}$ and $2\pi/\omega_0 = 100\,\mu$sec. If $\dot{\beta}_n$ be the amplitude of the nth Fourier component of the particle velocity, the contribution of this component to the response of a condenser unit will be proportional to $\mu_p\dot{\beta}_n$, $\mu_{ce}\dot{\beta}_n$ and $\mu_{cr}\dot{\beta}_n$ for a parallel-plate unit, a cylindrical unit measuring longitudinal displacement, and a cylindrical unit measuring radial displacement respectively. In the present case, it follows from equations (11·5) and (11·6) that

$$\dot{\beta}_n = \frac{2\omega_0[\hat{u}_{x0}]_0}{\pi^2 s}\,\frac{(-1)^{\frac{1}{2}(n-1)}}{n}\sin \pi n s \quad (n = 1, 3, 5, \ldots). \tag{11·17}$$

Table 11·5 gives the values of a/Λ, c/c_0, μ_p, μ_{ce}, μ_{cr}, $\pi^2 s\dot{\beta}_n/2[\hat{u}_{x0}]_0$ and $\pi^2 s\dot{\beta}_n/2\omega_0[\hat{u}_{x0}]_0$ for values of n up to 29.

The figures given in this table indicate that, in this particular case, the variation of stress and displacement over the cross-section will produce serious errors, especially with the two cylindrical condensers. For example, $\dot{\beta}_{29} = 0{\cdot}034\dot{\beta}_1$, whilst $\mu_p\dot{\beta}_{29} = 0{\cdot}06\dot{\beta}_1$, $\mu_{ce}\dot{\beta}_{29} = -0{\cdot}25\dot{\beta}_1$ and $\mu_{cr}\dot{\beta}_{29} = 0{\cdot}32\dot{\beta}_1$; the high magnification of the high-frequency components of the wave relative to the low-frequency components is obvious, and considerable caution must therefore be exercised in interpreting experimental results obtained with the cylindrical units.

TABLE 11·5. $\sigma = 0{\cdot}29$; $s = \frac{1}{10}$; $T = 100\,\mu$sec.; $a = 1{\cdot}27$ cm.; $x = 0$

n	a/Λ	c/c_0	μ_p	μ_{ce}	μ_{cr}	$\pi^2 s\dot{\beta}_n/2[\hat{u}_{x0}]_0$	$\pi^2 s\dot{\beta}_n/2\omega_0[\hat{u}_{x0}]_0$
1	0·0255	1·000	1·00	1·00	1·00	0·3090	0·3090
3	0·0766	0·995	1·00	0·99	1·06	−0·0899	−0·2697
5	0·1289	0·985	1·01	0·96	1·16	0·0400	0·2000
7	0·1852	0·962	1·04	0·88	1·32	−0·0165	−0·1155
9	0·2440	0·925	1·10	0·72	1·70	0·00382	0·0344
11	0·3350	0·836	1·20	0·29	2·80	0·00203	0·0223
13	0·4577	0·721	1·39	−0·60	4·69	−0·00479	−0·0623
15	0·5896	0·646	1·56	−1·90	6·71	0·00444	0·0666
17	0·7022	0·616	1·61	−3·05	7·81	−0·00280	−0·0476
19	0·8019	0·602	1·63	−3·90	8·42	$0{\cdot}00085_6$	0·0163
21	0·8921	0·594	1·64	−4·60	8·79	−0·00070	−0·0147
23	0·9823	0·586	1·68	−5·32	9·03	−0·00153	−0·0352
25	1·069	0·583	1·70	−6·00	9·21	0·00160	0·0400
27	1·156	0·580	1·71	−6·53	9·32	−0·00111	−0·0300
29	1·244	0·577	1·72	−7·17	9·40	$0{\cdot}00036_7$	0·0106

The errors will clearly decrease as the sharpness of the discontinuities in the disturbance decreases, and while it may be necessary to use a parallel-plate unit with very sharp pulses, it may be possible to use one or other of the cylindrical units with pulses in which the rate of change of pressure with time is not too large. For example, in some cases, it is very convenient to use a cylindrical condenser measuring radial displacements, since this type of unit measures the pressure rather than the longitudinal displacement; in other cases it may be convenient to use a cylindrical condenser measuring the longitudinal displacement at the end of the bar, since this type of unit possesses constant sensitivity even when dealing with large longitudinal displacements.

These considerations may be illustrated by the three photographs shown in figure 22, for which I am indebted to Dr E. Volterra; these records were taken with a cylindrical unit which measured the radial displacement on a pressure bar, 6 ft. long and 1 in. diameter.

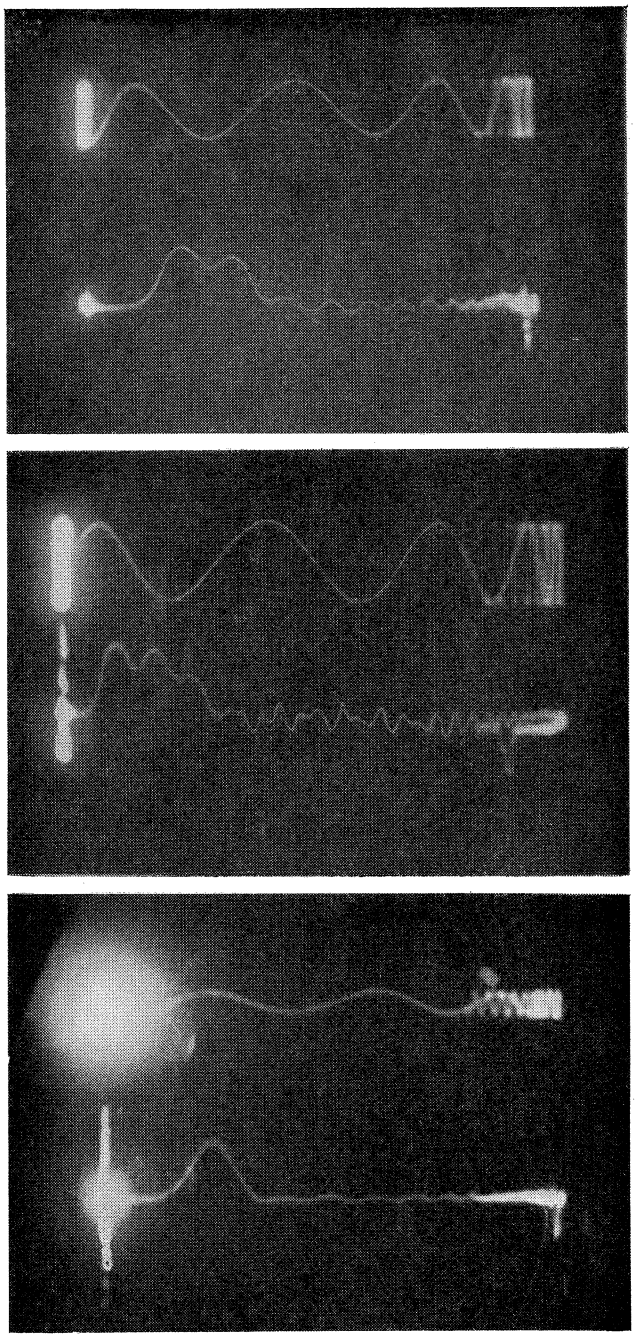

FIGURE 22. Oscillograms of pulses due to the impact of bullets. Pressure bar: length = 6 ft., diameter = 1 in. Condenser unit: cylindrical type, measuring radial displacement. Period of timing wave = 46·5 μsec.

	(*a*)	(*b*)	(*c*)
type of bullet	round-nosed	round-nosed	cone-shaped
velocity of bullet (ft./sec.)	1135	1171	1350
distance of condenser unit from pressure end of bar (cm.)	115	35	115

The difference between the internal radius of the insulated cylinder of the condenser unit and the radius of the bar was $\frac{1}{100}$ in. approximately, and the length of the insulated cylinder was 1·65 cm. The period of the timing wave was 46·5 μsec. In the experiments of figures 22*a* and 22*b*, the polarizing e.m.f., E_p of § 5, was 480 V, and in the experiment of figures 22*c*, 980 V; the values of the electrical components in the feed unit and in the amplifier were the same in the three experiments. The distance from the condenser unit to the pressure end of the bar was 115 cm. in the experiments of figures 22*a* and 22*c*, and 35 cm. in the experiment of figure 22*b*.

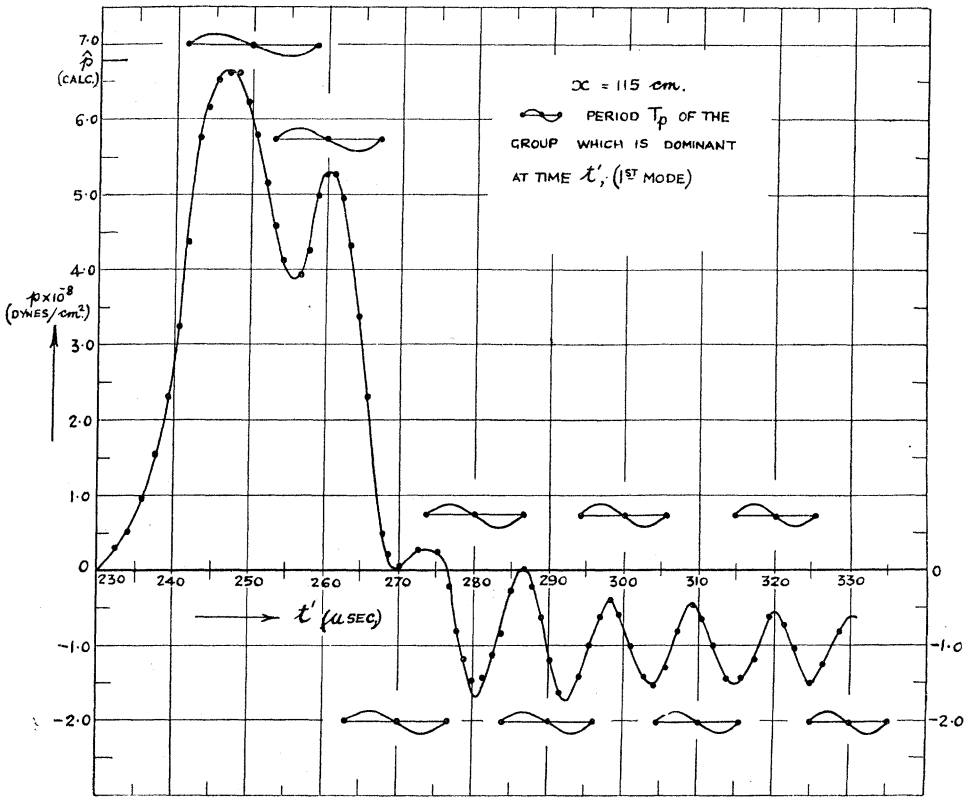

FIGURE 23. Analysis of the record shown in figure 22*a*.

Figures 22*a* and 22*b* show the radial displacement due to the impact of an ordinary round-nosed 0·22 lead bullet on the pressure end of the bar; the speed of the bullet was 1135 ft./sec. in figure 22*a* and 1171 ft./sec. in figure 22*b*. The (pressure, time) curves for these impacts are similar to the curve shown in figure 12; if a bullet moves with a speed equal to the average of the above speeds, and if the bullet behaves as a fluid, the time of impact is about 34 μsec., the maximum pressure in the bar is about $6{\cdot}8 \times 10^8$ dynes/sq.cm., and the time taken by the pressure to increase from zero to its maximum value is about 9 μsec.

The striking feature of these two photographs is the obvious distortion of the main pulse and the presence of a train of high-frequency oscillations following this pulse. It is clearly impossible to derive an accurate (pressure, time) curve from these records.

A full discussion of the distortion which appears when a parallel-plate unit is used with a similar pulse is given in § 12; in the meantime, comparison of figures 22*a* and 22*b* with figure 12 immediately brings out the fact that the slight oscillations of pressure which occur in the rising part of figure 12 (as shown by the periodic displacements of the experimental

points about the smoothed (ξ, t) curve) are very much smaller than the corresponding oscillations in figures 22*a* and 22*b*, whilst the high-frequency oscillations which follow the main pulse in the latter figures are absent from the former. This agrees with the conclusion reached above, and experiments to be described later (see figure 34) do in fact show that with a parallel-plate condenser unit, much sharper pulses are necessary to produce measurable amounts of high-frequency oscillations at the tail of the main pulse.

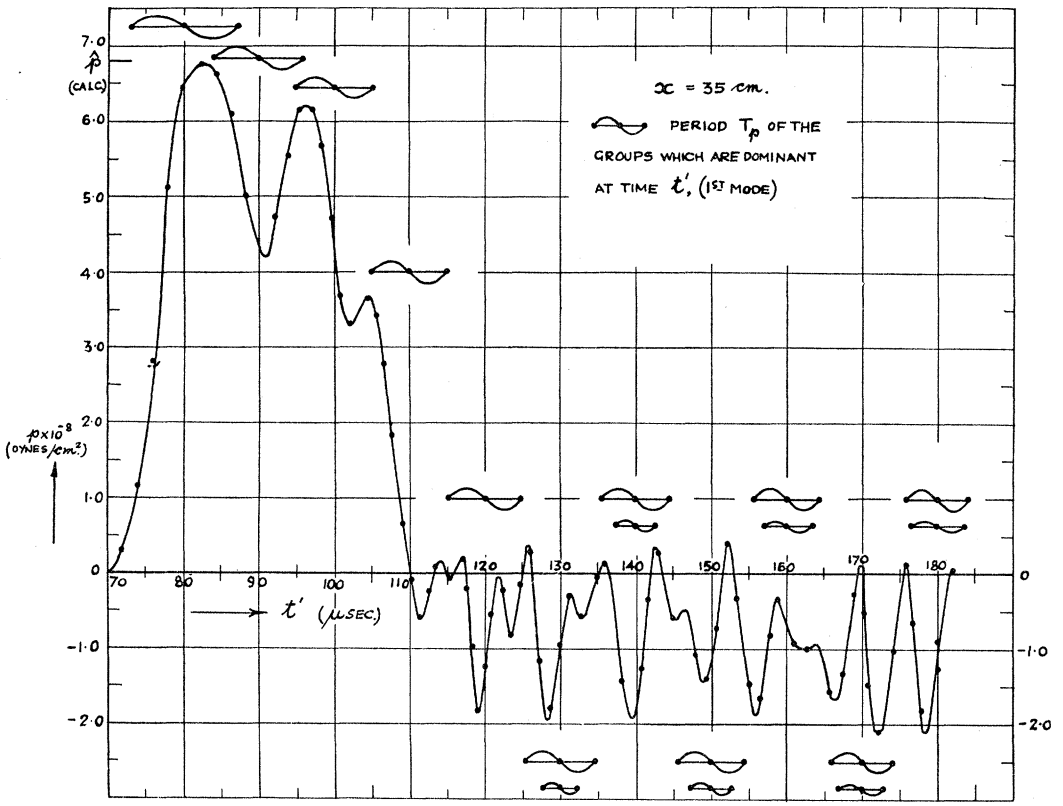

FIGURE 24. Analysis of the record shown in figure 22*b*.

It is interesting to consider the periods of the oscillations in the records shown in figures 22*a* and 22*b* from the standpoint of the method of stationary phase (see subsection (*b*) of this section). For this purpose, the analysis of the record of figure 22*a* is given in figure 23 and that of the record of figure 22*b* in figure 24. In these diagrams, time t', reckoned from the beginning of the impact of the bullet on the pressure end of the bar, is plotted as abscissa and pressure p, deduced by means of equations (1·3) and (A·1·4), is plotted as ordinate. The values of p and t' deduced from the readings of the measuring microscope are indicated by dots. The maximum pressure ($6{\cdot}8 \times 10^8$ dynes/sq.cm.) calculated from the speed of the bullet by equation (9·1) is shown in the diagrams by the short horizontal line marked 'p (calc.)' on the p-axis.

To a first approximation, the disturbance at a given point on the bar may be regarded as originating in a pulse of infinitely short duration, concentrated at the pressure end of the bar. With a pulse of finite duration, this assumption cannot be expected to be true for the values of t' corresponding to the main pulse, but it is a reasonably good approximation as far as the later stages of the record are concerned. On this assumption, the variation of

the period, T_p, of the dominant groups with time t', at $x = 35$ cm. and $x = 115$ cm., can be determined from the non-dimensional curves of figure 15, since $a = 1{\cdot}27$ cm. and $c_0 \simeq 5 \times 10^5$ cm./sec. The values of T_p corresponding to $x = 115$ cm. are shown in figure 25 in the curves marked '22 (*a*) (1st mode)' and '22 (*a*) (2nd mode)', derived respectively from curves (1) and (2) of figure 15. Figure 25 also shows the values of T_p corresponding to curves (1) and (2) of figure 15 for $x = 35$ cm.; these curves are marked '22 (*b*) (1st mode)' and '22 (*b*) (2nd mode)'. The values of T_p for the first mode are also shown diagrammatically in figures 23 and 24 by the small sine-curves placed at intervals of 10 μsec.; the length of these curves represents to scale the value of T_p for the value of t' corresponding to their mid-points.

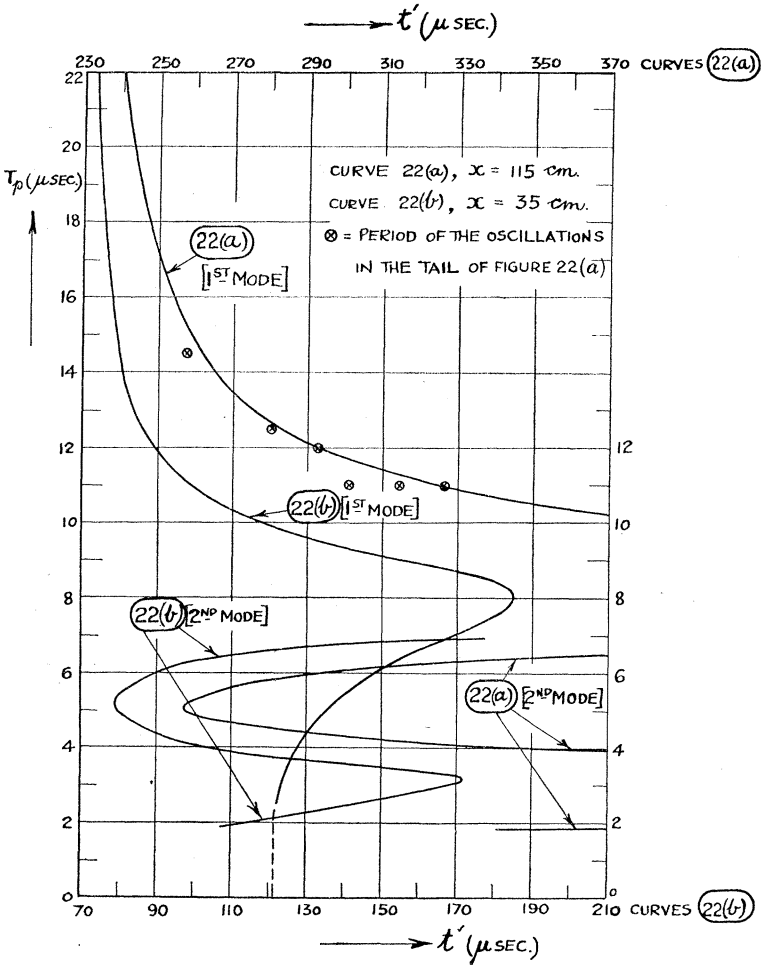

FIGURE 25. (T_p, t') curves for the records of figures 22*a* and 22*b*.
T_p = period of the groups which are dominant at time t'.

The values of t' included in the (p, t') curve of figure 23 range between $t' = 230$ μsec. and $t' = 330$ μsec. For vibrations of the first mode, the duration, at $x = 115$ cm., of a disturbance originating in an infinitely thin pulse at the pressure end of the bar is about $1{\cdot}64 \times 230 = 378$ μsec., whilst the duration of the impact of the bullet is about 35 μsec.; the duration of the disturbance, allowing for the finite time of impact of the bullet, is thus about 413 μsec. The curve of figure 23 would therefore have to extend to $t' = 643$ μsec. in order to include the whole of the disturbance, and, as figure 25 shows, the actual record in fact covers

only the main pulse and the initial stages of the tail, as far as vibrations in the first mode are concerned. The (T_p, t') curve (1st mode) will show two or more values of T_p for each value of t' when $t' \geqslant 1{\cdot}735 \times 230 \geqslant 399\,\mu$sec., so that the record stops short even of this point. It follows that if the vibrations excited by the bullet impact belong to the first mode, then the whole of the tail appearing in figure 23 should be composed of simple harmonic vibrations gradually decreasing in period from $15{\cdot}7\,\mu$sec. at $t' = 255\,\mu$sec. to $10{\cdot}5\,\mu$sec. at $t' = 350\,\mu$sec. If, however, the disturbance includes vibrations of the second mode, figure 25 shows that, when t' exceeds $256\,\mu$sec., two vibrations with periods ranging between 4·0 and $6{\cdot}4\,\mu$sec. will be superposed on the single vibration contributed by the first mode. In these circumstances, the resultant curve will show the sudden changes of slope which are characteristic of curves compounded of two or more vibrations which are varying in period and phase (see figure 24). There is no indication of this in the tail of figure 23, implying that if any vibrations of the second mode are present their amplitude is very small in comparison with those of the first mode. This conclusion is confirmed by the values of the periods of the oscillations in the later stages of the curve of figure 23; these values are shown in figure 25 by crosses in circles and the agreement between these points and the calculated (T_p, t') curve for the first mode is reasonably good. As far as this experiment is concerned, it may be concluded therefore that the waves excited by the impact of the bullet belong to the first mode of vibration.

Considering figure 24, the range of t' covered in the record extends from $t' = 70\,\mu$sec. to $t' = 182\,\mu$sec. The duration of the disturbance, allowing for the finite time of impact of the bullet, at the distance corresponding to the record (35 cm.) is about $155\,\mu$sec., assuming that the vibrations are of the first mode; the record would have to extend from $t' = 70\,\mu$sec. to $t' = 220\,\mu$sec. in order to contain the whole of the disturbance. The range of t' covered in figure 24 is thus a little less than the calculated duration of the disturbance, and, as figure 25 shows, the record should include the major portion of the high-frequency tail (1st mode), including that portion which consists of two or more superposed oscillations of different frequencies. The sudden, irregular changes of slope shown by the major part of the tail of the record of figure 24 agrees with this conclusion.* Although it is difficult to test matters quantitatively in this case, the sine-curves shown in the figure indicate that the periods of the oscillations at the end of the main pulse are in fair agreement with those deduced from figure 25.

Figure 22*c* shows a record of the radial displacement at a distance of 115 cm. from the pressure end of the bar, when the latter was hit by a lead bullet which had been machined so that the portion projecting from the cartridge case was in the form of a cone, 1 cm. axial length, and 32° vertical angle; the speed of the bullet was 1350 ft./sec. It is difficult to make an accurate estimate of the rate of rise of pressure and the maximum pressure in this case; in the initial stages, the bullet behaves as a fluid and the pressure increases parabolically with time; owing to the finite strength of the bullet, the parabolic law will later break down and ultimately the pressure will decrease. The maximum pressure will probably be reached when about 0·7 cm. of the bullet has been disintegrated and the maximum pressure in the bar is thus about 5×10^8 dynes/sq.cm. and it occurs about $17\,\mu$sec. after the beginning of the impact. In this experiment, the rate of rise of pressure is therefore much less than in the

* The regularity of the last two waves in the diagram is due to the small difference in the values of the periods of the two dominant groups in this region.

experiment corresponding to figures 22*a* and 22*b*, where the time to maximum pressure is about 9 μsec.

The record of figure 22*c* shows comparatively little trace of the oscillations which are so characteristic a feature of figures 22*a* and 22*b*; it therefore appears that the cylindrical unit measuring radial displacements can be used without excessive error due to oscillations, provided that the rate of rise of pressure does not greatly exceed that corresponding to figure 22*c*.

12. The propagation of a pulse in a bar of finite length according to Love's approximate wave equation

According to the simple theory, the differential equation for the longitudinal displacement, u_x, at a point abscissa x, at time t', in an extensional stress wave propagated in a bar is

$$\frac{\partial^2 u_x}{\partial t'^2} = \frac{E}{\rho}\frac{\partial^2 u_x}{\partial x^2} = c_0^2 \frac{\partial^2 u_x}{\partial x^2}. \tag{12·1}$$

Considering a bar of length l, let a constant force P per unit area be applied at time $t' = 0$ to the end $x = l$ (the pressure end) in the direction Ox, the other end, $x = 0$ (the measuring end) being free; it can be shown (Timoshenko 1929, p. 208) that the subsequent displacement at the point abscissa x at time t' is given by the equation

$$u_x = \frac{Pt'^2}{2m} + \frac{2Pl^2}{\pi^2 c_0^2 m}\sum_{n=1}^{n=\infty}\frac{(-1)^n}{n^2}\cos\frac{n\pi x}{l}\left(1-\cos\frac{n\pi c_0 t'}{l}\right) \quad (n = 1, 2, \ldots), \tag{12·2}$$

where m = mass per unit cross-sectional area of the bar.

The first term in this equation represents the displacement of the bar as a whole on account of the acceleration P/m due to the force P acting for time t', whilst the infinite series of the second term corresponds to the vibrations which are superposed on this motion. The contribution of the nth term in this series to u_x is equal to the displacement at the point x at time t' when a free-free bar of length l executes stationary longitudinal vibrations of period $2l/nc_0 = T_0/n$, where $T_0 = 2l/c_0$ is the period of vibration of the bar in its fundamental mode. The waves concerned in this vibration have velocity c_0 and wave-length $2l/n$.

From the solution (12·2) the effect of a pressure pulse in which the pressure applied at $x = l$ rises instantaneously from zero to a constant value P at time $t' = 0$ and falls instantaneously from P to zero at time $t' = T'$ can be found by superposing the solution for a pressure $-P$ applied at $t' = T'$ at $x = l$ on the solution given in equation (12·2). By considering the point $x = 0$, where $u_x = \xi$, it is easy to show that the solution obtained in this way agrees with the result which can be derived more directly from equation (1·2), and which is given with slightly differing notation in equation (A·1·1).

If the effect of the lateral inertia of the bar is taken into consideration, and if K is the radius of gyration of the cross-section of the bar about Ox, the wave equation takes the form given by Love (1934, § 278),

$$\frac{\partial^2 u_x}{\partial t'^2} - \sigma^2 K^2 \frac{\partial^4 u_x}{\partial x^2 \partial t'^2} = c_0^2 \frac{\partial^2 u_x}{\partial x^2}, \tag{12·3}$$

where the effect of the lateral inertia is represented by the second term on the left-hand side of the equation.

Since this section deals only with displacements parallel to Ox, the suffix in u_x may be dropped and the longitudinal displacements in the bar denoted by u.

Equation (12·3) may be written in the form

$$\frac{\partial^2 u}{\partial t'^2} - c_0^2\left(\frac{\partial^2 u}{\partial x^2} + H^2 \frac{\partial^4 u}{\partial x^2 \partial t'^2}\right) = 0, \tag{12·4}$$

where the parameter H, which is equal to $\sigma K/c_0$, is of the dimension of time.

This section is concerned with the derivation of the solution of equation (12·3) for the case of a uniform pressure P applied and sustained at the end $x = l$ of the bar, the end $x = 0$ being free; this solution, which is analogous to the solution (12·2) of the simple equation (12·1), is then extended to cover the case of a square-topped pressure pulse of duration T'. The section also includes a discussion of the bearing of the theory on the experimental results.

(*a*) *The phase and group velocities of sinusoidal waves*

For sinusoidal waves of unit amplitude, u will be of the form

$$u = e^{i(\gamma x + \omega t')}$$

in the notation of § 11; substituting in equation (12·3), it is easy to show that the phase velocity c of sinusoidal waves of wave-length Λ is given by the relationship

$$c^2 = c_0^2/(1 + 4\pi^2\sigma^2 K^2/\Lambda^2). \tag{12·5}$$

When the bar is a circular cylinder of radius a, $K^2 = \frac{1}{2}a^2$; neglecting terms of the fourth and higher powers in a/Λ, equation (12·5) agrees with the equation (Love 1934, § 201)

$$c = c_0(1 - \pi^2\sigma^2 a^2/\Lambda^2), \tag{12·5a}$$

which is derived from the Pochhammer-Chree theory as the second approximation for the phase velocity c.

From equation (11·2), the group velocity c_g corresponding to equation (12·5) is found to be

$$c_g = c_0/(1 + 4\pi^2\sigma^2 K^2/\Lambda^2)^{\frac{3}{2}}. \tag{12·6}$$

The $(c/c_0, a/\Lambda)$ and $(c_g/c_0, a/\Lambda)$ curves for a bar of circular cross-section, derived from equations (12·5) and (12·6), are given by the dotted curves labelled (1a) in figures 13 and 14 of §11. For small values of a/Λ, these curves agree, as they should, with the curves (1) which are derived from the accurate theory of §11. As a/Λ increases, the curves begin to differ, and when a/Λ becomes infinite, the values of c and c_g given by the accurate theory approach the velocity c_s asymptotically, whereas the values of c and c_g given by equations (12·5) and (12·6) tend to zero. Now when the phase and group velocities in a dispersive medium become zero for infinitely short wave-lengths, it can be shown (Havelock 1914, § 34) that if a discontinuity is possible at any point in the medium, it exists permanently at that point, i.e. the disturbance is propagated with infinite velocity from the source. In this respect the propagation of a pressure pulse in a bar, according to equation (12·3), is similar to the instantaneous propagation of a discontinuity in a deep liquid under gravity, where the phase and group velocities are proportional to $\sqrt{\Lambda}$.

In both cases the anomaly is due to the incompleteness of the theory on which the result is based. In the latter case the liquid is supposed to be incompressible; when the compressibility of the liquid is taken into account, a finite time elapses between the initiation of a disturbance and its appearance at a finite distance from the origin. Similarly, in the case of the bar, the anomaly would disappear if it were possible to use the accurate equations of § 11.

The method of stationary phase and figure 15 show that the solution derived from equation (12·3) will differ in other respects from the solution which would be given by the accurate theory. The $(T_p/T_a, t'/\frac{1}{2}T_0)$ curves deduced by the method of stationary phase are shown in figure 15, where the curves for the accurate and approximate theories (1st mode) are marked (1) and (1 *a*) respectively. It is clear from the curves that they give different values of T_p/T_a for the same value of $t'/\frac{1}{2}T_0$. Again, considering a point at a finite distance from the origin, as has been mentioned in § 11 (*b*), the disturbance represented by curve (1) is of finite duration, due to the fact that the $(c_g/c_0, a/\Lambda)$ curve shows a minimum at which c_g/c_0 differs from zero. In the case of curve (1 *a*), however, the disturbance is of infinite duration, due to the circumstance that, in this case, c_g/c_0 tends to zero as a/Λ becomes infinite.

These considerations indicate that the solutions derived from equation (12·3) will not be correct in all respects; nevertheless, the error in the main features of the results will probably be small if the important terms in the solution involve only values of a/Λ which lie in the region where the difference between the curves (1) and (1 *a*) in figures 13, 14 and 15 is small.

(*b*) *The displacement due to a sustained force acting on the pressure end of the bar*

Considering first the case of a constant pressure P applied at time $t' = 0$ to the end $x = l$ of the bar, in the direction Ox, a solution of equation (12·4) is required, subject to the following initial and boundary conditions:

(*a*) $u = \dfrac{\partial u}{\partial t'} = 0$, when $t' = 0$ and $0 \leqslant x \leqslant l$.

(*b*) $\dfrac{\partial u}{\partial x} = 0$, when $x = 0$, $t' \geqslant 0$.

(*c*) At the end $x = l$, the applied pressure P is equal to the elastic stress in the bar, i.e.

$$P = E\frac{\partial u}{\partial x}, \quad \text{when} \quad x = l, \ t' > 0.$$

The required solution can be obtained by the use of the Laplace transform (see, e.g., Carslaw & Jaeger 1941, chaps. 4, 5 and 7). In order to conform with the commonly accepted notation associated with the Laplace transform, it is necessary to use the symbols $\bar{u}$, p, γ, μ and M in the next few paragraphs to denote quantities different from those which they denote in the remainder of this report.

If p denotes here a positive number or a number whose real part is positive, then when equation (12·4) is multiplied by $e^{-pt'}dt'$ and integrated with respect to t' from 0 to infinity, the equation becomes an equation in $\bar{u}(p)$, the Laplace transform of u, defined by

$$\bar{u}(p) = \int_0^\infty e^{-pt'}u(t')\,dt'.$$

Since the initial displacements and velocities are zero, equation (12·4) becomes

$$p^2\bar{u}-c_0^2\frac{\partial^2\bar{u}}{\partial x^2}-c_0^2H^2p^2\frac{\partial^2\bar{u}}{\partial x^2}=0$$

or
$$\frac{\partial^2\bar{u}}{\partial x^2}-\frac{p^2\bar{u}}{c_0^2(1+H^2p^2)}=0. \tag{12·7}$$

The solution of this equation is

$$\bar{u}=N\sinh\frac{px}{c_0\sqrt{(1+H^2p^2)}}+N'\cosh\frac{px}{c_0\sqrt{(1+H^2p^2)}}, \tag{12·8}$$

where N and N' are constants to be determined from conditions (b) and (c) above. In terms of $\bar{u}$, these conditions become

$$x=0,\quad t'\geqslant 0,\quad \frac{\partial\bar{u}}{\partial x}=0;\qquad x=l,\quad t'>0,\quad \frac{\partial\bar{u}}{\partial x}=\frac{P}{p\bar{E}},$$

giving
$$N=0,\quad N'=\frac{Pc_0\sqrt{(1+H^2p^2)}}{p^2E}\Big/\sinh\frac{pl}{c_0\sqrt{(1+H^2p^2)}}.$$

Thus
$$\bar{u}=\frac{Pc_0\sqrt{(1+H^2p^2)}}{Ep^2}\frac{\cosh\dfrac{px}{c_0\sqrt{(1+H^2p^2)}}}{\sinh\dfrac{pl}{c_0\sqrt{(1+H^2p^2)}}}. \tag{12·9}$$

To determine u in terms of $\bar{u}$, we use the inversion theorem, namely, that if

$$\bar{u}(p)=\int_0^\infty e^{-pt'}u(t')\,dt'$$

and $|u(t')|$ is less than $Me^{\mu t'}$, where M and μ are positive constants, then

$$u(t')=\frac{1}{2\pi i}\lim_{w\to\infty}\int_{\gamma-iw}^{\gamma+iw}e^{\lambda t'}\bar{u}(\lambda)\,d\lambda,$$

where $\lambda=\gamma+iw$ is the complex variable, $\gamma>\mu$, and the integral is taken over a path in the complex plane of λ.

Thus, from equation (12·9),

$$u=\frac{Pc_0}{2\pi i\bar{E}}\int_{\gamma-i\infty}^{\gamma+i\infty}\frac{\sqrt{(1+H^2\lambda^2)}}{\lambda^2}e^{\lambda t'}\frac{\cosh\dfrac{\lambda x}{c_0\sqrt{(1+H^2\lambda^2)}}}{\sinh\dfrac{\lambda l}{c_0\sqrt{(1+H^2\lambda^2)}}}\,d\lambda. \tag{12·10}$$

The integrand is a single-valued function of λ with a triple pole at $\lambda=0$, and simple poles at the points determined by $\sinh[\lambda l/c_0\sqrt{(1+H^2\lambda^2)}]=0$, $\lambda\neq 0$, i.e. at the points given by

$$\lambda l/c_0=\pm n\pi i\sqrt{(1+H^2\lambda^2)}\quad(n=1,2,3,\ldots),$$

or
$$\lambda=\pm n\pi ic_0/\sqrt{(l^2+\pi^2H^2n^2c_0^2)}.$$

In addition, as $n\to\infty$, $\lambda\to\pm i/H$, i.e. the set of simple poles has two limit points which are essential singularities of the integrand.

Considering a suitable closed circuit in the complex plane in the usual way, the value of the integral in equation (12·10) can be shown, by Cauchy's theorem, to be equal to $2\pi i$

times the sum of the residues of the integrand at its poles; by excluding the two limit points by small circles and proceeding to the limit when these circles are infinitesimally small, it can be proved that the limit points make no contribution to the integral.

The residue at the pole $\lambda = 0$ is

$$\frac{c_0 t'^2}{2l} + \frac{x^2}{2lc_0} - \frac{l}{6c_0} + \frac{H^2 c_0}{l}.$$

The residue at the poles $\lambda = \pm n\pi i c_0/(l^2+\pi^2 n^2 H^2 c_0^2)^{\frac{1}{2}}$ is

$$-\frac{(-1)^n l}{\pi^2 n^2 c_0^2} \frac{l^2}{l^2+\pi^2 n^2 H^2 c_0^2} \cos\frac{n\pi x}{l} \exp\left[\pm n\pi i c_0 t'/\sqrt{(l^2+\pi^2 n^2 H^2 c_0^2)}\right].$$

The sum of the residues at the poles is thus

$$\frac{c_0 t'^2}{2l} + \frac{x^2}{2lc_0} - \frac{l}{6c_0} + \frac{H^2 c_0}{l} - \frac{2l}{\pi^2 c_0} \sum_{n=1}^{\infty} \frac{(-1)^n}{n^2} \frac{1}{1+n^2\psi^2} \cos\frac{n\pi x}{l} \cos\frac{n\pi c_0 t'}{l\sqrt{(1+n^2\psi^2)}},$$

where $\psi = \pi H c_0/l$. Hence, from equation (12·10),

$$u = \frac{Pc_0}{E}\left\{\frac{c_0 t'^2}{2l} + \frac{x^2}{2lc_0} - \frac{l}{6c_0} + \frac{H^2 c_0}{l} - \frac{2l}{\pi^2 c_0} \sum_{n=1}^{\infty} \frac{(-1)^n}{n^2} \frac{1}{1+n^2\psi^2} \cos\frac{n\pi x}{l} \cos\frac{n\pi c_0 t'}{l\sqrt{(1+n^2\psi^2)}}\right\}. \quad (12\cdot11)$$

Since $c_0^2 = E/\rho$ and $m = \rho l$, this equation may be written

$$u = \frac{Pt'^2}{2m} + \frac{PH^2}{m} + \frac{2Pl^2}{\pi^2 c_0^2 m}\left\{\frac{\pi^2}{4}\left(\frac{x^2}{l^2} - \frac{1}{3}\right) - \sum_{n=1}^{\infty} \frac{(-1)^n}{n^2} \frac{1}{1+n^2\psi^2} \cos\frac{n\pi x}{l} \cos\frac{n\pi c_0 t'}{l\sqrt{(1+n^2\psi^2)}}\right\}. \quad (12\cdot12)$$

Remembering that $$\frac{\pi^2}{4}\left(\frac{x^2}{l^2} - \frac{1}{3}\right) = \sum_{n=1}^{\infty} \frac{(-1)^n}{n^2} \cos\frac{n\pi x}{l} \quad (-l<x<l),$$

equation (12·12) may be written in the form

$$u = \frac{Pt'^2}{2m} + \frac{PH^2}{m} + \frac{2Pl^2}{\pi^2 c_0^2 m} \sum_{n=1}^{\infty} \frac{(-1)^n}{n^2} \left(\cos\frac{n\pi x}{l}\right)\left(1 - \frac{1}{1+n^2\psi^2} \cos\frac{n\pi c_0 t'}{l\sqrt{(1+n^2\psi^2)}}\right). \quad (12\cdot12a)$$

When $H = \psi = 0$, the solution becomes identical with the solution of the simple theory, given in equation (12·2).

In the general case, equation (12·12a) shows that u consists of (1) the displacement $\frac{1}{2}Pt'^2/m$ of the bar as a whole, due to the force P acting on a mass m for time t'; (2) the displacement PH^2/m, which represents a very small, constant displacement of the bar as a whole, independent of time, and connected with the instantaneous propagation of disturbances which is implicit in the present theory; (3) an infinite number of vibrations which are superposed on (1) and (2). The nth term in the series represents the displacement at the point x at time t' when a free-free bar of length l executes longitudinal vibrations of period $2l\sqrt{(1+n^2\psi^2)}/nc_0 = 2l/nc$, which agrees with the usual expression for the period of the vibration of a free-free bar in the nth mode, when lateral inertia is taken into account. The waves concerned in this vibration have velocity c and wave-length $2l/n$.

The displacement ξ of the measuring end of the pressure bar is obtained by substituting $x = 0$ in equation (12·12). In the remaining part of this section the discussion will be limited to bars of circular cross-section; thus

$$\psi^2 = \pi^2\sigma^2(a^2/2l^2). \quad (12\cdot13)$$

If $e_s = Pl/E$ = extension of the bar under a static load P per unit area, and as before $T_0 = 2l/c_0$ = the time taken by a longitudinal wave of infinite wave-length to traverse the bar twice, then, from equation (12·12), ξ/e_s may be written in the following non-dimensional form:

$$\frac{\xi}{e_s} = \frac{2t'^2}{T_0^2} + \frac{\psi^2}{\pi^2} - \frac{1}{6} - \frac{2}{\pi^2}\sum_{n=1}^{\infty} \frac{(-1)^n}{n^2} \frac{1}{1+n^2\psi^2} \cos \frac{2\pi n t'}{T_0\sqrt{(1+n^2\psi^2)}}. \qquad (12{\cdot}14)$$

This equation shows that ξ/e_s is a function of σ, t'/T_0 and a/l, and the similarity relationships which have been given in the preceding section will clearly hold in the present case.

To determine the values of ξ/e_s for given values of σ, a/l and t'/T_0, it becomes necessary to find the sum of the infinite series in equation (12·14); there does not seem to be any short method of doing this, so that each term in the series has to be evaluated separately and the sum found by adding these terms. A large number of terms has to be taken to obtain reasonable accuracy in the results, since the series converges comparatively slowly. Assuming, as in § 11, that $\sigma = 0{\cdot}29$ and $c_0 = 5 \times 10^5$ cm./sec., calculations have been carried out for two bars denoted by A and B; for bar A, $a = 1{\cdot}27$ cm. $= 0{\cdot}5$ in., $l = 193{\cdot}5$ cm. $= 6{\cdot}35$ ft., and for bar B, $a = 1{\cdot}905$ cm. $= 0{\cdot}75$ in., $l = 670{\cdot}_5$ cm. $= 22$ ft. The value of ψ^2 is $1{\cdot}786 \times 10^{-5}$ for bar A and $3{\cdot}349_5 \times 10^{-6}$ for bar B, whilst $T_0 = 774\,\mu$sec. for bar A and $2682\,\mu$sec. for bar B. In each case, the calculations extend from $t'/T_0 = 0{\cdot}485$ to about $t'/T_0 = 0{\cdot}57$.

In the calculations, some eighty or ninety terms of the infinite series of equation (12·14) have been evaluated and summed for each value of t'/T_0; in general, this number is necessary to ensure that the error due to the omission of the remaining terms of the series is small. The accuracy of the results of calculations made with this number of terms may be gauged by considering the value of the ratio ξ_0/e_s, where ξ_0 is the displacement at the measuring end of the bar when distortion is absent. On the one hand, ξ_0/e_s can be determined from equation (12·2), i.e. from equation (12·14) with $\psi = 0$. On the other hand, by integrating equation (1·2) for the case where the applied pressure is constant, it is found that if $t' < T_0/2$, $\xi_0/e_s = 0$ and if $t' > T_0/2$, then

$$\xi_0/e_s = (4t'/T_0) - 2; \qquad (12{\cdot}15)$$

this is clearly the true value of ξ_0/e_s, i.e. the value of the ratio when the summation in equation (12·14) is taken to infinity.

In table 12·1, the third column gives the value of ξ_0/e_s calculated from equation (12·2), the summation being stopped at the value of n ('$n_{\text{max.}}$') given in the second column; the last column in the table gives the value of ξ_0/e_s calculated from equation (12·15). The agreement between the figures in the last two columns shows that the errors are reasonably small when $n_{\text{max.}}$ is about 80.

TABLE 12·1

		ξ_0/e_s calculated from	
t'/T_0	$n_{\text{max.}}$	eqn. (12·2)	(eqn. 12·15)
0·490	78	0·00040	0·00
0·495	83	−0·00069	0·00
0·500	82	0·00229	0·00
0·505	80	0·01939	0·02
0·510	85	0·04040	0·04

The results of the calculations for the general case are given in table 12·2, in which $t\,(= t' - \frac{1}{2}T_0)$ denotes time reckoned from the instant at which a wave travelling with velocity c_0 arrives at $x = 0$.

The results are shown graphically in figures 26 and 27; the former is in terms of non-dimensional variables, and it gives the variation of ξ/e_s with t'/T_0. In the latter, time t is plotted as abscissa and $k'\xi/e_s$, where k' is a constant, as ordinate; for bar A, k' is unity and for bar B, k' is equal to 3·465, which is the ratio of the values of T_0 for bars B and A. This procedure makes the displacement ξ_0 and the velocity $\dot{\xi}_0$, at a given time t, the same for the two bars if the effect of the lateral motion is neglected, since equation (12·15), which applies under these conditions, may be written

$$\xi_0/e_s = 4t/T_0.$$

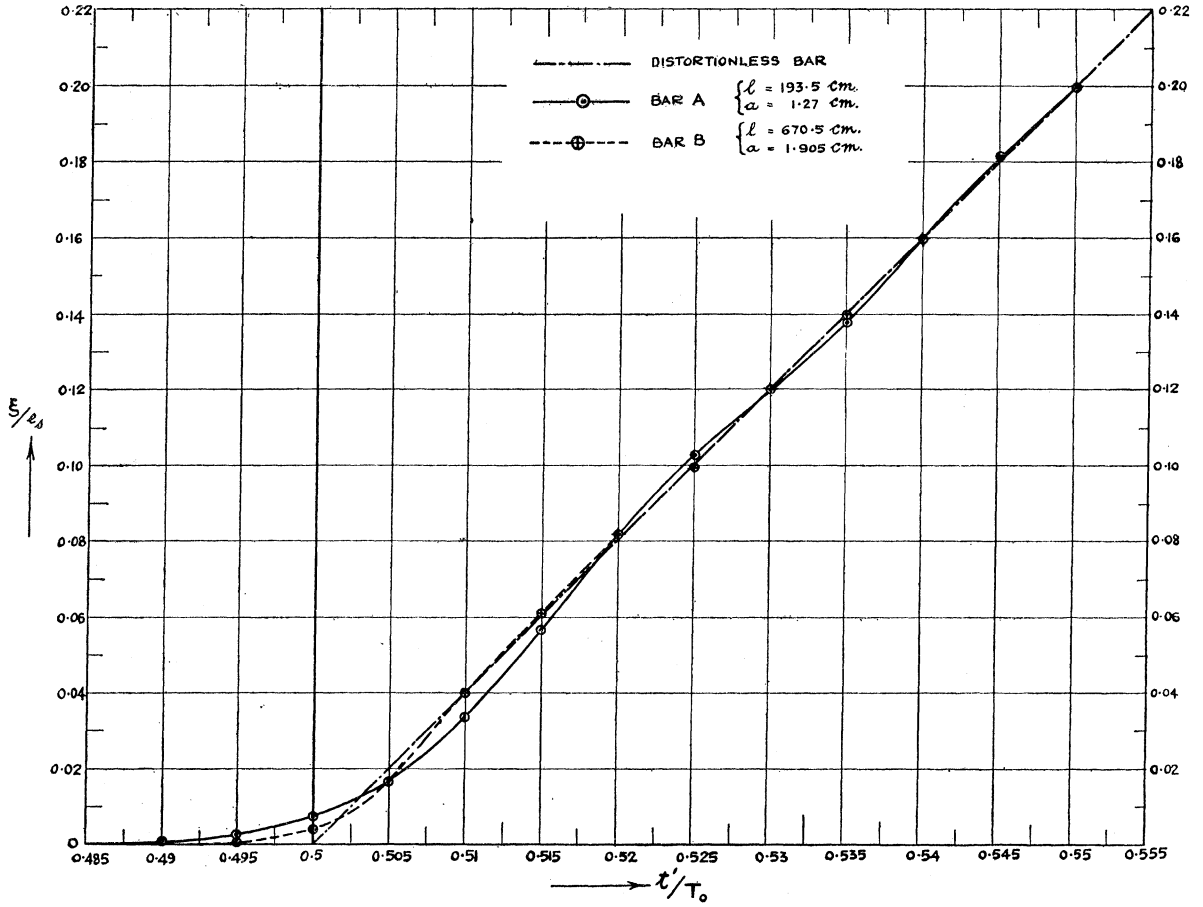

FIGURE 26. $(\xi/e_s, t'/T_0)$ curves for a sustained pressure. ξ = displacement at measuring end of bar; e_s = extension of bar under static load; t' = time; $T_0/2$ = time taken by a wave of velocity c_0 to travel the length of the bar.

Before discussing these results, it will be convenient to consider how far they are likely to differ from those which would be given by the accurate theory of § 11 if it were possible to derive a pulse solution using this theory. Any difference between the results will be due to the fact that the two theories lead to different values of c/c_0 for the same values of σ and a/Λ, and curves (1) and (1a) in figure 13 indicate that the difference in c/c_0 is small for small values of a/Λ and that it increases as a/Λ increases. Considering the nth term in the infinite series of equation (12·14), $\Lambda = 2l/n$ and $a/\Lambda = na/2l$; $a/2l$ is equal to 0·003280 for bar A and 0·001421 for bar B.

For bar A, table 12·3 gives (i) the amplitude $(-1)^n/n^2(1+n^2\psi^2)$ of the vibration represented by the nth term ($n = 1, 10, \ldots, 90$) in the infinite series of equation (12·14), (ii) the value of a/A for the wave concerned in this vibration, (iii) the value of c/c_0 according to equation (12·5), (iv) the value of c/c_0 according to the accurate theory, (v) the ratio of the two values of c/c_0.

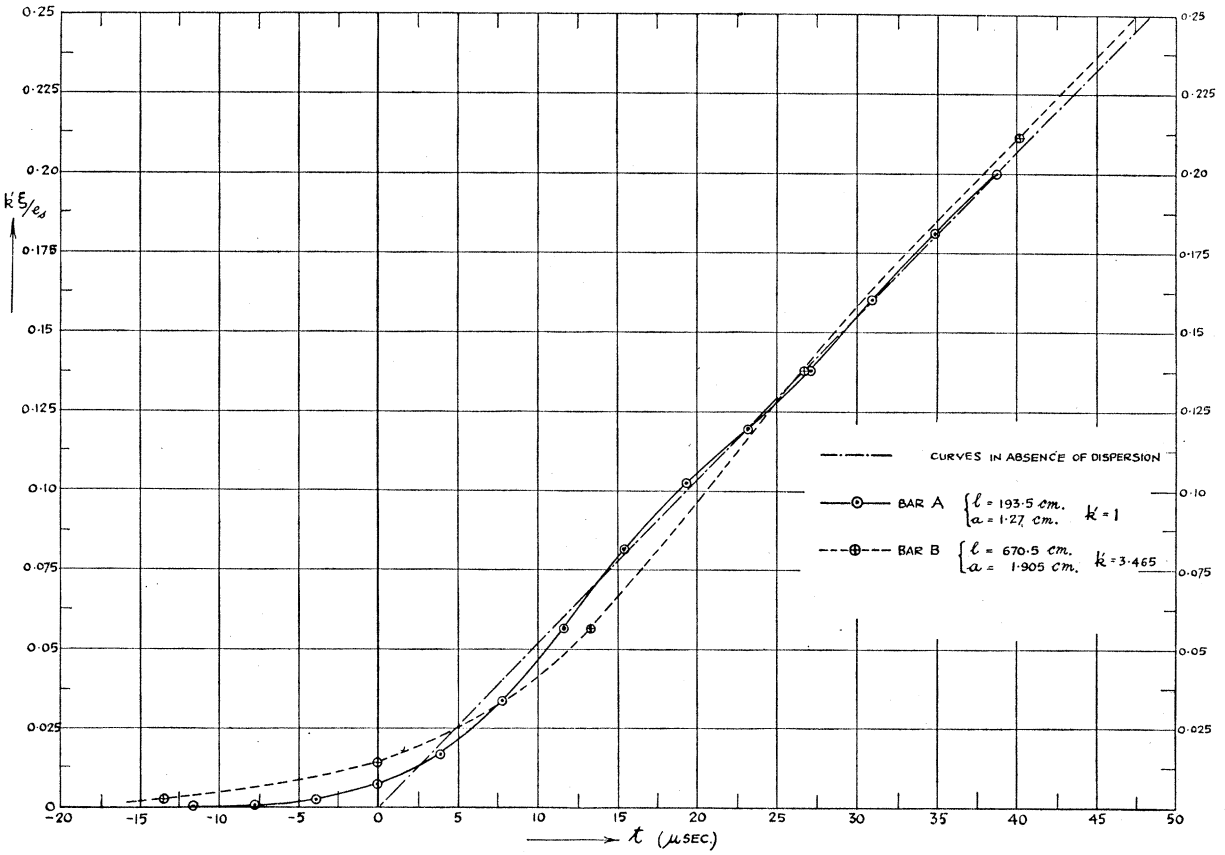

FIGURE 27. $(k'\xi/e_s, t)$ curves for a sustained pressure. t = time reckoned from instant of arrival of wave of velocity c_0 at the measuring end of the bar.

TABLE 12·2

	bar A			bar B		
t'/T_0	t (μsec.)	$n_{max.}$	ξ/e_s	t (μsec.)	$n_{max.}$	ξ/e_s
0·485	−11·61	85	0·00024	−40·2	84	0·00015
0·490	− 7·74	78	0·00087	−26·8	81	0·00021
0·495	− 3·87	83	0·00268	−13·4	85	0·00075
0·500	0	82	0·00736	0	84	0·00404
0·505	3·87	80	0·01692	13·4	85	0·01637
0·510	7·74	85	0·03373	26·8	91	0·03994
0·515	11·61	76	0·05685	40·2	67	0·06107
0·520	15·48	82	0·08185	53·6	85	0·08196
0·525	19·35	88	0·10287	67·0	85	0·09994
0·530	23·22	85	0·11968	80·4	85	0·11993
0·535	27·09	85	0·13807	93·8	85	0·13988
0·540	30·96	83	0·16036	107·2	80	0·16014
0·545	34·83	91	0·18145	120·6	—	—
0·550	38·70	90	0·19960	134·0	85	0·20015
—	—	—	—	—	—	—
0·570	—	—	—	187·6	82	0·28002
0·575	—	—	—	201·0	84	0·30007

Even when $n = 90$, the difference between the two values of c/c_0 is only 7 %, and, at the same time, the amplitude of the term is only about $\frac{1}{9300}$ of the amplitude of the first term. The difference between the results of the present theory and the accurate theory cannot therefore be large.

TABLE 12·3. BAR A

				c/c_0		
n	$1/n^2$	$(-1)^n/n^2(1+n^2\psi^2)$	a/A	eqn. (12·5)	§ 11	ratio
1	1	1	0·00328	1·000	1·000	1·00
10	0·01	0·009980	0·0328	0·999	0·999	1·00
20	0·0025	0·002482	0·0656	0·997	0·997	1·00
30	0·00111	0·001093	0·0984	0·993	0·993	1·00
40	0·000625	0·000607	0·1312	0·986	0·986	1·00
50	0·000400	0·000383	0·1640	0·978	0·970	1·01
60	0·000278	0·000261	0·1968	0·969	0·956	1·01
70	0·000204	0·000188	0·2296	0·959	0·937	1·02
80	0·000156	0·000140	0·2624	0·948	0·908	1·04
90	0·000123	0·000108	0·2952	0·935	0·877	1·07

For bar B, when $n = 90$, $a/A = 0{\cdot}1279$, the two values of c/c_0 differ by less than 0·5 %, and the amplitude of the term is about $\frac{1}{8200}$ of the amplitude of the first term; the difference between the results of the two theories is therefore even less than in the case of bar A.

The curves given in figures 26 and 27 indicate that dispersion, in so far as it can be represented by the $\partial^4 u/\partial x^2 \partial t'^2$ term in equation (12·3), has two effects on the (ξ, t) curves.

(1) The initial portions of the curves are not straight lines and they do not intersect the t-axis at a finite angle as they would do if dispersion is absent; instead, they are curved and tangential to the t-axis. It should be pointed out that the curves begin to rise before the arrival of the wave of velocity c_0 at the measuring end of the bar; this effect is to be expected from the discussion given in the first part of this section.

(2) Beyond their initial curved portions, the (ξ, t) curves oscillate, to varying degrees, about the straight lines which would be obtained with a distortionless bar. The periods of these fluctuations agree reasonably well with those given by the group-velocity theory of § 11 (*b*). In figure 26, for bar A, one half-period of the oscillation (reckoned as the difference in the values of t' corresponding to consecutive intersections of the $(\xi/e_s, t'/T_0)$ curve with the straight line for a distortionless bar) extends from $t'/T_0 = 0{\cdot}503$ to $t'/T_0 = 0{\cdot}519$, giving a period of $4 \times 0{\cdot}016 \times \frac{1}{2}T_0 = 0{\cdot}064 \times \frac{1}{2}T_0$, corresponding to a mean value of $t'/\frac{1}{2}T_0 = 1{\cdot}022$. For bar A, $l = 193{\cdot}5$ cm., $a = 1{\cdot}27$ cm., and therefore $\frac{1}{2}T_0 = 193{\cdot}5T_a/1{\cdot}27 = 152{\cdot}5T_a$; from figure 26 the period of the oscillation is thus $0{\cdot}064 \times 152{\cdot}5T_a = 9{\cdot}76T_a$. From curve (1*a*) of figure 15, the value of T_p corresponding to $t'/\frac{1}{2}T_0 = 1{\cdot}022$ is $10{\cdot}4T_a$. The two succeeding half-oscillations in figure 26 give periods equal to $6{\cdot}7T_a$ and $6{\cdot}1T_a$ when $t'/\frac{1}{2}T_0$ is $1{\cdot}04_9$ and 1·07 respectively; from curve (1*a*) of figure 15, the corresponding values of T_p are $7{\cdot}3T_a$ and $6{\cdot}1T_a$, respectively. It is worth noticing that the values of T_p given by the accurate theory (curve (1) in figure 15) for $t'/\frac{1}{2}T_0 = 1{\cdot}022$, $1{\cdot}04_9$ and 1·07 are $11{\cdot}6T_a$, $8{\cdot}4T_a$ and $7{\cdot}6T_a$ respectively.

The discussion given in connexion with table 12·1 shows that the two above effects are real characteristics of the propagation of waves in the bar, and that they are not due to errors such as would be caused, for example, by taking too few terms in the summation in equation (12·14); comparison of figures 26 and 27 with figures 17 and 18 shows that the main features

of the distortion in the two cases agree as well as one would expect when comparing the distortion of a pulse with that of a periodic wave of the type considered in § 11, in which the duration of the inclined portions of the wave is comparable with its period.

Experimental evidence for the existence of the above forms of error was obtained in a series of experiments in which the pressure bar was used with a parallel-plate condenser unit to measure the pressure in detonation waves in explosive gaseous mixtures contained in a long tube. In the initial portions of such waves, the pressure rises practically instantaneously from zero to a constant value which can be calculated from thermo-chemical data.

The phtograph shown in figure 28 is an enlargement of a plate taken when a pressure bar 1 in. diameter, 2 ft. 2 in. long, was sealed into the end of a steel tube in which a mixture of unknown composition, containing hydrogen, oxygen and air, was detonated by a spark; the bar and the explosion tube were coaxial, so that the apparatus measured the stagnation or Pitot pressure in the wave.

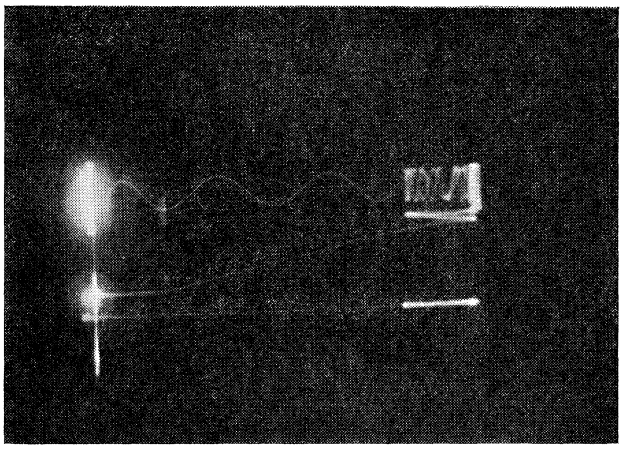

FIGURE 28. Oscillogram of the pulse due to the Pitot pressure in a detonation wave in a mixture of air, oxygen and hydrogen. Pressure bar: length = 2 ft. 2 in., diameter = 1 in. Condenser unit: parallel-plate type. Upper trace: timing wave, period = 41 μsec. Middle trace: amplified p.d. from condenser unit. Lower trace: datum line.

The analysis of the record is given in figure 29, in which the ordinate is the vertical deflexion δ on the photographic plate of the recording spot of the oscillograph, and the abscissa is the horizontal distance, $X-X_0$, on the plate, reckoned from the point where the recording spot begins to move vertically upwards. The points which were measured with the microscope are indicated in the diagram, which also gives the relationships connecting the displacement ξ with δ and time with $X-X_0$.

In this diagram the curve passing through the measured points is initially concave upwards and then it oscillates about the straight line of closest fit drawn through these points. If this straight line is produced back to cut the axis of time, the length of the intercept on this axis corresponds to 4·5 μsec.; the mean of the length of this intercept for this and two other plates taken under the same conditions is 4·6 μsec.

Whilst the initial curvature of the $(\delta, X-X_0)$ curve of figure 29 and the fluctuations of the experimental points about the smoothed curve agree qualitatively with the effects of dispersion in the pressure bar, it is important to make certain that they are not spurious

effects due to imperfections in some other part of the apparatus. The main source of effects of this type, apart from the bar, is the amplifier, and an analysis of the behaviour of the amplifier was undertaken in order to see whether defects in the amplifier could account for the effects in question. This analysis shows that, whilst imperfections of the amplifier are partly responsible for the initial curvature of the $(\delta, X-X_0)$ curves, the effect actually observed is much too large to be attributed to the amplifier, since the length of the intercept on the t-axis, due to the amplifier alone, is only about $0{\cdot}4\,\mu$sec., i.e. about one-tenth of the observed value.

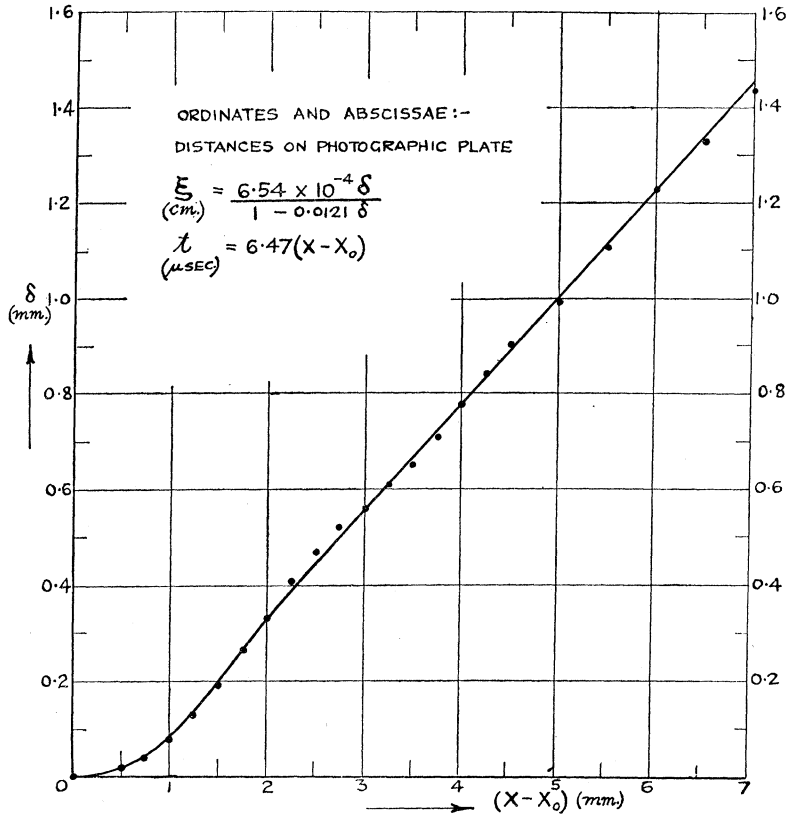

FIGURE 29. Analysis of the record shown in figure 28.

Considering the oscillations of the experimental points in the record about the straight line of closest fit, it should be pointed out that the scatter of the points actually measured is greater than the error in the measurement of the photographic plate; for example, in the case of the point at $X-X_0 = 2{\cdot}5$ mm., the vertical distance between the measured point and the straight line is equivalent to 0·02 mm. on the plate, which is about four times as great as the normal error in measuring a plate. These oscillations are undoubtedly due to dispersion in the bar, and their periods agree with the values deduced from curve (1) of figure 15. In figure 29, the first well-defined half-oscillation extends from $X-X_0 = 1{\cdot}9$ mm. to $X-X_0 = 3{\cdot}05$ mm.; the corresponding value of the period is $14{\cdot}88\,\mu$sec., which is equal to $6{\cdot}12T_a$, since $a = 1{\cdot}27$ cm. and $c_0 = 5{\cdot}23 \times 10^5$ cm./sec. The mean value of $t'/\frac{1}{2}T_0$ for this half-oscillation is 1·126; the corresponding value of T_p from figure 15 is $6{\cdot}1T_a$ from curve (1), or $4{\cdot}72T_a$ from curve (1a). The next half-oscillation in figure 29, extending from $X-X_0 = 3{\cdot}05$ mm. to $X-X_0 = 4{\cdot}1$ mm., corresponds to $t'/\frac{1}{2}T_0 = 1{\cdot}18_3$ and the period

is $5{\cdot}58T_a$; from figure 15 this value of $t'/\frac{1}{2}T_0$ gives $T_p = 5{\cdot}3T_a$ from curve (1), and $T_p = 3{\cdot}8T_a$ from curve (1a). It is interesting to note that the experimental results agree better with the results of the accurate theory (curve (1)) than with those of the approximate theory of this section (curve (1a)).

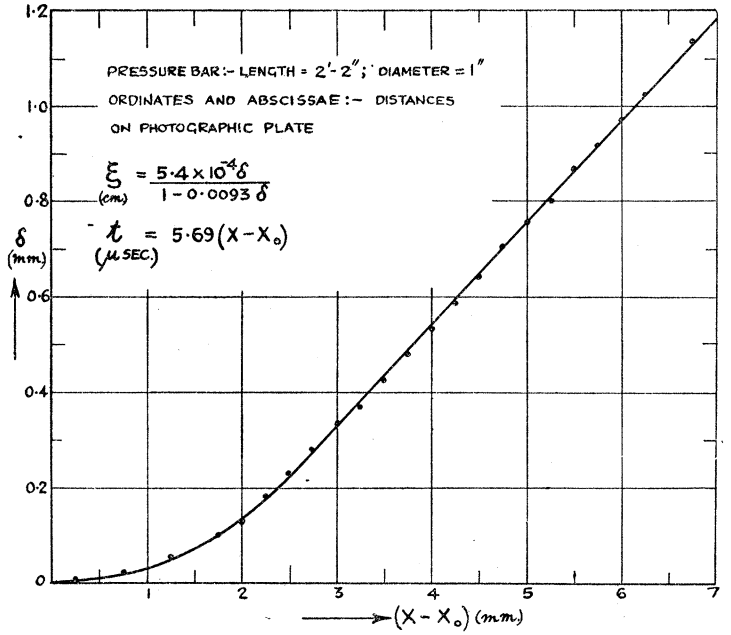

FIGURE 30. Record from bar arranged to measure static pressure in a detonation wave in a mixture of equal volumes of acetylene and oxygen.

Figure 30, with the same variables as figure 29, gives the analysis of a plate taken with a mixture of equal volumes of oxygen and acetylene when the same pressure bar was sealed into the wall of the explosion tube with its axis at right angles to the axis of the tube, the pressure end of the bar being flush with the inside surface of the tube; this arrangement therefore measures the 'static' pressure in the detonation wave. The length of the explosion tube was 12 ft., and the distance from the centre of the pressure bar to the closed end of the tube was 16 in. The record is similar to that shown in figure 29, the main difference being in the length of the intercept on the horizontal axis of the straight line of closest fit drawn through the observed points; in this case the length of the intercept corresponds to about 8 μsec., compared with about 4·6 μsec. in the previous case. This difference is due to the fact that the force on the pressure end of the bar does not rise instantaneously to its final value, since the detonation wave takes a finite time to travel across the face of the bar when the static pressure is being measured; since the velocity of the detonation wave in a mixture of equal volumes of oxygen and acetylene is $2{\cdot}96\times10^5$ cm./sec., the time taken by the force on the face of the bar to rise to its constant value is $2{\cdot}54/2{\cdot}96\times10^5$ sec. $= 8{\cdot}6\,\mu$sec.

Figure 31 gives the $(\delta, X-X_0)$ curve derived from a plate taken under the same conditions as figure 30, except that the diameter of the pressure bar in this experiment was 0·5 in., and its length was 2 ft. 3 in., so that the time taken by the detonation wave to traverse the diameter of the bar was 4·3 μsec. Comparison of this diagram with the preceding one shows, as one would expect, that if the length of the bar is the same the errors decrease as the radius of the bar decreases.

When (ξ, t) curves similar to those given in figures 26 to 31 are differentiated, the derived (p, t) curves show a gradual initial rise followed by oscillations about an approximately constant value. These effects are shown in figure 32, where $2t'/T_0$ is taken as abscissa and p/p_0 as ordinate, p being the pressure given by differentiation of the curves of figure 26 and p_0, the pressure which would be obtained with a distortionless bar.

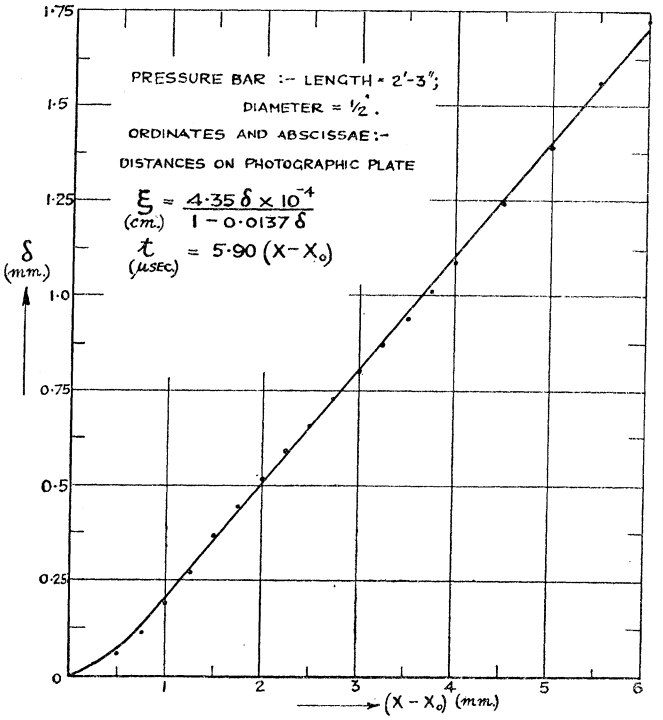

FIGURE 31. Record from a bar arranged to measure static pressure in a detonation wave in a mixture of equal volumes of acetylene and oxygen.

A Hopkinson bar, used with a very short time-piece, in the way described by Hopkinson, measures the maximum value of the pressure p. On the present theory, and with a pulse of the form considered here, it follows that the maximum pressure deduced from the observations will exceed the true maximum pressure and that the discrepancy will be greater as the ratio a/l increases, i.e. as l decreases, if a is constant. Qualitatively, this agrees with the experimental results of Landon & Quinney (1923), who found that the momentum trapped in a short time-piece, used with a bar of given diameter, increases as the length of the bar decreases. The effects to be expected with a pulse of finite duration are discussed below (subsections (*c*) and (*d*)).

It follows from figures 26, 27 and 32 that if the fluctuations in a (ξ, t) curve observed with a constant, sustained pressure are smoothed out by drawing the straight line which best fits the experimental data (excluding the initial, curved portion of the curve), then the average value, $\bar{p}$, of the pressure p deduced in this way will depend on the range of t over which the average is taken. This can be seen from table 12·4 which gives the values of $\bar{p}/p_0$ for different ranges of $t'/\frac{1}{2}T_0$, calculated by finding, by the method of least squares, the straight line of closest fit through the points corresponding to the values of ξ/e_s and t'/T_0 given in table 12·2. Table 12·4 is useful in that it enables a quantitative estimate to be made of the inaccuracy

in the value of p when it is deduced by smoothing the observational data; it is clear from the table that errors up to about 10 % will occur in the value of p if the average is taken over time intervals which are too small.

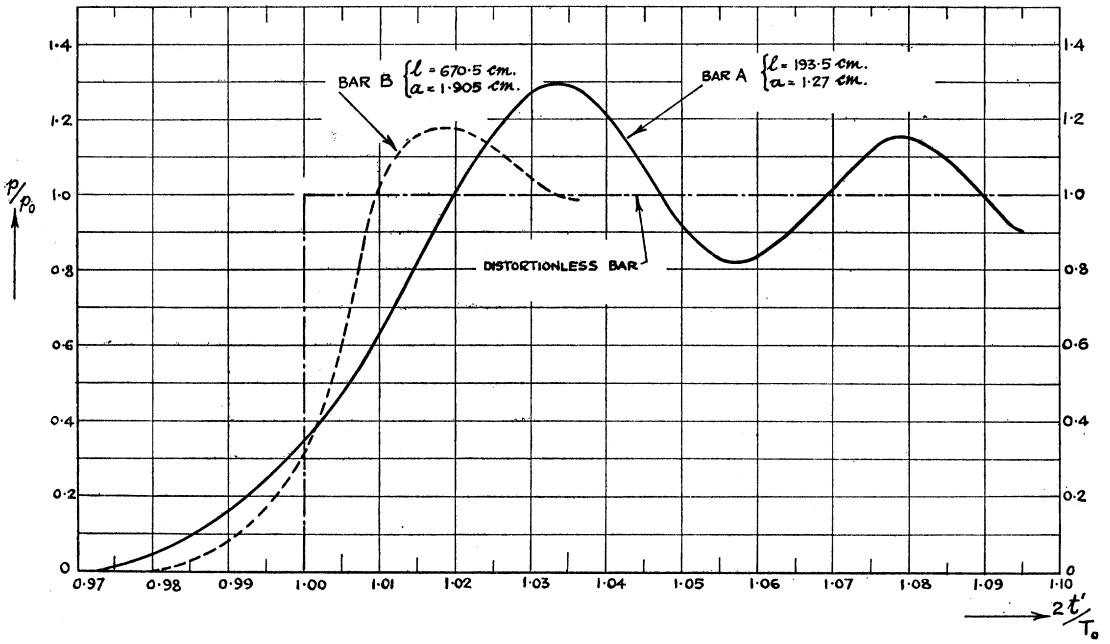

FIGURE 32. (Pressure, time) curves derived from figure 26. p = pressure derived by differentiating the curves of figure 26; p_0 = pressure in the absence of dispersion.

TABLE 12·4

	bar A		bar B	
range of $2t'/T_0$	range of t (μsec.)	$\bar{p}/p_0$	range of t (μsec.)	$\bar{p}/p_0$
1·01 to 1·04	3·87 to 15·5	$1{\cdot}10_1$	13·4 to 53·6	$1{\cdot}08_4$
1·06	23·2	$1{\cdot}09_4$	80·4	$1{\cdot}02_5$
1·08	31·0	$1{\cdot}03_7$	107·2	$1{\cdot}00_5$
1·10	38·7	$1{\cdot}01_4$	—	—

(c) The displacement due to a force of finite duration acting on the pressure end of the bar

Considering next the case of a pressure pulse in which the pressure applied at $x = l$ rises instantaneously from zero to a constant value P at time $t' = 0$ and falls instantaneously from P to zero at time $t' = T'$, the displacement ξ at the measuring end can be found by superposing the solutions appropriate to the case of a pressure $-P$ applied at time $t' = T'$ on the solution given in (12·14). The results of calculations on these lines, for bar A and for pulses in which $2T'/T_0 = 0{\cdot}04$, $0{\cdot}06$, $0{\cdot}08$, are given in figure 33; since $T_0 = 774\,\mu$sec., the corresponding values of T' are 15·48, 23·22 and 30·96 μsec. respectively. The diagram is plotted using non-dimensional variables, namely $2t'/T_0$ as abscissa and the ratio of the value of ξ to the maximum value $\hat{\xi}_0$ of the displacement ξ_0 for a distortionless bar as ordinate; the values of the ratio of the displacement ξ_0 to $\hat{\xi}_0$ are included to help in estimating the error.

The curves in this diagram show, of course, the two forms of error which have already been mentioned in discussing the response of the bar to a sustained force applied to the pressure end. In addition, it is clear, as one would expect, that dispersion gives rise to errors towards

the end of the pulse; here the displacement ξ first overshoots the value $\hat{\xi}_0$ and then oscillates about a value which is a little greater than $\hat{\xi}_0$ in the range covered in the diagram. It is obvious from the diagram that these oscillations at the end of the main pulse are relatively more important in the case of pulses of short duration involving sudden change of pressure.

The period of the oscillations following the main pulse corresponds to the period of the oscillation of the $(\xi/e_s, t'/T_0)$ curves of figure 26 about the inclined straight line for a distortionless bar, or the oscillations of the $(p/p_0, 2t'/T_0)$ curves of figure 32 about the horizontal straight line for a distortionless bar. Thus, in experiments where the oscillations at the end of the main pulse are absent, such as the experiments on the pressure in detonation waves in gaseous mixtures, the period of oscillation of the observed curve around the straight line of closest fit should agree for a given value of t' with the period of the oscillations obtained, with the same bar, at the end of a sudden pulse.

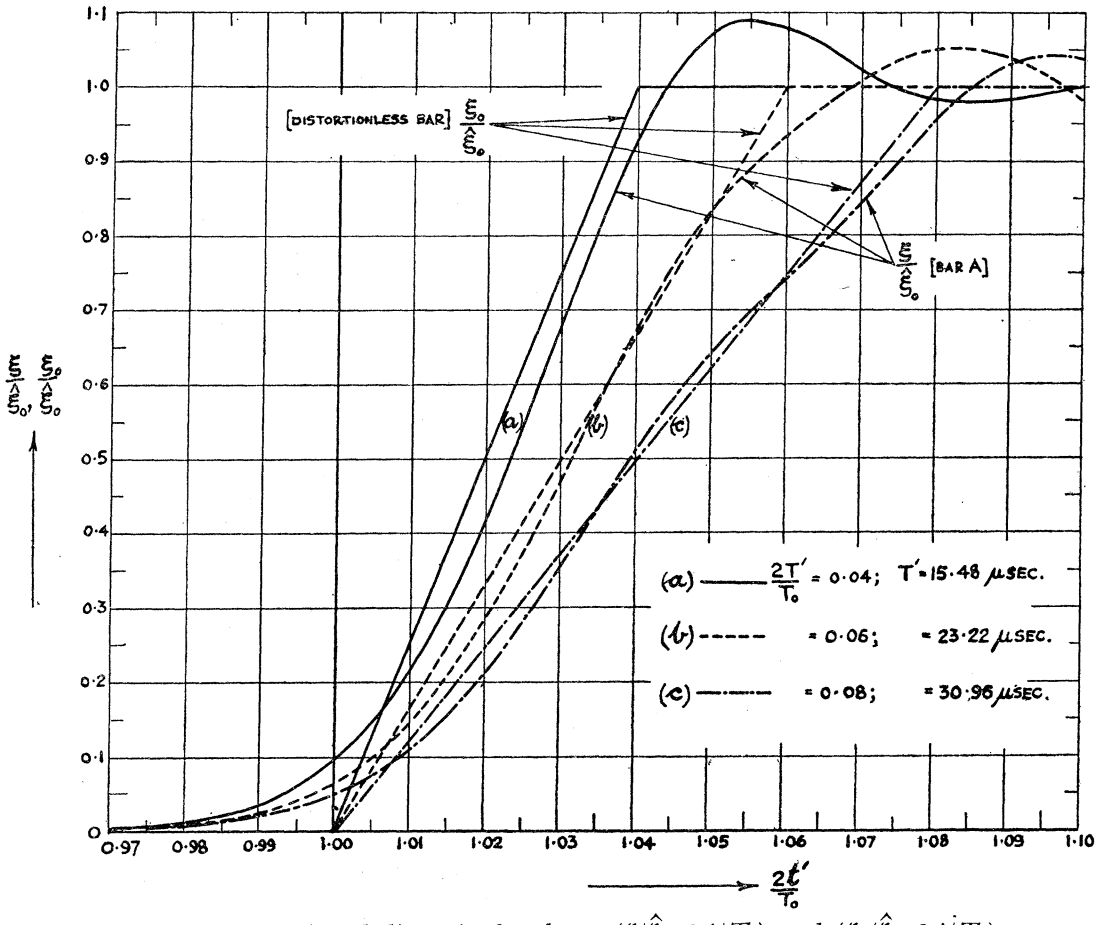

FIGURE 33. Bar A and distortionless bar. $(\xi/\hat{\xi}_0, 2t'/T_0)$ and $(\xi_0/\hat{\xi}_0, 2t'/T_0)$ curves for a force of finite duration, T'.

The phenomenon of the oscillations following the main pulse has already been discussed to some extent in connexion with the comparative response of a parallel-plate unit and a cylindrical unit measuring radial displacement; when the latter type of unit is used, the effect is shown very clearly in the photographs of figure 22 and the oscillations persist to some extent even when the rate of change of pressure is small, as in the case of the impact of a cone-shaped bullet.

With a parallel-plate condenser unit, for the reasons given in § 11 (*c*), these oscillations do not become prominent unless the pressure pulse is much sharper than that due to the impact of lead bullets, and figure 34 shows two photographs, taken with bars 1 in. diameter and 6 ft. long, to illustrate this. Figure 34*a* was obtained in the course of experiments on the measurement of pressure near a bare cylindrical charge of C.E.; the diameter of the charge was 2 in. and the axis of the charge was at right angles to the axis of the bar. In this experiment, the pressure end of the bar was in the form of a cone of 30° semi-vertical angle and the distance from the centre of the charge to the tip of the cone was 3·5 in. The value of the maximum pressure calculated from this record is $1{\cdot}3_9$ tons/sq.in. Figure 34*b* was taken when a steel ball, 0·5 in. diameter, was fired at the end of the bar from a smooth-bore pneumatic gun with a velocity of 182 ft./sec.

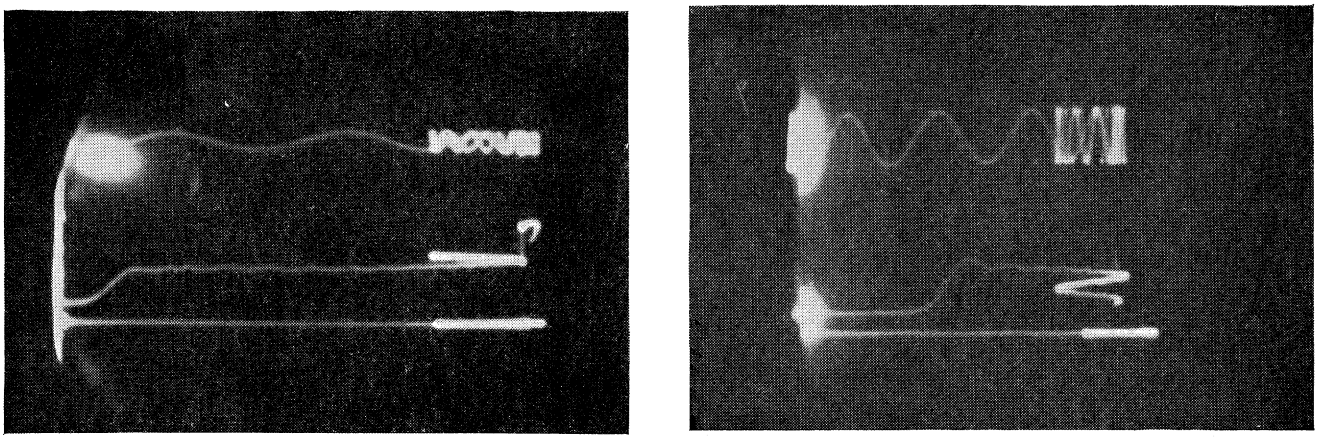

(*a*) (*b*)

FIGURE 34. Oscillograms showing the oscillations following the main pulse. Pressure bar: length = 6 ft., diameter = 1 in. Condenser unit: parallel plate type. (*a*) Pulse due to 1 oz. charge of C.E. Upper trace: timing wave of period 57·3 μsec. Middle trace: amplified output from condenser unit. Lower trace: datum line. (*b*) Pulse due to the impact of a steel ball, 0·5 in. diameter. Velocity of ball = 182 ft./sec. Upper trace: timing wave of period 40·9 μsec. Middle trace: amplified output from condenser unit. Lower trace: datum line.

In the two photographs of figure 34, the main pulse is followed by a tail of high-frequency oscillations; the tail appears to be composed of a single vibration whose period clearly decreases as time increases, as one would expect from figure 15, since $t'/\frac{1}{2}T_0$ is of the order of 1·1 in these records.

The oscillogram of figure 34*a* was analyzed in order to find the degree of agreement between the values of the periods of the oscillations in the tail, and the values of T_p deduced from the group velocity theory (figure 15). The results are summarized in table 12·5, in which the first half-oscillation, extending from the first minimum in the tail to the adjacent maximum on the right, is denoted by number 1, and the succeeding half-oscillations to the right by numbers 2, 3 and 4 respectively.

Remembering that the values of $t'/\frac{1}{2}T_0$ lie in the region of the $(T_p/T_a, t'/\frac{1}{2}T_0)$ curve, where T_p/T_a varies very rapidly with $t'/\frac{1}{2}T_0$, the agreement between the experimental results (3rd row) and the results derived from the accurate theory of Pochhammer and Chree (6th row) is satisfactory. As one would expect, the agreement between the experimental

results and the results deduced from the approximate theory (7th row) of this section is less good.

TABLE 12·5

$l = 6$ ft. $= 183$ cm.; $a = 0{\cdot}5$ in. $= 1{\cdot}27$ cm.; $c_0 = 5{\cdot}23 \times 10^5$ cm./sec.; $\frac{1}{2}T_0 = 350$ μsec.; $T_a = 2{\cdot}42$ μsec.

half-oscillation number	1	2	3	4
time between max. and min. (μsec.)	$9{\cdot}8_5$	$8{\cdot}4_5$	$7{\cdot}7_5$	$6{\cdot}7_0$
period of the oscillation (expt.)	$8{\cdot}1_2 T_a$	$6{\cdot}8_9 T_a$	$6{\cdot}3_9 T_a$	$5{\cdot}5_2 T_a$
t' for mid-point of the half-oscillation (μsec.)	$380{\cdot}_5$	390	398	$405{\cdot}_5$
$t'/\frac{1}{2}T_0$	$1{\cdot}08_7$	$1{\cdot}11_4$	$1{\cdot}13_7$	$1{\cdot}15_8$
T_p for this value of $t'/\frac{1}{2}T_0$ from figure 15:				
(i) curve (1)	$6{\cdot}7 T_a$	$6{\cdot}1 T_a$	$5{\cdot}7 T_a$	$5{\cdot}4 T_a$
(ii) curve (1a)	$5{\cdot}5_5 T_a$	$4{\cdot}9 T_a$	$4{\cdot}3 T_a$	$4{\cdot}0 T_a$

From figure 33 it follows that if the slope and therefore the pressure is averaged by drawing the straight line of closest fit through the points observed in an experiment, the result will be too high and the magnitude of the error will be of the same order as the error in the case of a sustained pulse (see table 12·4). At the same time, at the end of a pulse of finite duration, $\xi/\hat{\xi}_0$ oscillates about a mean value which appears from figure 33 to be a little greater than unity; this implies that if a parallel plate condenser unit is used to measure the displacement ξ, and if the unit is calibrated from momentum measurements as described in § 5 (c), then the observed value of the separation, D, of the plates of the unit will be in error.

To estimate this error and its effect on the measured values of the pressure, consider the particular case of the first set of readings shown in table 5·1. Assuming first that the bar is distortionless, and that, as shown in the table, $\hat{\xi} = 2{\cdot}28 \times 10^{-3}$ cm., $\hat{V} = 0{\cdot}0525$ V, $E_p = 193$ V, equation (5·16a) then gives $D = 5{\cdot}60 \times 10^{-2}$ cm. Assuming next that dispersion modifies the $(\xi/\hat{\xi}_0, 2t'/T_0)$ curves as shown in figure 33 and that the duration of the pulse due to the impact of the ball is such that $2T'/T_0 = 0{\cdot}04$, this diagram shows that the mean value of $\xi/\hat{\xi}_0$ at the end of the pulse is about 1·03. This does not affect the value of $\hat{\xi}$ used in equation (5·16a) since this value is deduced from the momentum communicated to the bar by the impact of the ball; on the other hand, it does affect the total change in capacity, $\hat{\gamma}$, of the bar condenser and the maximum p.d., $\hat{V}$, across R_s and C_s of figure 4. $\hat{\gamma}$ is, in fact, proportional to the average value of ξ at the end of the pulse in figure 33 (see equation (5·8) and $\hat{V}$, in turn, is proportional to $\hat{\gamma}$ (see equation (5·5a)). Thus the value of $\hat{V}$ appropriate to the present case is $0{\cdot}0525 \times 1{\cdot}03 = 0{\cdot}05408$ V, and substituting this value of $\hat{V}$, together with the values of $\hat{\xi}$ and E_p already given, in equation (5·16a), it is found that $D = 5{\cdot}51 \times 10^{-2}$ cm., compared with its previous value of $5{\cdot}60 \times 10^{-2}$ cm. Thus curve (a) of figure 33 leads to a value of D which is about 2 % less than the value corresponding to the case of a distortionless bar, and since displacement and pressure are proportional to D^2 (see equation (5·10b)), other quantities remaining unchanged, it follows that the values of ξ and p deduced from the lower value of D will be about 4 % too small. The average value of the pressure deduced from the slope of curve (a) of figure 33 is about 10 % higher than the value deduced from the slope of the curve for a distortionless bar; thus, when a pressure measurement is combined with a calibration experiment, the net result, on our present assumptions, is to give a value of the pressure which is about 6 % greater than the true value. The same considerations will apply to some extent in every case, and in calibration experiments, such as those summarized in table 5·1, the scatter of the values of D is undoubtedly

due partly to the effect which has just been discussed; in addition, the errors due to the alteration of the slope of the (ξ, t) curves, caused by dispersion, are partly neutralized when the momentum method is used to find the value of the separation D of the plates of a parallel plate condenser unit.

(*d*) *Summary of the general conclusions*

It will be convenient at this point to summarize the results of the experiments and the discussion given in this and the preceding sections. The summary will be restricted to the performance of the parallel plate type of condenser unit; the behaviour of the two types of cylindrical units can be deduced from that of the parallel plate unit by means of the discussion already given in the concluding part of § 11. At the same time, no attempt is made here to discuss the performance of the bar when used mechanically, although some of the statements given below will obviously apply to this case.

1. The pressure bar is incapable of accurate measurement of pressures which are subject to rapid changes in times of the order of 1 μsec.

2. When the force applied to the pressure end of the bar changes instantaneously from zero to a finite value, the pressure deduced from the displacement at the measuring end takes a finite time (after the arrival of the wave) to rise to an approximately constant value. This time depends on Poisson's ratio and on the radius and length of the bar; when $\sigma = 0{\cdot}29$, with a bar 0·5 in. diameter, 2 ft. 3 in. long, the time is of the order of 2 μsec.; with a bar 1 in. diameter, 2 ft. 2 in. long it is of the order of 3 μsec., and with a bar 1 in. diameter, 6 ft. long, about 5 μsec.

3. Similar considerations hold when the force at the pressure end is instantaneously reduced from a finite value to zero.

4. It follows that if the pressure to be measured consists of a force which rises instantaneously from zero to a finite value, which is maintained for a time T', and then drops instantaneously to zero, no pretence at accuracy can be made if T' is less than 4 μsec. with a bar 0·5 in. diameter, 2 ft. 3 in. long, less than 6 μsec. with a bar 1 in. diameter, 2 ft. 2 in. long, and less than 10 μsec. with a bar 1 in. diameter, 6 ft. long.

5. With constant or slowly varying forces, the pressure derived from the displacement at the measuring end fluctuates slightly about its true value; these fluctuations decrease, and the accuracy increases, as T' increases. Apart from the initial and final portions of the pulse, an accuracy of about 2 % can be obtained theoretically by averaging, if T' is not less than about six times the time taken by the pressure (deduced from the displacement at the measuring end) to reach its final value.

(*e*) *The accuracy of the experiments*

In addition to these errors which are inherent in the pressure bar itself, each measurement of pressure with the apparatus described in this paper is subject to errors due to inaccuracies in the measurement of (i) the record on the photographic plate, (ii) the electrical quantities —p.d.'s, resistances, capacities and frequency—involved, (iii) the separation, D, of the plates of the condenser unit, when a parallel plate unit is used, or the capacity per unit length when either of the cylindrical units is used.

(i) The microscope used to measure the oscillograms reads directly to 0·01 mm., and in most cases, two independent settings of the microscope on a given point on a trace agree to

within 0·005 mm. In the case of the record shown in figure 12, an uncertainty of $\pm 0{\cdot}002_5$ mm. in the measured values of the vertical displacement leads to an uncertainty in the value of p of about ± 1 to $\pm 2{\cdot}5$ % in the initial stages of the record and about $\pm 0{\cdot}5$ % in the region of maximum pressure. It should be pointed out that the scatter of the points actually measured in figure 12 about the curve marked 'ξ(experiment)' is much greater than the error in the measurement of the plate and it is undoubtedly caused by dispersion in the bar; for example, in the case of the point at $t = 13{\cdot}20\,\mu$sec., the vertical distance between the measured point and the curve is equivalent to 0·1 mm. on the photographic plate, i.e. to one-tenth of a revolution of the screw of the microscope.

(ii) The uncertainty in the measured values of the electrical quantities does not usually exceed $\pm 0{\cdot}5$ %.

(iii) With a parallel plate condenser unit, ξ and p are proportional to D^2, other quantities remaining constant; under these conditions, the percentage error in p is therefore twice the percentage error in D. The error in the value of D is caused partly by the distortion of the pressure pulse in the bar and partly by errors in the measurement of the records and the electrical quantities. Table 5·1 shows that the uncertainty in D is about $\pm 1{\cdot}5$ %, when the diameter of the pressure bar is 1 in. Since all sources of error contribute to the uncertainty in the measured value of D, it seems legitimate to conclude that twice the uncertainty in D, i.e. $\pm$ 3 % is a fair measure of the over-all accuracy of a pressure measurement in a given experiment, provided, of course, that the pressure does not vary too rapidly with time.

Measurement of the pressure due to bullet impacts and the pressure in detonation waves in gaseous mixtures confirms that the over-all error is of the order of the figure just given and that normally it is less than this.

The results shown in figure 12 are typical of those obtained with bullet impacts. Here the agreement between the experimental and theoretical (p, t) curves is reasonably satisfactory, since it is difficult to be certain about the accuracy of the initial and final portions of either curve. The difference between the two curves in their middle sections is within the limits stated above and the maximum pressures agree to within 2·5 %.

The work described in this paper was carried out between 1939 and 1943 at the Engineering Laboratory, Cambridge, at the suggestion of Sir Geoffrey Taylor, to whom I am greatly indebted for advice and help throughout the course of the work.

I am also indebted to the University College of Wales, Aberystwyth, for leave of absence from my post; to the Trustees of the Leverhulme Research Fellowships for the grant of a Fellowship for the period 1939 to 1941; to the Research and Experiments Department of the Ministry of Home Security, to whom I was seconded from 1941 to 1943, for permission to publish the work; to Professors Sir Charles Inglis, Sir B. Melville Jones and Sir Lawrence Bragg for laboratory facilities and to Mr W. E. Thompson for his help in the construction of apparatus.

Appendix 1

The effect of radial displacements on the response of a cylindrical condenser unit

When a longitudinal elastic wave is propagated along a bar, it gives rise to both longitudinal and radial displacements, a longitudinal wave of compression being accompanied

by radial expansion and a longitudinal wave of extension by radial contraction; the radial displacement ζ on the cylindrical surface of the bar is given by equation (1·3): $\zeta = \sigma a p/E$.

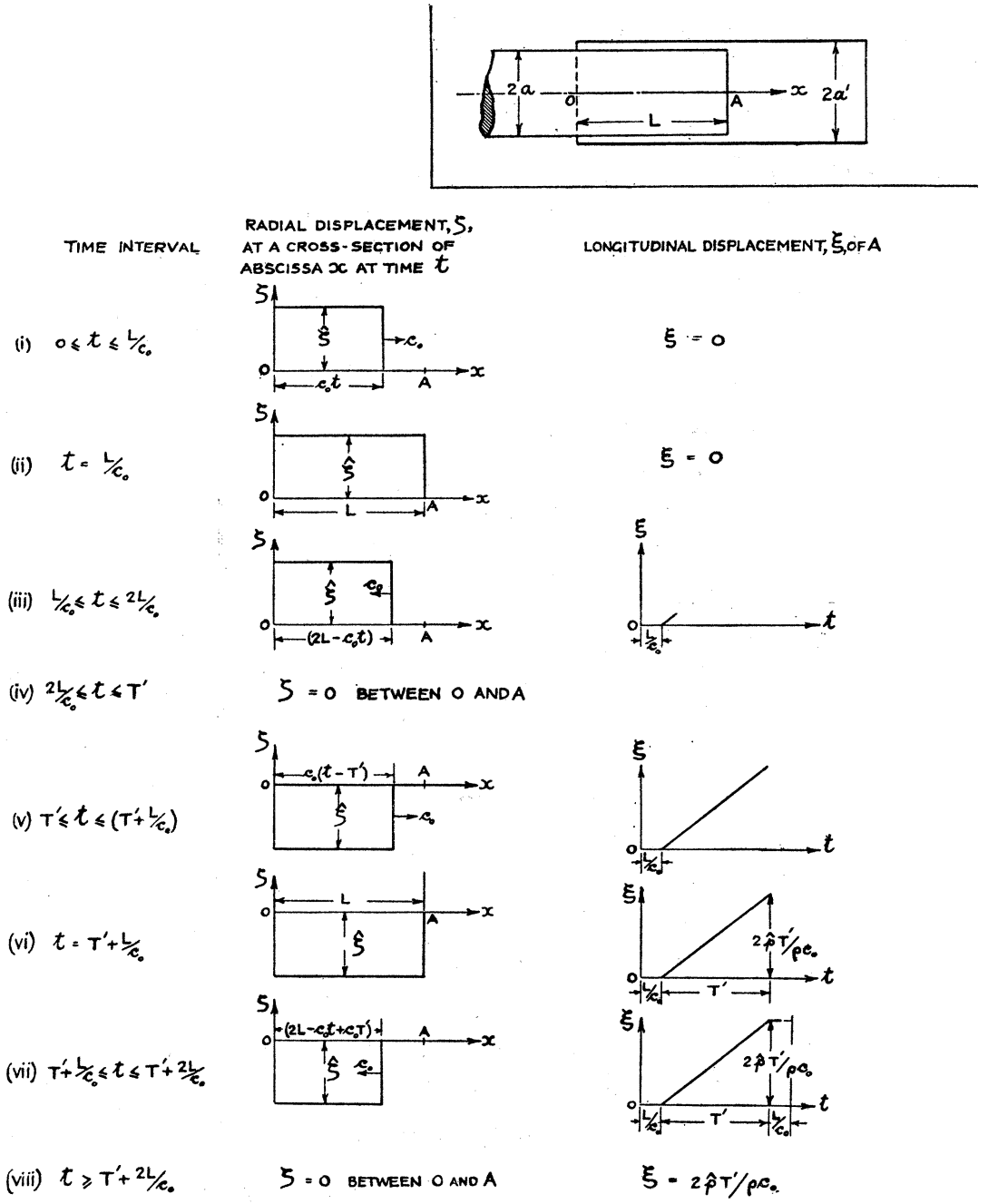

FIGURE 35. The variation of the longitudinal and radial displacements in a cylindrical condenser unit with a square-topped pressure pulse of duration T'.

Consider a pressure bar of radius a and take the axis of the bar as the axis of x; suppose that the cylindrical condenser unit consists of an insulated cylinder of internal radius a' coaxal with the earthed pressure bar as shown in the inset of figure 35. Let the origin of x be taken at O, the point of intersection of the axis of x with the cross-section passing through the inner end of the insulated cylinder; let the abscissa of the end A of the bar be L.

In order to find the net change γ in the capacity of this condenser due to a pressure pulse, it will be assumed, for simplicity, that a square-topped pulse of compression of duration T' is propagated along the bar in the positive direction of x, so that the pressure p at a given point in the bar rises instantaneously from zero to a value $\hat{p}$, say, and remains at this value for time T', when it falls instantaneously to zero.

Let the origin of time be taken as the instant at which this pulse of compression arrives at the point O. As the pulse travels in the positive direction of x, it gives rise to a radial expansion $\zeta = \hat{\zeta} = \sigma a\hat{p}/E$. When it arrives at A, it is reflected as a pulse of extension which travels in the negative direction of x and causes a radial contraction of amount $\hat{\zeta}$. The resultant radial displacement ζ at a point in the portion OA of the bar at time t is found by superposing the separate displacements due to the incident and the reflected waves; figure 35 shows the values of ζ plotted as ordinate against x as abscissa at different values of t in the interval $0 \leqslant t \leqslant (T'+2L/c_0)$, assuming that $T' > 2L/c_0$.

From equation (1·2), it follows that the longitudinal displacement ξ of the end A of the bar at time t is given here by the equations

$$\left.\begin{array}{ll} 0 \leqslant t \leqslant L/c_0, & \xi = 0, \\ L/c_0 \leqslant t \leqslant (T'+L/c_0), & \xi = 2\hat{p}(t-L/c_0)/\rho c_0, \\ t \geqslant (T'+L/c_0), & \xi = 2\hat{p}T'/\rho c_0. \end{array}\right\} \qquad \text{(A·1·1)}$$

The relationship between ξ and t is shown in figure 35.

Let γ_l be the increase in the capacity of the bar condenser at time t due to the longitudinal displacement ξ, and γ_r the increase in capacity at the same instant, due to the radial displacement ζ. Assuming that end-effects are unchanged by the motion of the surfaces of the bar, $\gamma_l = k\xi$ where k, the capacity per unit length of the bar condenser, is given by the equation

$$k = \frac{0{\cdot}2416}{\log(a'/a)} = \frac{10}{18\ln(a'/a)} \quad (\mu\mu\text{F/cm.}). \qquad \text{(A·1·2)}$$

If the radius of the inner conductor of the condenser increases by the amount Δa, it follows from this equation that the increase Δk in k is

$$\Delta k = \frac{k\Delta a}{a\ln(a'/a)} = 1{\cdot}8k^2\frac{\Delta a}{a}. \qquad \text{(A·1·3)}$$

If the radius of the bar has been increased by the radial displacement ζ over a length L' of the common portion OA of figure 35 at time t, then

$$\gamma_r = L'\Delta k = 1{\cdot}8L'k^2\zeta/a. \qquad \text{(A·1·4)}$$

The total change in capacity, γ, of the condenser unit at time t is therefore

$$\gamma = \gamma_l + \gamma_r = k(\xi + 1{\cdot}8kL'\zeta/a). \qquad \text{(A·1·5)}$$

The value of γ corresponding to a given value of t can thus be calculated from these equations, the appropriate value of L' being found from figure 35.

The full-line curve in figure 36 shows the results of numerical calculations for a condenser consisting of an insulated cylinder of internal diameter $1\frac{1}{16}$ in. and a bar 1 in. diameter, the overlap L being 1·3 cm. In this curve, γ is plotted as ordinate against t as abscissa, and for the purpose of calculation, it has been assumed that $\sigma = 0{\cdot}29$, $\rho = 7{\cdot}85$ g./cu.cm.,

$c_0 = 5{\cdot}23 \times 10^5$ cm./sec., and $\hat{p} = 5 \times 10^8$ dynes/sq.cm., $T' = 30\,\mu$sec., corresponding approximately to the impact of a lead bullet 0·36 in. long, moving with a velocity of 1000 ft./sec. The value of (L/c_0) is $2{\cdot}5\,\mu$sec., and the (γ_l, t) curve consists of the inclined straight line joining the points $(2{\cdot}5, 0)$ and $(32{\cdot}5, 6{\cdot}7_2)$ when t lies between 2·5 and 32·5 μsec., and the horizontal straight line of ordinate $6{\cdot}7_2$ when t exceeds 32·5 μsec.

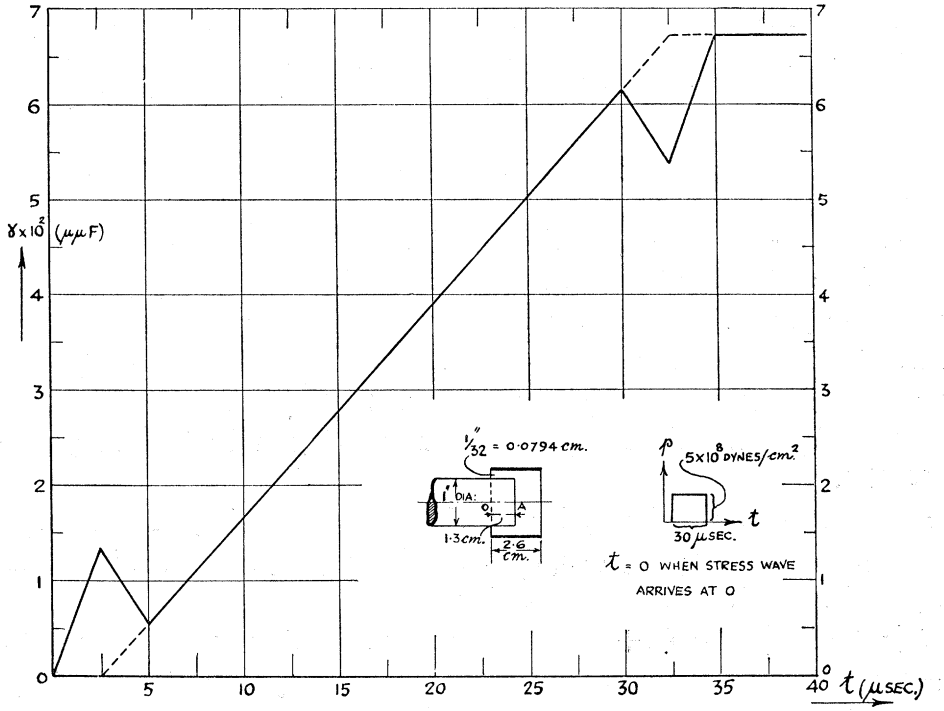

FIGURE 36. The net response of a cylindrical condenser unit to a square-topped pulse.

The resultant radial displacement in the overlap L differs from zero only in the time intervals 0 to 5 μsec. and 30 to 35 μsec., and the diagram shows that in these intervals, the contribution of γ_r to γ is appreciable, even though the value of $\hat{\zeta}$ is only $8{\cdot}56 \times 10^{-5}$ cm., whereas the maximum displacement $\hat{\xi}$ of the end of the bar is $7{\cdot}32 \times 10^{-3}$ cm. Clearly, a cylindrical condenser unit can only give unambiguous results when the clearance $(a' - a)$ is fairly large and then only when the unit is used with pulses whose duration T' is sufficiently long to make $(2L/c_0)$ small in comparison with T'. It must be remembered in this connexion that, in practice, L cannot be decreased indefinitely in an attempt to satisfy the latter condition, since an indeterminate factor, due to the variation of the end-correction with the displacement ξ, enters into the theory given in § 5 when L is too small.

In estimating the effect of the radial displacement in any given instance, it is useful to find the ratio of the maximum values $\hat{\gamma}_r$ and $\hat{\gamma}_l$ of the changes in capacity γ_r and γ_l respectively; $\hat{\gamma}_r$ is the value of γ_r when $L' = L$, whilst $\hat{\gamma}_l$ is the value of γ_l when $\xi = \hat{\xi} = 2\hat{p}T'/\rho c_0$. From equations (1·3) and (A·1·5), it can be shown that

$$\frac{\hat{\gamma}_r}{\hat{\gamma}_l} = \frac{0{\cdot}9kL\sigma}{2c_0 T'} = \frac{5kL}{T'} \times 10^{-7} \qquad \text{(A·1·6)}$$

with the values assumed above for σ and c_0.

In a condenser unit which was designed to measure the pressure due to underwater explosions, $2a' = 1{\cdot}625$ in. $= 4{\cdot}128$ cm., $2a = 1{\cdot}5$ in. $= 3{\cdot}81$ cm., $L = \frac{3}{8}$ in. $= 0{\cdot}95$ cm.; from equation (A·1·2), $k = 6{\cdot}94\,\mu\mu$F/cm. $= 6{\cdot}25$ e.s.u./cm. If $T' = 300\,\mu$sec., then from equation (A·1·6), $\hat{\gamma}_r/\hat{\gamma}_t = 0{\cdot}01$, whilst $(2L/c_0) = 3{\cdot}6\,\mu$sec. In this case γ, and consequently the vertical deflexion on the oscillogram, will be liable to an error of about 1 % in the first and the last $3{\cdot}6\,\mu$sec. of the record. The effect of an error of this magnitude on the performance of this particular unit can be neglected, since all measurements made with the unit will be subject, in the initial and final portions of the pressure pulse at any rate, to a greater error than this, by reason of the distortion of the pulse by the pressure bar (see §§ 10 to 12).

Appendix 2

A more exact theory of the condenser feed-unit circuit

In the discussion of the circuit of the condenser feed-unit given in § 5, it was assumed that the shunt resistance, R_s, of figure 4 was infinite; this appendix deals with the behaviour of the circuit when this restriction is removed. It will be assumed, as in § 5, that the circuit can be regarded as being charged by the polarizing battery to a potential E_p at time $t = 0$, and isolated from it during the motion of the measuring end of the bar, i.e. during the interval $0 \leqslant t \leqslant T'$.

With the notation used previously for the electrical quantities, when $t = 0$, $C = C_1$, the charge on C is $\pm C_1 E_p$ and on C_0, $\pm C_0 E_p$; C_s is uncharged, since it is in parallel with the resistance R_s, and the p.d. across R_s and C_s is zero.

At time t $(0 \leqslant t \leqslant T')$, $C = C_1 + \gamma$, and the p.d. across R_s and C_s is equal to V, and, if $\pm q$, $\pm q_0$, $\pm q_s$ be the charges on the condensers C, C_0 and C_s respectively, and i_s the current through the resistance R_s, then the circuit equations are

$$-\dot{q} = \dot{q}_0 = \dot{q}_s + i_s, \tag{A·2·1}$$

$$V = R_s i_s = q_s/C_s, \tag{A·2·2}$$

$$q/C = q_s/C_s + V, \tag{A·2·3}$$

and, since the loss of charge of C is equal to the gain of charge of C_0, in time t,

$$C_1 E_p - q = q_0 - C_0 E_p. \tag{A·2·4}$$

Differentiating equation (A·2·3), then

$$\frac{1}{C}\frac{dq}{dt} - \frac{q}{C^2}\frac{dC}{dt} = \frac{1}{C_s}\frac{dq_s}{dt} + \frac{dV}{dt}. \tag{A·2·5}$$

Substituting in this equation the values of q, $\dot{q}$ and $\dot{q}_s$ given in equations (A·2·1), (A·2·2) and (A·2·4), the following differential equation for V is obtained:

$$\left(C_s + \frac{CC_0}{C+C_0}\right)\frac{dV}{dt} + \left\{\frac{1}{R_s} + \frac{C_0^2}{(C+C_0)^2}\frac{dC}{dt}\right\} V = -\frac{E_p(C_1+C_0)\,C_0}{(C+C_0)^2}\frac{dC}{dt}. \tag{A·2·6}$$

Since C_0 is of order $10^5\,\mu\mu$F, whilst C and C_1 are of order $10\,\mu\mu$F, C and C_1 will be neglected in comparison with C_0 and this equation written in the form

$$(C_s + C)\frac{dV}{dt} + \left(\frac{1}{R_s} + \frac{dC}{dt}\right) V = -E_p \frac{dC}{dt}. \tag{A·2·7}$$

Remembering that $C = C_1+\gamma$, $\frac{dC}{dt} = \frac{d\gamma}{dt}$, this equation may be rewritten

$$(E_p+V)\frac{d\gamma}{dt}+\frac{dV}{dt}\gamma+(C_1+C_s)\frac{dV}{dt}+\frac{V}{R_s} = 0. \qquad \text{(A·2·8)}$$

Thus $$d[\gamma(V+E_p)] = -(C_1+C_s)\,dV-V\,dt/R_s,$$

and, since $\gamma = V = 0$ at time $t = 0$, on integration,

$$\gamma = -\frac{(C_1+C_s)\,V}{E_p+V}\left\{1+\frac{\int_0^t V\,dt}{R_s(C_1+C_s)\,V}\right\}. \qquad \text{(A·2·9)}$$

Writing $\overline{V} = \left(\int_0^t V\,dt\right)\Big/t$ for the average value of V in the time interval $(0, t)$, this equation becomes

$$\gamma = -\frac{(C_1+C_s)\,V}{E_p+V}\left\{1+\frac{t}{R_s(C_1+C_s)}\frac{\overline{V}}{V}\right\}. \qquad \text{(A·2·10)}$$

When R_s is infinite, the value of γ given by this equation agrees, as it should, with the valued derived from equation (5·4) when C_0 is much greater than C and C_s.

The correction for the leakage through the shunt resistance R_s is thus given by the term $\frac{t}{R_s(C_1+C_s)}\frac{\overline{V}}{V}$ in equation (A·2·10). Normally in these experiments the (V, t) curve does not differ greatly from a straight line passing through the origin and inclined to the V and t axes, so that V and $\overline{V}$ are of the same order. The magnitude of the correction term in question is thus effectively determined by the ratio of the time t to the time-constant $R_s(C_1+C_s)$, and for accurate work it is therefore essential either to allow for leakage by evaluating the correction term, or to make the product $R_s(C_1+C_s)$ large in comparison with the duration T' of the pressure pulse. In practice, it is so easy to satisfy the condition $R_s(C_1+C_s) \geqslant T'$, and, at the same time, ensure sufficient over-all sensitivity of the apparatus, that this procedure has been adopted in this series of experiments.

Appendix 3

The propagation of a pulse of flexural waves in a cylindrical bar

If the forces applied to the pressure end of a bar are unsymmetrical with respect to the axis of the bar, the forces are equivalent to a longitudinal force along the axis, together with a couple; the longitudinal force gives rise to a stress pulse composed of longitudinal or extensional waves and the couple to a pulse consisting of flexural or transverse waves. Since a cylindrical condenser unit designed to measure the longitudinal displacement of the measuring end of a bar can respond to flexural waves, it is important to find the conditions under which the oscillograms given by this type of condenser unit are free from the effects of flexural waves. This appendix deals with the propagation of a flexural wave pulse from the standpoint of the method of stationary phase, following the lines of the discussion given in § 11 (*b*) for extensional wave pulses.

The differential equations, which have been used for describing flexural vibrations in a bar, fall into two classes—the exact equations, due to Pochhammer and to Chree, derived

from the general equations of the theory of elasticity, and the simpler less exact equations, derived in a more elementary manner from a consideration of the stresses in the bar. The former have been summarized by Love (1934, § 202), and calculations, based on these equations, giving the phase velocity of flexural waves for different wave-lengths, have been published recently by Hudson (1943). The simpler equations, and the assumptions on which they are based, have been summarized by Timoshenko (1929, §§ 40 to 43); more recently, a very thorough discussion of the problem has been given by Prescott (1942).

Considering a cylindrical bar of radius a, let the axis of the bar (assumed straight when in equilibrium) be taken as the axis of x, and let the direction of the displacement of the bar in flexural or transverse vibration be taken as the axis of y. Assuming that the bar is uniform and that the displacements are small, let

u_y = flexural displacement at time t at a cross-section of abscissa x.

c', c'_g = phase and group velocities respectively of flexural waves of wave-length Λ, period T, in the bar.

$K' = a/2$ = radius of gyration of the cross-section of the bar about an axis through the centre of gravity, perpendicular to the xy plane.

R' = a non-dimensional constant, depending on the shape of the cross-section of the bar. For a circular cross-section, $R' = 10/9$.

$\epsilon = R'E/\mu = 2R'(1+\sigma)$.

$\gamma = 2\pi/\Lambda$; $\omega = 2\pi/T = \gamma c' = 2\pi c'/\Lambda$.

The simplest theory of the flexural vibrations of a bar assumes that the displacement of an element of the bar consists solely of translation parallel to Oy; the differential equation may be written in the form

$$c_0^2 K^2 \frac{\partial^4 u_y}{\partial x^4} + \frac{\partial^2 u_y}{\partial t^2} = 0. \tag{A·3·1}$$

For sinusoidal waves of unit amplitude, u_y will be of the form

$$u_y = e^{i(\gamma x + \omega t)}, \tag{A·3·2}$$

and, substituting in equation (A·3·1), it is easy to show that the phase velocity c' of sinusoidal flexural waves of wave-length Λ is given by the equation

$$c' = \gamma c_0 K = \frac{\pi c_0 a}{\Lambda}. \tag{A·3·3}$$

The corresponding value of the group velocity, c'_g, given by the equation

$$\frac{c'_g}{c_0} = \frac{c'}{c_0} + \frac{a}{\Lambda} \frac{d(c'/c_0)}{d(a/\Lambda)}, \tag{A·3·4}$$

is here

$$c'_g = 2c' = 2\pi c_0 a/\Lambda. \tag{A·3·5}$$

This theory leads to results which are physically absurd, namely that a wave-packet consisting of waves of infinitely short wave-lengths will be propagated with an infinite velocity, and that a wave-packet consisting of waves of infinitely long wave-lengths will be propagated with an infinitesimally small velocity.

When the elements of the bar are considered to undergo rotation (without distortion) in addition to lateral displacement, the differential equation (A·3·1) is modified to the form (due apparently to Rayleigh (1894, p. 294))

$$c_0^2 K^2 \frac{\partial^4 u_y}{\partial x^4} - K^2 \frac{\partial^4 u_y}{\partial x^2 \partial t^2} + \frac{\partial^2 u_y}{\partial t^2} = 0. \tag{A·3·6}$$

The effect of the rotation of the elements of the bar is represented by the term

$$-K^2 \partial^4 u_y / \partial x^2 \partial t^2.$$

Proceeding as before, it may be shown that the phase and group velocities derived from this equation are given by

$$c' = \frac{c_0}{\sqrt{\left(1+\frac{\Lambda^2}{\pi^2 a^2}\right)}}, \quad c'_g = \frac{c_0}{\sqrt{\left(1+\frac{\Lambda^2}{\pi^2 a^2}\right)}} \left\{1+\frac{1}{1+\frac{\pi^2 a^2}{\Lambda^2}}\right\}. \tag{A·3·7}$$

When a/Λ is small, the values of c' and c'_g given by this equation become equal to those given in equation (A·3·6); when a/Λ is large, both c' and c'_g approach the value c_0 asymptotically, so that a wave-packet consisting of waves of infinitely short wave-lengths will be propagated not with infinite velocity but with a velocity equal to the velocity of extensional waves of infinite wave-length.

When the shearing, the rotation and the lateral displacements of the elements of the bar are taken into account, the differential equation takes the form given by Timoshenko (1921) and by Prescott (1942):

$$c_0^2 K^2 \frac{\partial^4 u_y}{\partial x^4} + \frac{\partial^2 u_y}{\partial t^2} - K^2(1+\epsilon) \frac{\partial^4 u_y}{\partial x^2 \partial t^2} + \frac{\epsilon K^2}{c_0^2} \frac{\partial^4 u_y}{\partial t^4} = 0. \tag{A·3·8}$$

This equation differs from equation (A·3·7) by the terms involving the non-dimensional parameter ϵ as a factor.

It can be shown that the phase and group velocities derived from equation (A·3·8) are given by the relationships

$$\left.\begin{aligned} \frac{c_0^2}{c'^2} + \epsilon \frac{c'^2}{c_0^2} &= 1 + \frac{\Lambda^2}{\pi^2 a^2} + \epsilon, \\ \frac{c'_g}{c_0} &= \frac{c'}{c_0}\left[1 + \frac{1}{1+\frac{\pi^2 a^2}{\Lambda^2}\left(1+\epsilon-2\epsilon\frac{c'^2}{c_0^2}\right)}\right]. \end{aligned}\right\} \tag{A·3·9}$$

For a given value of a/Λ, the first of these equations becomes a quadratic in c^2/c_0^2; the two roots are real, the larger giving a value of c' which exceeds c_0 except in the limiting case where $a/\Lambda \to \infty$, whilst the smaller gives a value of c' which is always less than c_0. The larger root does not appear to have any physical significance under ordinary conditions of experiment (cf. Prescott 1942), and moreover the exact theory shows that c/c_0 is a single-valued function of a/Λ; this root will therefore be ignored, and, with this restriction, it follows that the values of c'/c_0 and c'_g/c_0 given by equation (A·3·9) reduce to those given by equations (A·3·3) and (A·3·5) when a/Λ is small. When a/Λ is large, c'/c_0 and c'_g/c_0 approach the value $1/\sqrt{\epsilon}$ asymptotically.

Assuming that $\sigma = 0{\cdot}29$, the variation of c'/c_0 and c'_g/c_0 with a/Λ given by equations (A·3·3), (A·3·5), (A·3·7) and (A·3·9) is shown graphically in figures 37 and 38; the values given by equations (A·3·3) and (A·3·5) are shown in the broken-line curve labelled 'Flexural waves (elementary theory)', those given by equation (A·3·7) in the chain-dotted curve labelled 'Flexural waves (Rayleigh theory)', and those derived from equation (A·3·9) by the points marked by crosses. These diagrams also show the values of c'/c_0 and c'_g/c_0 deduced from the data given by Hudson; these values are given by the curve labelled 'Flexural waves (exact theory)' and, for purposes of comparison, the values of c/c_0 and c_g/c_0, for extensional waves (1st mode, exact theory) have been included in the curves marked 'Extensional waves'.

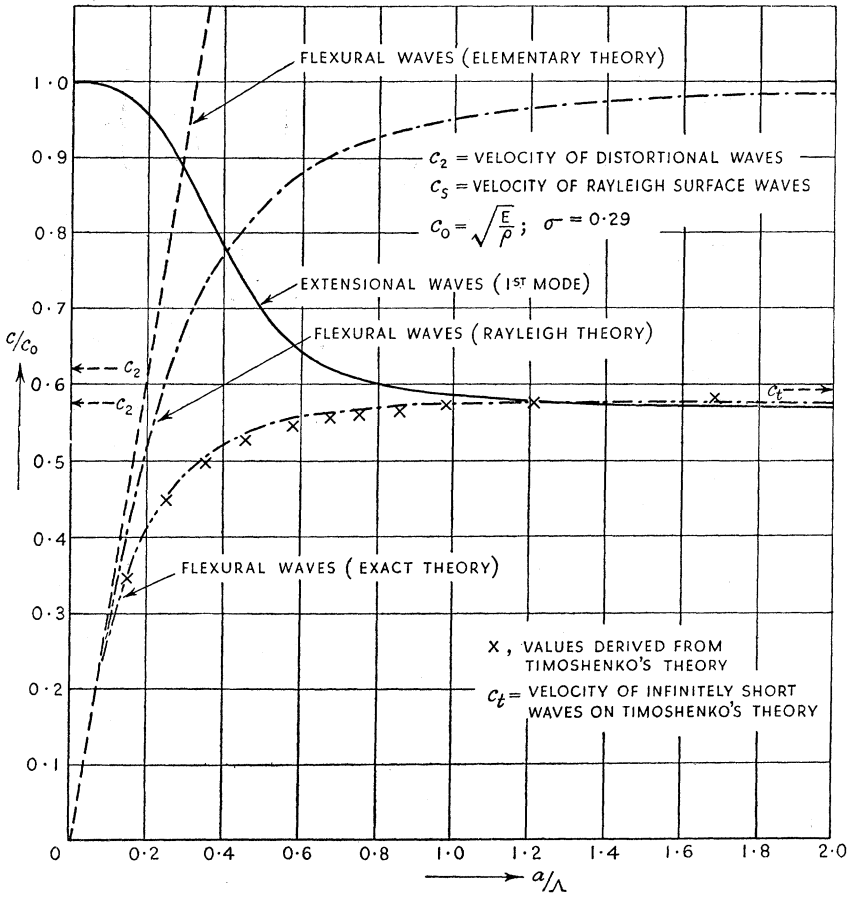

FIGURE 37. Phase velocity, c, c' of extensional and flexural waves of wave-length Λ in cylindrical bars of radius a.

The curves given in these diagrams show a number of points of interest. When a/Λ is small, the elementary theory gives the correct result. As a/Λ increases from zero, the values of c'/c_0 and c'_g/c_0 given by the elementary theory and by the Rayleigh theory are greater than those given by the exact theory. When a/Λ becomes large, the phase and group velocities become infinite on the elementary theory and equal to c_0 on the Rayleigh theory, whereas on the exact theory they become equal to c_s, the velocity of the Rayleigh surface waves. One interesting feature of the curves is the degree of agreement between the values of c'/c_0 and c'_g/c_0 given by the exact theory and by the Timoshenko theory, and even when the error is a maximum, i.e. when a/Λ is very large, the error of the Timoshenko theory is not excessive,

since the limiting values of c'/c_0 and c'_g/c_0 (when $\sigma = 0{\cdot}29$) are 0·5764 in the exact theory and 0·5906 in the Timoshenko theory. This feature of the Timoshenko theory justifies its use in dealing with problems such as the determination of the frequency of lateral vibrations of bars, where the exact theory cannot be employed because of its complexity (see, for example, Davies 1937).

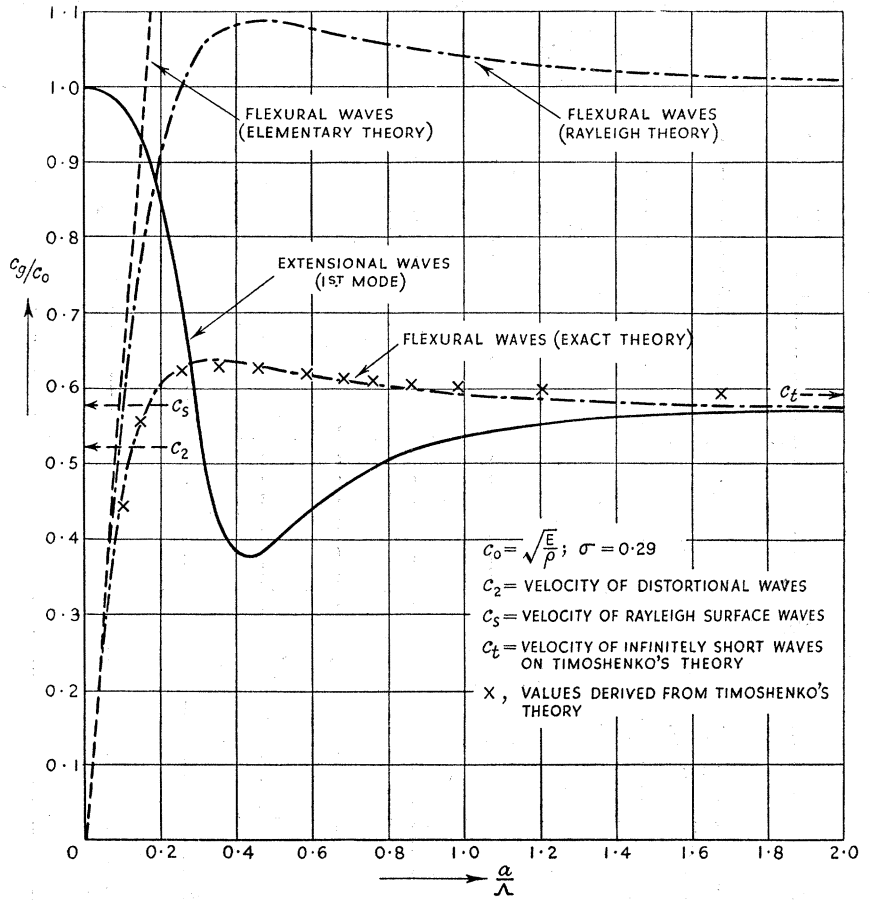

FIGURE 38. Group velocity, c_g, c'_g of extensional and flexural waves of wave-length Λ in cylindrical bars of radius a.

For the purpose of discussing the propagation of a pulse of flexural vibrations, consider a bar which is stressed initially so that the flexural displacement is zero everywhere except at a certain cross-section where it is infinite; this cross-section will be taken as the origin of x. If the stress is released at time $t' = 0$, the period T_p of the dominant group in the disturbance at a cross-section of abscissa x at time t' can be deduced by group-velocity methods. As in § 11 (b), it is convenient to take the non-dimensional ratio $t'/\frac{1}{2}T_0$ as the independent variable and the non-dimensional ratio T_p/T_a as the dependent variable, T_a and $\frac{1}{2}T_0$ being equal to the times taken by an extensional wave of infinite wave-length to traverse the distances a and x respectively. Since

$$\frac{T_p}{T_a} = \frac{\Lambda}{a}\frac{c_0}{c'} \quad \text{and} \quad \frac{t'}{\frac{1}{2}T_0} = \frac{c_0}{c'_g}, \tag{A·3·10}$$

the values of these non-dimensional variables can be derived from the curves of figures 37 and 38.

The $(T_p/T_a, t'/\frac{1}{2}T_0)$ curves deduced in this way are shown in figure 39. According to the elementary theory, $T_p/T_a = \Lambda^2/\pi a^2$, $t'/\frac{1}{2}T_0 = \Lambda/2\pi a$; the $(T_p/T_a, t'/\frac{1}{2}T_0)$ curve is thus a parabola passing through the point $t'/\frac{1}{2}T_0 = 0$ and symmetrical about the axis of T_p/T_a through this point. This implies, as has already been pointed out, that wave-packets consisting of infinitely short waves arrive at the cross-section of abscissa x at the instant at which the disturbance departs from the origin. As a/Λ decreases, the values of T_p/T_a and $t'/\frac{1}{2}T_0$ both increase, and for large values of a/Λ (outside the range of figure 39) the curve given by the elementary theory coincides with the curves given by the more exact theories.

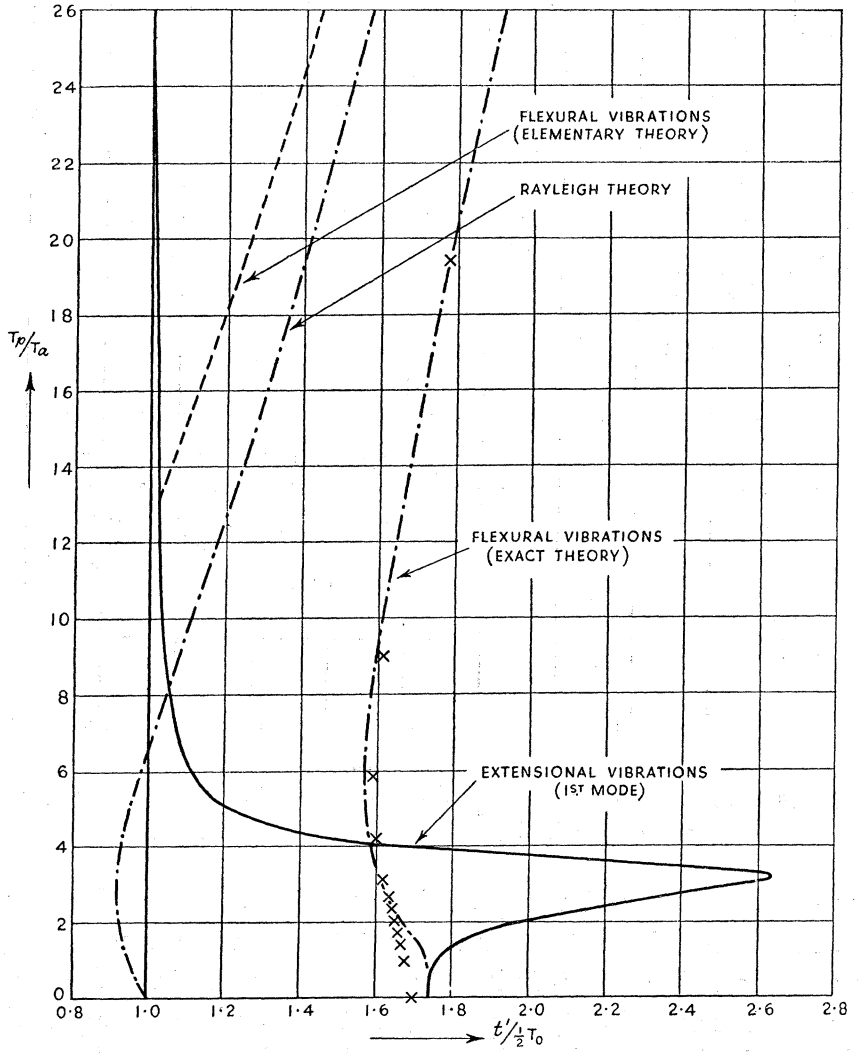

FIGURE 39. The periods, T_p, of the dominant groups in a bar of length l, radius a, at a point abscissa x, at the time t' after the departure of an infinitely thin pulse from the origin. $T_a = a/c_0$; $\frac{1}{2}T_0 = x/c_0$. ×, values derived from Timoshenko's theory.

According to the curve given by the Rayleigh theory, wave-packets consisting of infinitely short flexural waves take the same time to travel through a given distance as wave-packets composed of infinitely long extensional waves. As T_p/T_a increases (or a/Λ decreases) $t'/\frac{1}{2}T_0$ decreases until it reaches a minimum value at $t'/\frac{1}{2}T_0 = 0{\cdot}92$, when T_p/T_a is about 3 and a/Λ is about 0·8; beyond this point $t'/\frac{1}{2}T_0$ decreases as T_p/T_a increases. Thus, according to this theory, when an infinitely intense flexural disturbance initially concentrated at the origin

is released, the first components to arrive at a given point do so at time $t' = 0{\cdot}92T_0/2$; their period is about $3T_a$ and their wave-length about $1{\cdot}25a$. In the interval between the arrival of these components and time $t' = T_0/2$, two groups of different wave-lengths and period arrive simultaneously at each instant; finally when t' exceeds $T_0/2$, only one group arrives at a given instant, the period and the wave-length of the group increasing as t' increases.

Considering the results of the exact theory, it is clear that the faster components, originating in an infinitely intense disturbance at the origin, arrive at the cross-section of abscissa x at time $t' = 1{\cdot}56_8T_0/2$; the period of these components is $5{\cdot}29T_a$ and their wave-length is equal to $2{\cdot}7a$. Between this value of t' and $t' = 1{\cdot}73_5T_0/2$, two groups of different wave-lengths and periods arrive simultaneously at each value of t'; at $t' = 1{\cdot}73_5T_0/2$, the Rayleigh surface waves and waves of period $17{\cdot}3T_a$ arrive simultaneously. When t' exceeds $1{\cdot}73_5T_0/2$, only one group will arrive at each instant.

It is clear that the elementary theory and the Rayleigh theory give results which are very wide of the truth, and any solutions based on these theories of problems of the action of transient flexural stresses on bars are unlikely to be accurate unless it happens that the disturbances are such that waves of short wave-length are unimportant. Again, it is interesting to notice that the results derived from the Timoshenko theory are in excellent agreement with those deduced from the exact theory.

As far as the present experiments are concerned, the main interest of the curves of figure 39 is that they show that, on the exact theory, no flexural displacements will occur at the cross-section of abscissa x until $t' \geqslant 1{\cdot}56_8T_0/2$, i.e. $t' \geqslant 1{\cdot}56_8x/c_0$; remembering that the record in a given experiment begins when extensional displacements of infinite wave-lengths arrive at the cross-section, i.e. when $t' = T_0/2 = x/c_0$, it follows that displacements due to flexural waves will not appear on the record until a time $0{\cdot}568x/c_0$ after the beginning of the record. The length of the shortest bar used in the present series of experiments was 2 ft. 2 in. $= 66{\cdot}0_4$ cm.; assuming that $c_0 = 5{\cdot}26 \times 10^5$ cm./sec., $0{\cdot}568x/c_0 = 71{\cdot}3_1\,\mu$sec., and since the duration of the pulses measured with a bar of this length was usually of order $50\,\mu$sec., the record would normally be free from effects due to flexural waves.

References

Bancroft, D. 1941 *Phys. Rev.* **59**, 588.

Carslaw, H. S. & Jaeger, J. C. 1941 *Operational methods in applied mathematics.* Oxford: Clarendon Press.

Chree, C. 1889 *Proc. Camb. Phil. Soc.* **14**, 250.

Davies, R. M. 1937 *Phil. Mag.* **23**, 1129.

Havelock, T. H. 1914 *The propagation of disturbances in dispersive media.* Cambridge: University Press.

Hopkinson, B. 1914 *Phil. Trans.* A, **213**, 437.

Hudson, G. E. 1943 *Phys. Rev.* **63**, 46.

Kohlrausch, F. 1930 *Lehrbuch der praktischen Physik.* Berlin: Teubner.

Lamb, H. 1924 *Hydrodynamics.* Cambridge: University Press.

Landon, J. W. & Quinney, H. 1923 *Proc. Roy. Soc.* A, **103**, 622.

Love, A. E. H. 1934 *Mathematical theory of elasticity.* Cambridge: University Press.

Pochhammer, L. 1876 *J. reine angew. Math.* **81**, 324.

Prescott, J. 1942 *Phil. Mag.* **33**, 703.

Rayleigh, Lord 1894 *Theory of sound*, **1**. London: Macmillan and Co.

Robertson, R. 1921 *Trans. Chem. Soc.* **119**, 1.

Russell, A. 1914 *Alternating currents*, **1**. Cambridge: University Press.

Timoshenko, S. 1921 *Phil. Mag.* **41**, 744.

Timoshenko, S. 1929 *Vibration problems in engineering.* New York: van Nostrand.

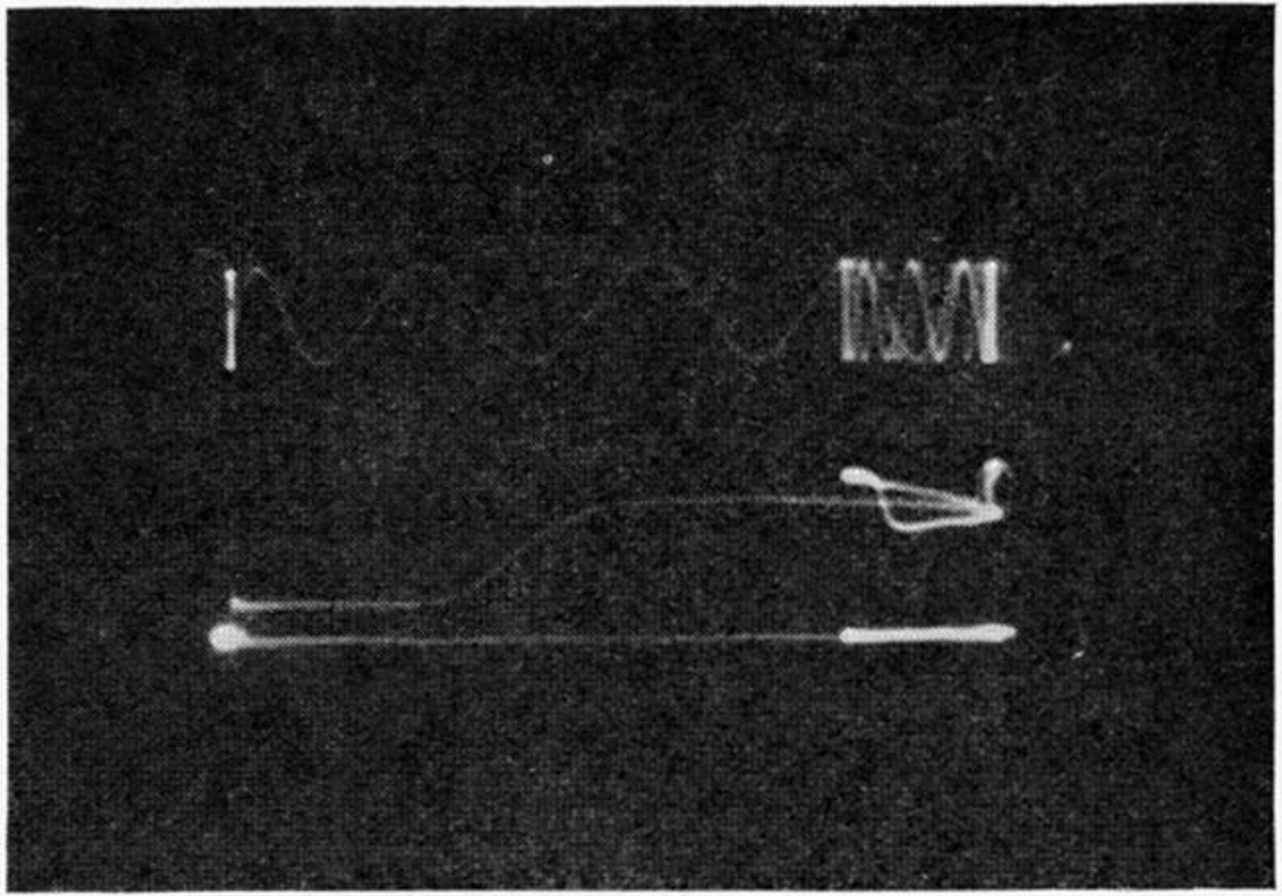

FIGURE 10. Oscillogram of a pulse due to the impact of a bullet. Pressure bar: length = 2 ft. 2 in., diameter = 1 in. Condenser unit: parallel-plate type. Velocity of bullet = 998 ft./sec. Upper trace: timing wave of period $40{\cdot}3_2$ μsec. Middle trace: amplified p.d. from condenser unit. Lower trace: datum line.

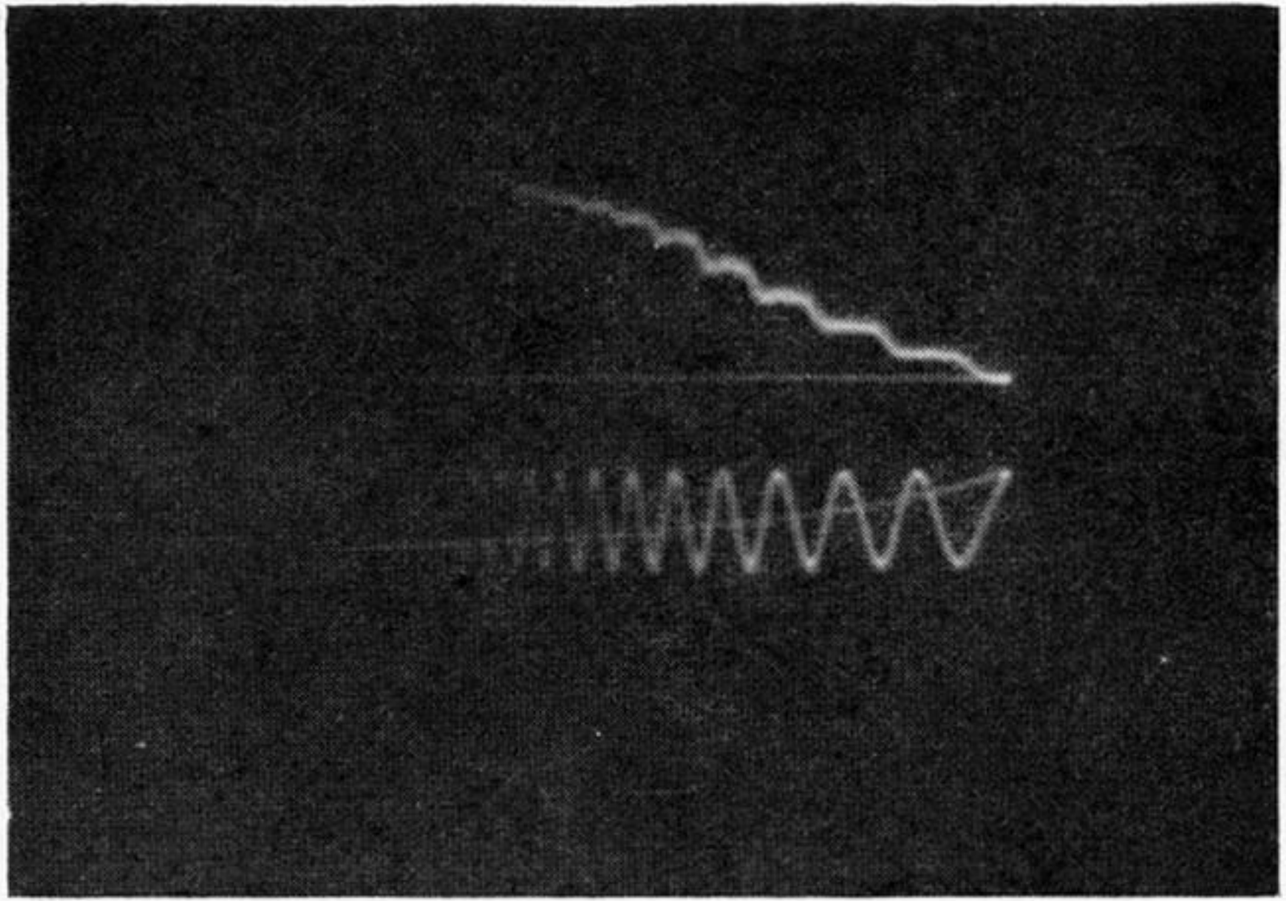

FIGURE 11. Oscillogram showing the discontinuous motion of the measuring end of a bar, caused by the impact of a steel ball on the pressure end. Pressure bar: length = 3 ft. $9\frac{1}{2}$ in., diameter = $1\frac{1}{2}$ in. Condenser unit: parallel-plate type. Upper trace: amplified p.d. from condenser unit. Lower trace: timing wave of period 435 μsec.

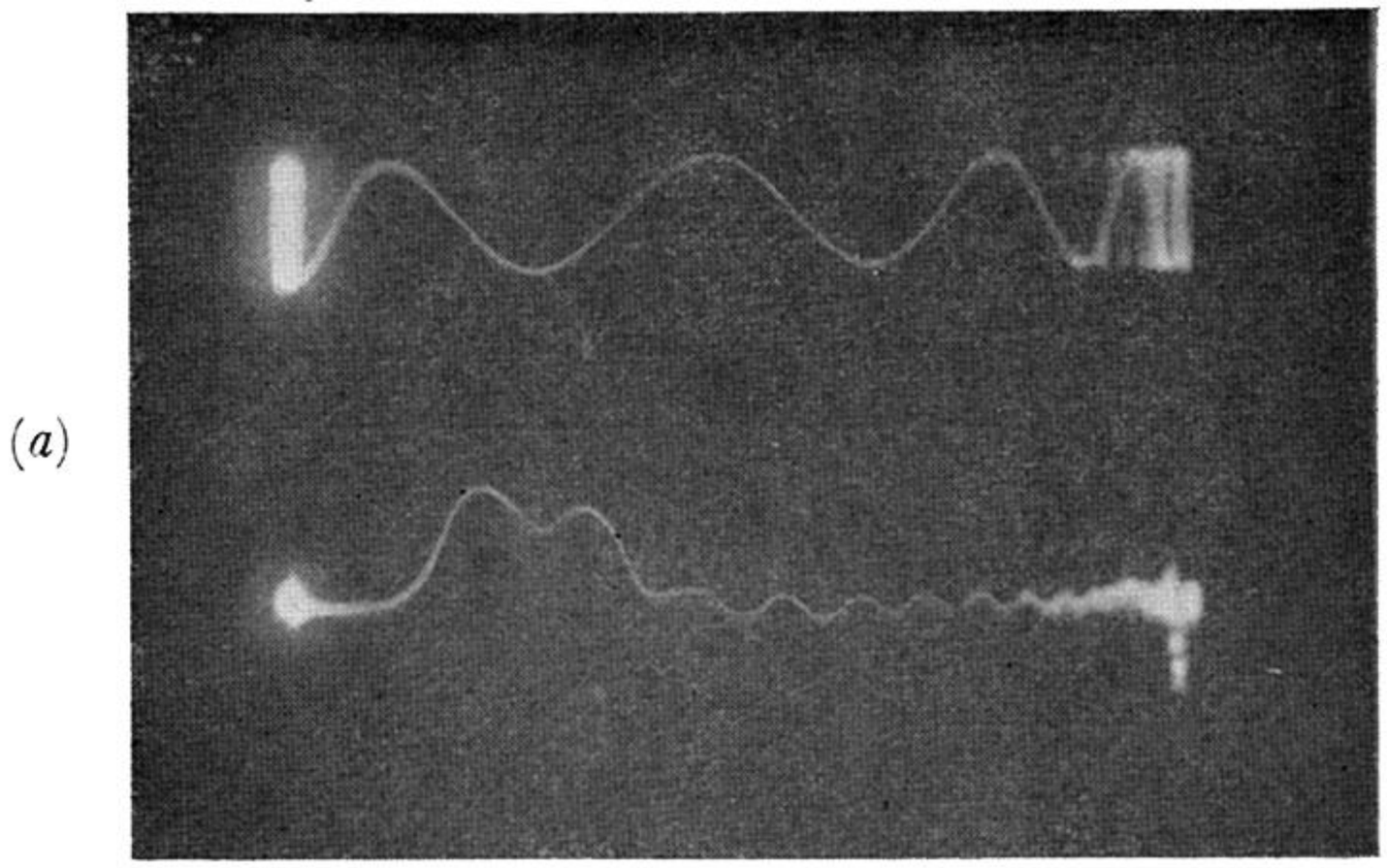

(*a*)

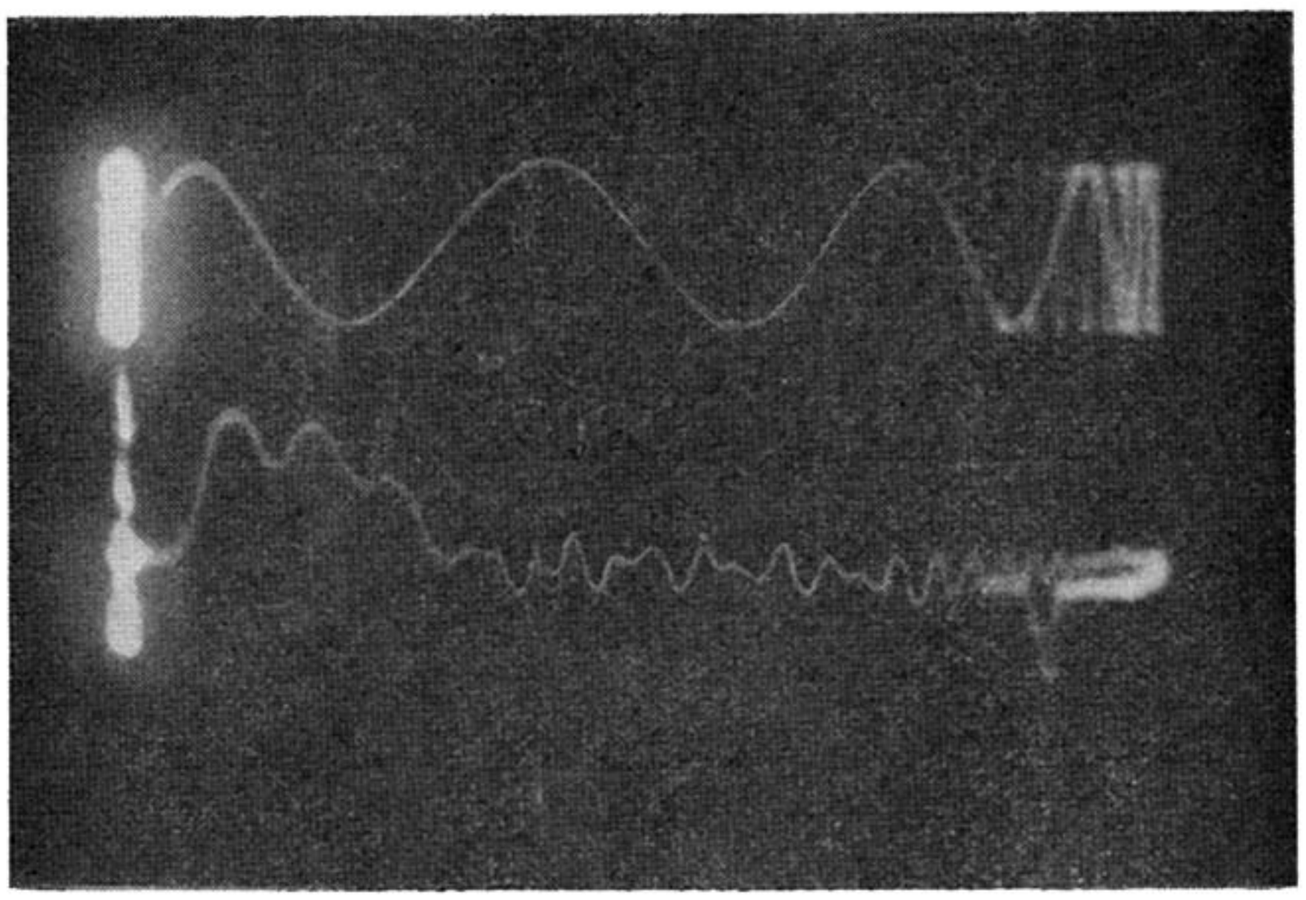

(*b*)

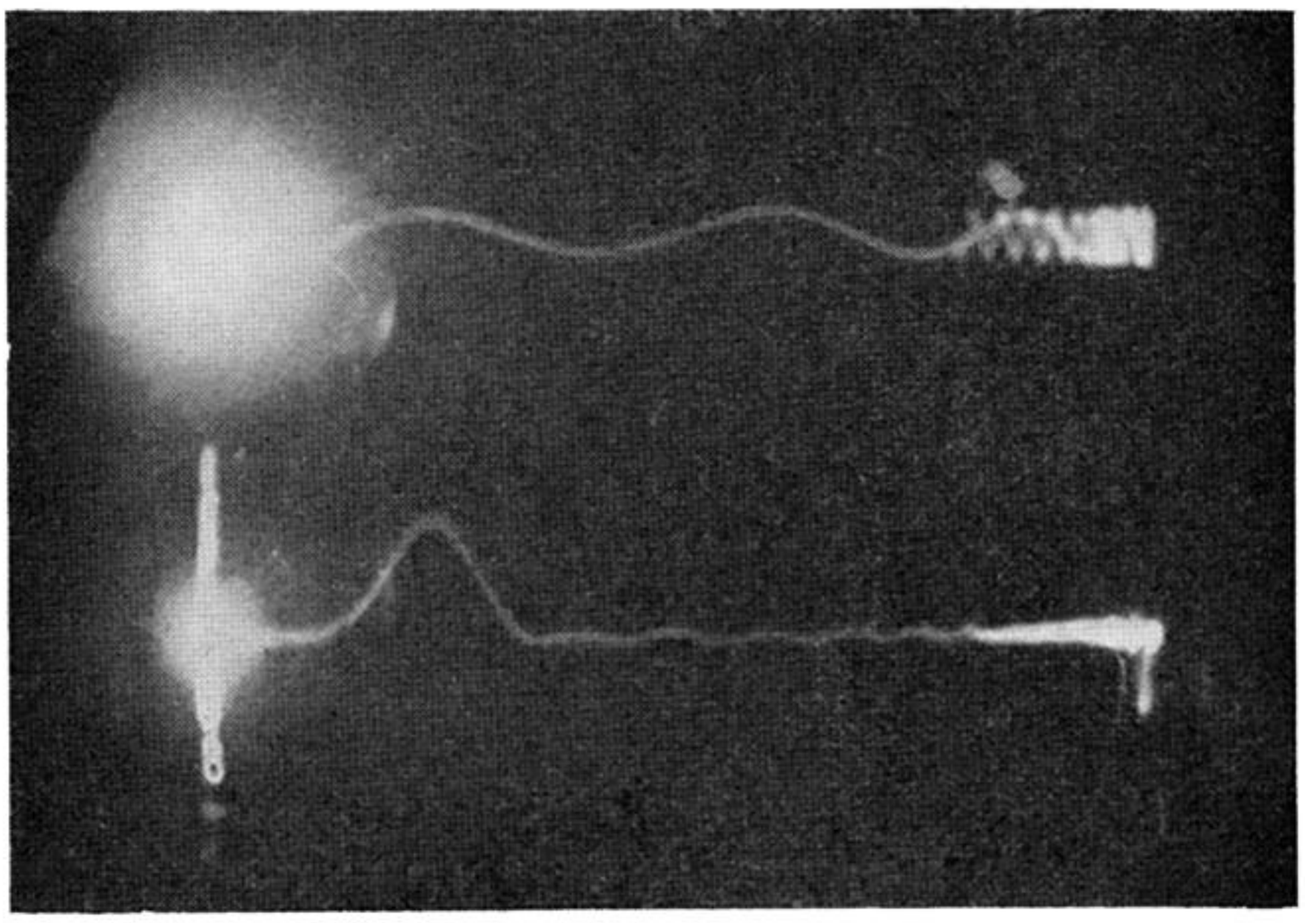

(*c*)

FIGURE 22. Oscillograms of pulses due to the impact of bullets. Pressure bar: length = 6 ft., diameter = 1 in. Condenser unit: cylindrical type, measuring radial displacement. Period of timing wave = 46·5 μsec.

	(*a*)	(*b*)	(*c*)
type of bullet	round-nosed	round-nosed	cone-shaped
velocity of bullet (ft./sec.)	1135	1171	1350
distance of condenser unit from pressure end of bar (cm.)	115	35	115

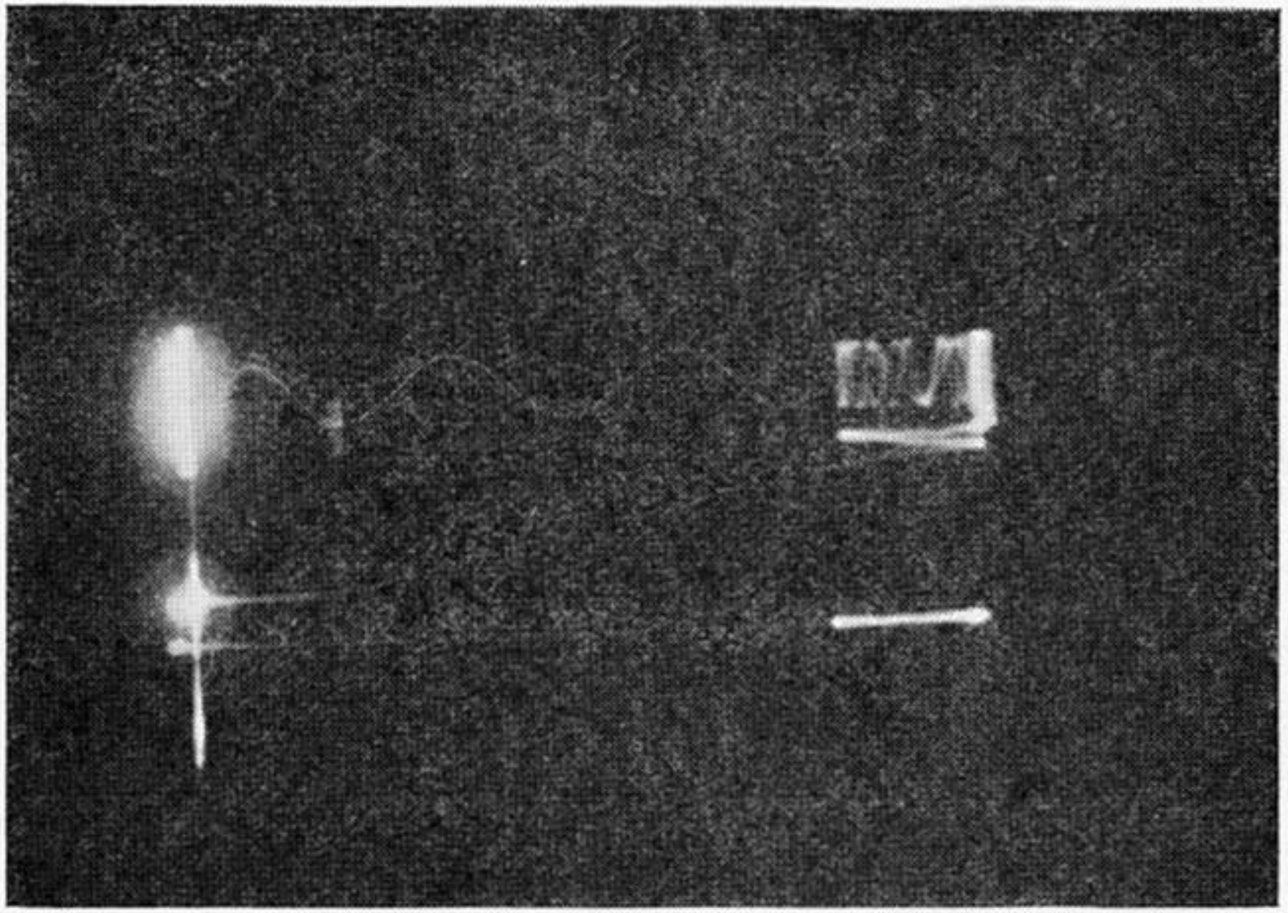

FIGURE 28. Oscillogram of the pulse due to the Pitot pressure in a detonation wave in a mixture of air, oxygen and hydrogen. Pressure bar: length = 2 ft. 2 in., diameter = 1 in. Condenser unit: parallel-plate type. Upper trace: timing wave, period = 41 μsec. Middle trace: amplified p.d. from condenser unit. Lower trace: datum line.

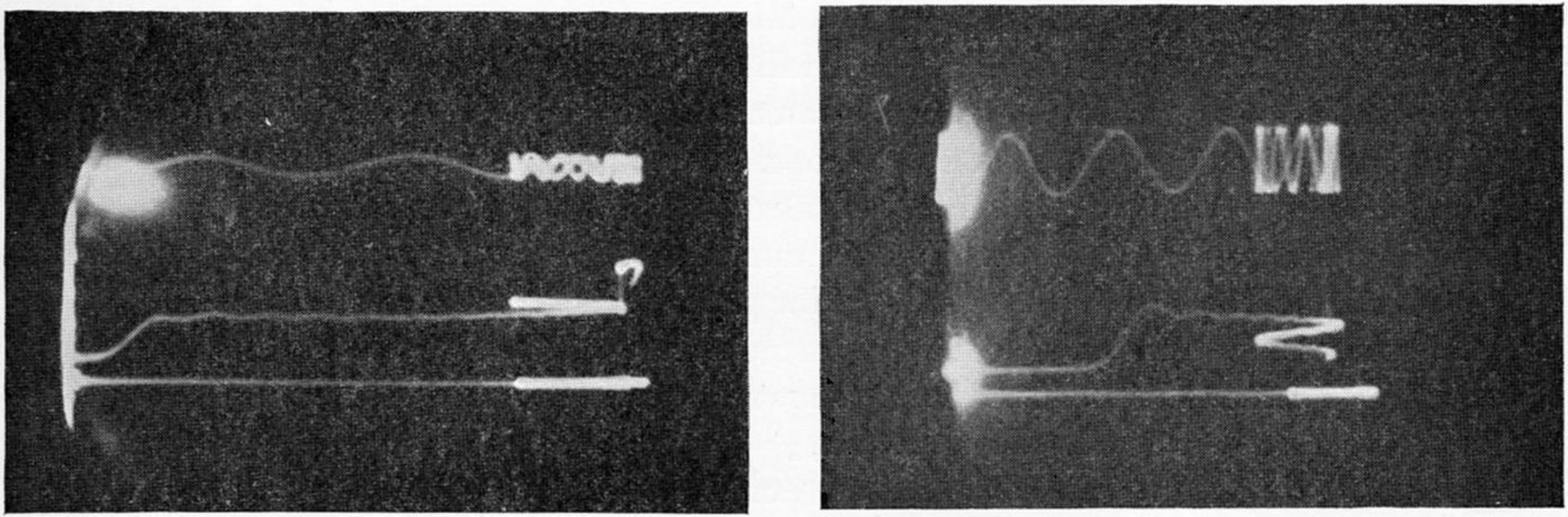

(*a*) (*b*)

FIGURE 34. Oscillograms showing the oscillations following the main pulse. Pressure bar: length = 6 ft., diameter = 1 in. Condenser unit: parallel plate type. (*a*) Pulse due to 1 oz. charge of C.E. Upper trace: timing wave of period 57·3 μsec. Middle trace: amplified output from condenser unit. Lower trace: datum line. (*b*) Pulse due to the impact of a steel ball, 0·5 in. diameter. Velocity of ball = 182 ft./sec. Upper trace: timing wave of period 40·9 μsec. Middle trace: amplified output from condenser unit. Lower trace: datum line.